VALIDATION

ATMOSPHERIC EXPANSION MODELLING
Literature review, Model refinement and Validation

REPORT No: 984B0034, Rev. 6

DATE: April 2018

Project name:	SAFETI-NL Innovative Maintenance	DNV Services UK Limited
Report title:	Atmospheric expansion modelling – Literature review, Model refinement and Validation	Vivo Building 30 Stamford Street
Customer:	RIVM, P.O. Box 1, 3720BA Bilthoven	London
Contact person:	Paul Uijt de Haag	SE1 9LQ
Date of issue:	21/12/2015	Tel: +44(0)20 357 6080
Project No.:	984B0034	
Organisation unit:	DNV	
Report No.:	984B0034, Rev. 6	
Document No.:	1	

Prepared by:	Verified by:	Approved by:
[Name] H.W.M. Witlox, DNV Senior Principal Engineer	[Name] Jan Stene, DNV Senior Mathematical Modeller	[Name]
[Name] [title]	[Name] [title]	
[Name] [title]	[Name] [title]	

☐ Unrestricted distribution (internal and external)
☒ Unrestricted distribution within DNV
☐ Limited distribution within DNV after 3 years
☐ No distribution (confidential)
☐ Secret

Keywords:
[Keywords]

Reference to part of this report which may lead to misinterpretation is not permissible.

Reference to part of this report which may lead to misinterpretation is not permissible.

No.	Date	Reason for Issue	Prepared by	Verified by	Approved by
1	2014-06-20	Phase I – 1st preliminary draft	H.W.M. Witlox	Jan Stene	
2	May 2015	Added validation (2-phase releases	Witlox & Fernandez		
3	July 2015	Added validation H2 (Shell/HSL)	Witlox		
4	Dec. 2015	Added validation NG/ethylene (BG)	Witlox		
5	Oct 2017	Phast/Safeti 8.0 version	Witlox	Jan Stene	
6	April 2018	Phast/Safeti 8.1 version	Witlox & Stene		
7	May 2021	Apply new template	D. Vatier		

Date: May 2021

Prepared by: Digital Solutions at DNV

Table of contents

1 EXECUTIVE SUMMARY

The consequence modelling package Phast includes steady-state and time-varying discharge models for vessel orifice releases of toxic or flammable materials. These models first calculate the depressurisation between the stagnation and orifice conditions and subsequently impose the ‘Atmospheric Expansion model’ ATEX for modelling the expansion from orifice conditions to the final conditions at atmospheric pressure. The latter post-expansion conditions are used as the source term for the Phast dispersion model UDM.

The ATEX mathematical model determines the unknown post-expansion variables (diameter, velocity, temperature, liquid fraction, density and enthalpy) by imposing conservation of mass, conservation of energy, and equations of state for density and enthalpy. In addition, either conservation of momentum or conservation of entropy is imposed; by default the conservation option which results in the minimum change in temperature and/or liquid fraction is used. Finally a maximum is imposed for the post-expansion velocity.

This report includes results of a literature review on atmospheric expansion modelling, and provides recommendations on selection of ATEX model equations to ensure a most accurate prediction for the near-field UDM jet dispersion against available experimental data.

First, the correctness of the numerical solution to the ATEX equations has been verified against an analytical solution of ideal-gas releases for both cases of isentropic and conservation-of-momentum assumptions, including comparison against published data in the literature. Also the importance of non-ideal gas effects is investigated.

Secondly, both ATEX expansion options have been applied to known available experimental data for orifice releases. This includes gas jets (natural gas and ethylene – British gas experiments, hydrogen - Shell/HSL experiments) and flashing liquid jets (ammonia – Desert Tortoise, Fladis; propane – EEC; HF – Goldfish; CO2 – CO2PIPETRANS). For these experimental data it was confirmed that the ATEX conservation-of-momentum option without a velocity cap provides overall more accurate concentration predictions than the isentropic assumption. However the existing default ‘minimum thermodynamic change’ option was found to mostly impose conservation of entropy (velocity cap not applicable) for two-phase releases and conservation of momentum (velocity cap applicable) for the sonic gas jets. For flashing two-phase releases including rainout a further investigation is recommended, as rainout calculations are currently based on the isentropic assumption.

2 INTRODUCTION

The hazard assessment software package Phast and the QRA software package Safeti include the discharge models DISC and TVDI for modelling steady-state or time-varying discharge from vessel orifices or pipes, and the models GASPIPE and PIPEBREAK for modelling of discharge of vapour or two-phase flashing liquids from long pipes. These discharge models all impose the 'Atmospheric Expansion' model ATEX[/2/] to calculate the expansion from the orifice conditions to the atmospheric pressure (see Figure 2-1). The 'final' ATEX atmospheric conditions (post-expansion conditions) are used as the starting conditions for the Phast dispersion model UDM and the Phast jet-fire model JFSH.

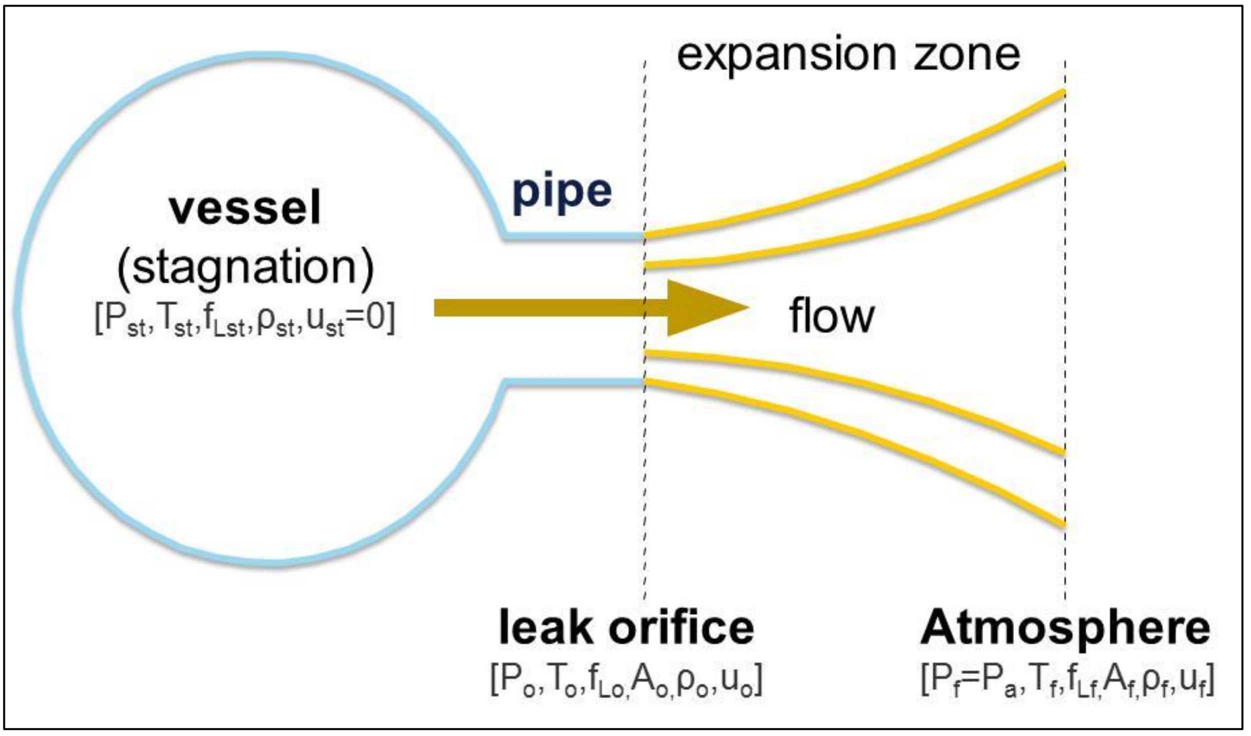

Figure 2-1 ATEX expansion from orifice to ambient conditions

For a liquid release from a vessel orifice ('leak' scenario), the orifice is at metastable equilibrium while for all other cases the orifice is at thermodynamic equilibrium. The final state is always at thermodynamic equilibrium.

Flow regimes for orifice release

Figure 2-2a illustrates the subsequent zones in the flow for the case of the discharge from an orifice:

- (st) stagnation point (zero velocity)
- (o) upstream orifice (nozzle entrance; area A_o, velocity u_o, pressure P_o)
- (vc) downstream orifice (nozzle throat; vena contracta area A_{vc}, velocity u_{vc}, pressure P_{vc}, temperature T_{vc})
- (f) end of atmospheric expansion zone (area A_f, velocity u_f, pressure P_f =ambient pressure P_a, temperature T)

The vena contracta area equals $A_{vc} = C_d A_o$, where C_d equals the discharge coefficient (C_d=1 for pipeline release). At the final conditions (f) the flow is presumed to be thermodynamic stable, while in case of a liquid release the metastable liquid assumption applies at (o).

The Phast model ATEX (see Chapter 1) currently assumes that the final conditions are given by a planar surface; see Figure 2-2b1. On the other hand Spicer et al.[/13/,/14/] (see Section 5.2) presume the final surface to be part of a sphere with radius R_f (enclosing an angle of 2Φ, with final velocity u_f normal to final surface); see Figure 2-2b2.

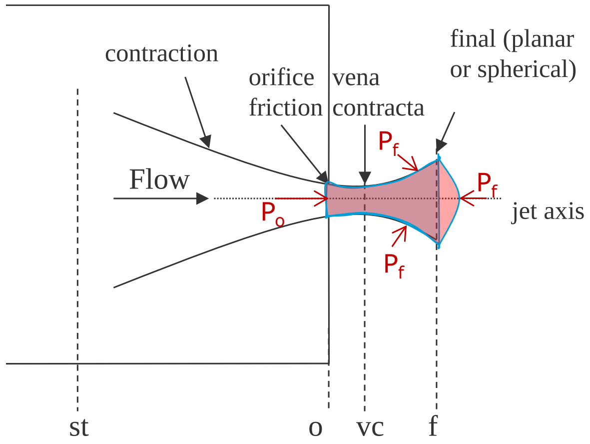

(a) Zones in flow for discharge from orifice

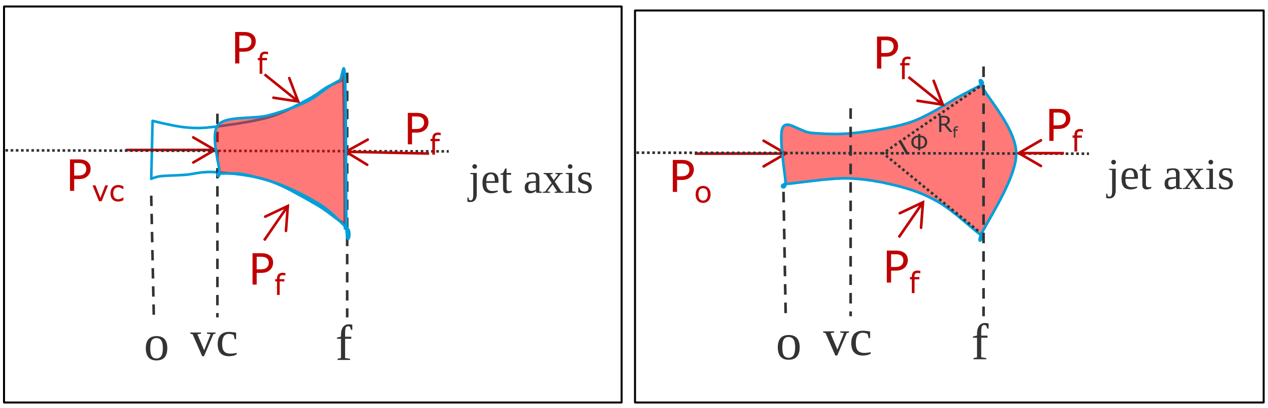

(b1) control volume (ATEX) (b2) control volume (Spicer and Paris)

Figure 2-2 Control volume for expansion to ambient conditions

General equations for atmospheric equation (integral formulation)

Let us now consider the coloured control volume as depicted in Figure 2-2b, and let B its volume and S its surface area. The integral form of the general fluid-dynamics equations for this control volume is now as follows (ignoring air entrainment):

$$\frac{\partial}{\partial t}\left\{\iiint_B \rho\, dB\right\} + \iint_S \rho(\underline{V}\bullet\underline{n})dS = 0 \quad \text{, mass} \tag{1}$$

$$\frac{\partial}{\partial t}\left\{\iiint_B \rho\underline{V}\, dB\right\} + \iint_S \rho\underline{V}(\underline{V}\bullet\underline{n})dS = \iint_S\left[-p\underline{n}+\underline{t}_{fr}\right]dS + \iiint_B \rho\underline{g}\, dB \text{ , momentum} \tag{2}$$

$$\frac{\partial}{\partial t}\left\{\iiint_B \rho\left(\frac{1}{2}V^2+e\right)dB\right\} + \iint_S \rho\left(\frac{1}{2}V^2+e\right)(\underline{V}\bullet\underline{n})dS = \iint_S\left[-p\underline{n}+\underline{t}_{fr}\right]\bullet\underline{V}\, dS + \iiint_B \rho\underline{g}\bullet\underline{V}\, dB - \iint_S \underline{q}\bullet\underline{n}\, dS \text{ ,energy} \tag{3}$$

Here ρ is the fluid density, $\underline{V}$ is the fluid velocity, $\underline{n}$ is a unit vector pointing outward normal to the surface S, p the pressure, $\underline{g}$ the gravitational acceleration vector (pointing downwards; g = 9.81m/s^2), $\underline{t}_{fr}$ surface friction forces, e the internal energy, and $\underline{q}$ the heat flux from the surroundings.

Presuming a steady-state release and ignoring friction forces, gravity forces, viscous dissipation, and heat flux from the wall, and using e=h–p/ρ (h = specific enthalpy), the above equations reduce to

$$\iint_S \rho(\underline{V} \bullet \underline{n})dS = 0 \text{ , mass} \quad (4)$$

$$\iint_S \{\rho \underline{V}(\underline{V} \bullet \underline{n}) + p\underline{n}\}dS = 0 \text{ , momentum} \quad (5)$$

$$\iint_S \rho\left(\frac{1}{2}V^2 + h\right)(\underline{V} \bullet \underline{n})dS = 0 \text{ , energy} \quad (6)$$

Outcome of previous literature review (Phase I droplet modelling JIP)

Phases I-IV of the droplet modelling JIP (Witlox et al.[/3/,/15/]) very much focussed on the correct evaluation of the flow rate (kg/s) and initial post-expansion droplet size distribution (micrometre), but did not focus on correct evaluation of the post-expansion velocity, post-expansion liquid fraction (case of 2-phase releases) and temperature (case of vapour releases).

The arbitrary ATEX default cap of 500 m/s for post-expansion velocity is a known issue alongside the appropriate default choice of the ATEX expansion method (isentropic, conservation of momentum, or minimum thermodynamic change).

A very brief review of external expansion calculations available in the literature was carried out by Witlox and Bowen (2002)[/1/] as part of the first phase of the droplet modelling JIP.

The most common approach in the literature may be the absence of a cap combined with the conservation of momentum method (particularly for releases from pipes). ATEX currently also allows for an alternative cap (sonic velocity). However in case of choked flow (sonic velocity at orifice), supersonic turbulent flow (shock waves) is known to occur downstream of the orifice and the sonic cap may not be appropriate. Moreover the thermodynamic path may need to include non-equilibrium effects and/or slip. So far we are not aware of a published and validated formulation, which takes these effects into account.

Also important to note is that for choked flows the final velocity u_f does not necessarily correspond to a physically real velocity, and is therefore sometimes referred to in literature as a *'pseudo-velocity'*. The key important aspect is that this *pseudo-velocity* produces the correct amount of (jet) entrainment in the UDM dispersion model to ensure accurate predictions of the concentrations in the near-field. It is therefore NOT important that the predicted post-expansion velocity is close to the actual post-expansion velocity.[i]

Model validation (discharge in conjunction with dispersion model)

As detailed in the UDM validation manual (part of UDM Technical Reference Manual[/5/]), so far the UDM dispersion model has been largely validated independently of the discharge model, with post-expansion data (velocity, liquid fraction, temperature) as provided by Hanna (MDA database) and/or SMEDIS (REDIPHEM database). Thus these data are not in any way reliant on excessive post-expansion velocities predicted by the discharge model. In these experiments it was observed that the 'conservation of momentum' assumption provided the closest values to the SMEDIS data. As part of the current proposed work, a range of ATEX expansion methods will be utilised to a dataset of dispersion experiments to further evaluate which one gives the closest results. Furthermore it is noted that the CCPS flashing correlation (used both in the original and modified CCPS droplet size correlations present in Phast) has been derived based on a best fit against experimental data presuming the isentropic expansion method. The use of this correlation in conjunction with the conservation-of-momentum method may therefore lead to less accurate predictions of rainout.

Current work

The current work constitutes the results of a separate research project involving a literature survey and validation. Given the observations above, this also includes the accuracy and validation of the near-field concentrations. Furthermore distinction has been made in the project between vapour releases and two-phase releases. Finally the emphasis of the current work is on conventional pseudo-source models (as could be used in Phast). CFD modelling is not considered as part of the current scope of work. For example, Leeds University (Wareing et al., 2013)[/25/] developed a CFD method solving rigorously the Navier Stokes equations to define the shape, velocity and temperature distribution downstream of the Mach shock region, where the flow expands to atmospheric pressure.

Plan of report

[i] The final velocity is also used by the jet fire model, and therefore also the 'pseudo-velocity" should result in accurate jet fire predictions (shape of jet fire, surface emissive power, radiation)

Chapter 3 summarises the mathematical model for the atmospheric expansion model as currently implemented in Phast (versions 6.54 up to and including the latest version). This model imposes conservation of mass, conservation of energy, and conservation of either momentum or entropy.

Chapter 4 describes the analytical verification of this model for the special cases of incompressible liquids (Bernoulli law) and ideal gases.

Chapter 5 summarises the results of the literature review on atmospheric expansion. Here both experimental and theoretical work is considered, with focus on releases that do not rain out. Section 5.1 summarises the outcome of previous literature reviews carried out as part of DNV's droplet modelling JIP (Witlox and Bowen, 2002)[/1/] and EU project FLADIS and USA DTRA project (Britter et al.[/7/,/8/,/10/]). Sections 5.2, 5.3 and 5.4 consider flashing liquid jets (Spicer and Paris[/13/,/14/], Arkansas University), gas jets (including model by Birch et al.[/21/] and air, methane and hydrogen experiments) and multicomponent releases, respectively.

Chapter 6 discusses the validation of the Phast discharge model DISC (including ATEX model) and the Phast dispersion model UDM for both two-phase flashing jets and sonic gas jets, where a range of atmospheric expansion options has been applied.

Chapter 7 summarises the main conclusions and Chapter 8 includes final recommendations for the atmospheric expansion model to be applied in conjunction with potential future work.

3 ATMOSPHERIC EXPANSION MODEL ATEX

This section provides a brief summary of the ATEX mathematical model currently implemented in Phast and Safeti.

Non-instantaneous releases are considered in Section 3.1 and instantaneous releases briefly in Section 3.2. For further details the reader is referred to the detailed description of the ATEX model included in the ATEX theory document (Witlox, Harper and Stene, 2011)[/2/].

A number of correlations for predicting initial droplet sizes and droplet size distributions are available as part of the ATEX model. The associated theory and validation can be found in Droplet size theory document (Witlox et al., 2011)[/3/] and is not discussed in the current section.

3.1 Continuous or time-varying releases

ATEX input (vena contacta data or pipe exit data; see Figure 2-2b1 and Figure 2-1)

Input to the ATEX model are:

- orifice or pipe exit diameter d_o
- vena contracta temperature T_{vc} (for pure vapour or liquid) or liquid fraction f_{Lvc} (two-phase)
- vena contracta pressure P_{vc}
- exit velocity u_o or flow rate Q (kg/s)

For a liquid release from a vessel orifice ('leak' scenario), the orifice is at metastable equilibrium (P_o = ambient pressure, $f_{Lo}=1$) while for all other cases the orifice/pipe-exit is at thermodynamic equilibrium.

If the flow rate Q is specified, the exit velocity is u_o set using $u_o = Q / [0.25 \pi d_o^2 \rho(P_{vc},T_{vc},f_{Lvc})]$, where ρ is the density. For pipeline scenarios, the discharge coefficient $C_d=1$ and therefore vena contracta data are equal to the pipe exit data. For leak scenarios the vena contracta diameter $d_{vc} = C_d^{0.5} d_o$, where C_d is the discharge coefficient.[ii]

ATEX output (final post-expansion data)

Output from the ATEX model are the data at the end of expansion to atmospheric pressure (see Figure 2-1), which are used as the starting conditions for the UDM dispersion modelling. The final conditions are given by the 5 unknown post-expansion data: area A_f, velocity u_f, temperature T_f or liquid fraction f_{Lf}, density ρ_f, and specific enthalpy h_f. Along the expansion zone one-dimensional homogeneous flow is assumed in thermal equilibrium and with zero air entrainment.

The ATEX model calculates the expansion from the vena-contracta to the final post-expansion conditions, where the final conditions are imposed at a planar surface as shown in Figure 2-2b1. ATEX contains two models for the expansion from the conditions in the exit plane down to atmospheric, called 'conservation of momentum' and 'isentropic'.

ATEX 'conservation of momentum' model

For the case of a planar surface for the final conditions, Equations **(4)**, **(5)** and **(6)** reduce to the existing ATEX Equations **(7)**,**(8)**, **(9)**. Thus the ATEX 'conservation of momentum' model imposes three conservation equations (conservation of mass, momentum and energy) and two equations of state for density and enthalpy) for the five unknown variables:

$$\rho_f A_f u_f = \rho_{vc} A_{vc} u_{vc} \text{ , mass conservation} \quad \textbf{(7)}$$

$$\rho_f A_f u_f^2 = \rho_{vc} A_{vc} u_{vc}^2 + (P_{vc} - P_f) A_{vc} \text{ , momentum conservation} \quad \textbf{(8)}$$

[ii]IMPROVE/CHECK. The vena contract velocity u_{vc} is derived by ATEX from the orifice velocity as $u_{vc} = u_o / C_d$; furthermore $P_{vc} = P_o$, $T_{vc} = T_o$, $f_{Lvc} = f_{Lo}$, $\rho_{Lvc} = \rho_{Lo}$. Please note that in fact DISC first calculates the expansion from stagnation to vena contracta conditions, and not expansion from stagnation to exit conditions. Thus in fact actual inputs to ATEX are the vena contracta conditions, and ATEX calculates the expansion from vena contracta conditions to final conditions. At both the vena contracta conditions and the final conditions the velocity is presumed to be perpendicular to the vessel wall (case of leak scenario) or pipe cross-section (case of line rupture or long pipeline). In fact the orifice pressure P_o could be different to the vena contracta pressure P_a (and likewise for temperature density, enthalpy; also $u_{vc} = u_o / C_d$ may not apply. It may be recommended to update the DISC/ATEX theory documents to account for this. In this context it would be logical that the vena contracta velocity and the vena contracta diameter are input to the ATEX spreadsheet (to avoid any confusion).

$$\rho_f A_f u_f \left[h_f + \frac{1}{2} u_f^{\,2} \right] = \rho_{vc} A_{vc} u_{vc} \left[h(P_{vc}, T_{vc}; f_{Lvc}) + \frac{1}{2} u_{vc}^{\,2} \right] \text{, energy conservation} \quad \textbf{(9)}$$

$$\rho_f = \rho_f\,(P_a, T_f; f_{Lf}) \text{, density equation of state} \quad \textbf{(10)}$$

$$h_f = h(P_a, T_f; f_{Lf}) = f_{Lf} h_L(P_a, T_f) + (1 - f_{Lf}) h_V(P_a, T_f) \text{, enthalpy equation of state} \quad \textbf{(11)}$$

The unknown post-expansion data can subsequently be determined as follows:

a) The post-expansion mass rate $m_f = \rho_{vc}A_{vc}u_{vc}$ is set from Equation **(7)**

b) Set post-expansion speed u_f from Equation **(8)**

$$u_f = u_{vc} + \frac{P_{vc} - P_a}{\rho_{vc} u_{vc}} \quad \textbf{(12)}$$

c) Set post-expansion specific enthalpy h_f from Equation **(9)**

$$h_f = h_{vc} + \frac{1}{2}\left[u_f^{\,2} - u_{vc}^{\,2} \right] \quad \textbf{(13)}$$

d) For a two-phase release T_f equals the boiling temperature and the post-expansion liquid fraction f_{Lf} can be set from Equation **(11)**. Otherwise $f_{Lf} = 0$ (vapour release) or $f_{Lf} = 1$ (liquid release) and the temperature T_f can be set from Equation **(11)**.

e) Set post-expansion density ρ_f from Equation **(10)**

f) Set post-expansion jet area: $A_f = m_f/(u_f\rho_f)$.

ATEX 'isentropic' model

In the ATEX 'isentropic' model the above momentum conservation equation is replaced by the following entropy conservation equation:

$$s(T_{vc}, P_{vc}, f_{Lvc}) = s(T_f, P_a, f_{Lf}) \text{, entropy conservation} \quad \textbf{(14)}$$

The unknown post-expansion data can now be determined as follows:

a) The post-expansion mass rate $m_f = \rho_f A_f u_f$ is set from Equation **(7)**
b) For a two-phase release T_f equals the boiling temperature and the post-expansion liquid fraction f_{Lf} can be set from Equation **(14)**. Otherwise $f_{Lf} = 0$ (vapour release) or $f_{Lf} = 1$ (liquid release) and the temperature T_f can be set from Equation **(14)**.
c) Set post-expansion density ρ_f from Equation **(10)**
d) Set final enthalpy h_f using Equation **(11)**
e) Set post-expansion speed u_f from Equation **(9)**
f) Set post-expansion jet area: $A_f = m_f/(u_f\rho_f)$.

Final velocity capping (non-default option, not recommended)

ATEX allows the final velocity to be capped, to either a user-specified value or to the sonic velocity of the gas:

- In case of the conservation-of-momentum option, this capped velocity is then used in conjunction with conservation of energy equation to determine the final temperature and liquid fraction[iii]. This presents difficulties, as sonic velocity calculation itself requires temperature. Where the above solution yields u_f >

[iii] CHECK (JS). To check algorithm for capping logic (isentropic and conservation of momentum options) including sonic speed option – testing spreadsheet?

$u_{max}(T_f)$, the equation $u_f = u_{sonic}(T_f)$ replaces the conservation of momentum equation **(8)**. h_f is obtained by iteration when an equilibrium calculation at P_a and h_f yields a sonic velocity equal to that calculated from the conservation of energy equation.

- In case of the isentropic option, the final temperature and liquid fraction are based on the uncapped equations and only the final velocity is modified to the velocity cap.

Selection of expansion models

The continuous discharge models can use either the isentropic or conservation of momentum models. The isentropic model is the original Phast model, while the conservation of momentum model was introduced at a later stage. Phast now provides the users the option to select "conservation of momentum", "conservation of entropy" or the "results closest to the initial conditions":

- If the user chooses a specific model, then ATEX will perform the expansion modelling using only that model, and if that model fails, then ATEX will not produce a valid result.
- If the user chooses "Closest to Initial Conditions", then ATEX will perform the expansion modelling using both models, and will use the results for the model which gives the highest final temperature. If both models give the same final temperature, then ATEX will use the results for the model which gives a final liquid fraction that is closest to the orifice liquid fraction. If one of the models fails, then ATEX will use the results for the other model.

Following the validation described later in this report, it has been decided to apply the following default expansion model selection:

- Conservation of momentum is always applied for those releases where rainout cannot occur, i.e. for the following cases:
  - All CO_2 releases (solid deposition is assumed never to occur)
  - Case of rigorous multi-component modelling (not pseudo-component modelling)
  - Vapour releases with zero liquid fraction following depressurisation to atmospheric pressure
- In all other cases (releases with positive liquid fraction following depressurisation to atmospheric releases, where released material is not CO_2 and where rigorous multi-component modelling is not applied) the option of 'Closest to initial conditions' is always applied; however in case rainout is expected not to occur it is recommended for the user to change this into 'Conservation of momentum' in order to increase the accuracy of the concentration predictions.

Metastable liquid assumption

This metastable liquid assumption is applied by default[iv] for non-flashing and flashing liquid release from an orifice (Phast Leak Scenario). This means that the values of the orifice velocity u_o, the orifice liquid fraction η_{Lo}=1, the orifice temperature T_o, the orifice pressure P_o=P_a and the superheat ΔT_{sh} correspond to the meta-stable liquid assumption. The meta-stable assumption is strictly speaking applied to the vena-contracta state and not the orifice state, i.e, using u_{vc}, η_{vc}=1, P_{vc}= P_a, and superheat ΔT_{sh}. These vena contracta data are input to ATEX, and the post-expansion data are calculated by ATEX from these data. Since $P_{vc} = P_a$, it follows from Equation **(12)** that $u_f = u_{vc}$ in case of conservation of momentum.

3.2 Instantaneous releases

The instantaneous expansion model is used only by the instantaneous discharge models for catastrophic ruptures. It conforms to the isentropic model above, except that the final velocity u_f is calculated from the expansion energy[v,vi,vii]

$$E_{\exp} = h_o - h_f - (P_o - P_a)v_o \tag{15}$$

[iv] From Phast 6.7 (patch 2), the user can change from the metastable liquid assumption by changing a parameter and thereby allowing liquid to flash in the expansion to the orifice as a non-default option.

[v] JUSTIFY. Unsure where this comes from. It appears that for unpressurised releases, expansion energy is negative when tank head is greater than zero (see DISC theory), and consequently release velocity is set to zero (VI3027).

[vi] JUSTIFY (possible). This expansion energy is used for flashing break up calculations, but unlike the continuous models, enthalpy change is between storage and ambient conditions.

[vii] JUSTIFY: There are scenarios in which the calculated expansion energy for releases other than described in v above is negative. This is usually observed when the Pseudo-component thermodynamic assumption is applied to wide boiling mixtures. For this, special logic is applied which is discussed in Appendix B.

by means of the following equation[viii]

$$u_f = \sqrt{2E_{\exp}} \quad \textbf{(16)}$$

The solution can be carried out by the following procedure:

1. Calculate temperature and liquid fraction from isentropic expansion, Equation **(14)**. The procedure used is the same as described for the Isentropic Model described in the previous section.
2. Calculate final enthalpy from **(11)**
3. Calculate final specific volume ν_f from the equation of state **(10)**
4. Calculate expansion energy and final velocity from **(15)** and **(16)**

[viii] JUSTIFY. This implies that the expansion energy is fully converted into kinetic energy. To check this formula against the literature and that one used by the UDM for pressurised instantaneous releases.

4 ANALYTICAL VERIFICATION OF DISC/ATEX MODEL

4.1 Bernoulli equation for incompressible liquids

The metastable liquid DISC/ATEX implementation for an incompressible liquid (Bernoulli equation) and using the conservation of momentum option was verified analytically using the following equations: $C_d = 0.6$, $P_{vc} = P_a$, $D_{vc} = D_oC_d^{0.5}$, $u_f = u_{vc}$, $D_f = D_{vc}$. Here u_{vc} and the flow rate G (kg/s) are given by

$$u_{vc} = \sqrt{\frac{2(P_{st} - P_{a})}{\rho_L}}\ ,\ \ G = \rho_L\, A_{vc}\, u_{vc} = C_d A_o \sqrt{2\rho_L (P_{st} - P_{a})} \tag{17}$$

4.2 Ideal-gas law

4.2.1 Analytical verification for sonic air jets

The DISC/ATEX implementation for an air release was checked analytically against well-known ideal-gas equations. For air the heat capacity ratio $\gamma = C_p/C_v = 1.4$.

First DISC results were verified against well-known ideal-gas analytical equations and close agreement was obtained. The case was considered of a sonic air jet with 25mm orifice and stagnation data 300K and pressures 1.5, 1.1895, 1.896, 2, 3, 11 bara; both the default equation of state and the non-default ideal-gas law were considered.

First the value P_{cr}^{sonic} of the stagnation pressure was verified above which choked flow occurs (vena contracta velocity = speed of sound; vena contracta pressure > ambient pressure), and below which un-choked flow occurs (vena contracta velocity below the speed of sound; vena contracta pressure = ambient pressure),

$$\frac{P_{cr}^{\ sonic}}{P_a} = \left(\frac{2}{1+\gamma}\right)^{-\gamma/(\gamma-1)} \tag{18}$$

Subsequently data at the vena contracta[ix] were verified using the following well-known analytical solutions:

- Vena contracta choke pressure (for $P_{st} \geq P_{cr}^{sonic}$)

$$\frac{P_{vc}}{P_{st}} = \left(\frac{2}{1+\gamma}\right)^{\gamma/(\gamma-1)} \tag{19}$$

- Vena contracta temperature

$$\frac{T_{vc}}{T_{st}} = \left(\frac{P_{vc}}{P_{st}}\right)^{(\gamma-1)/\gamma} = \frac{2}{1+\gamma} \tag{20}$$

- Vena contracta velocity equal to speed of sound (for for $P_{st} \geq P_{cr}^{sonic}$; R = gas constant = 8314 J/K/kmol, M_w = dry air molecular weight = 28.95 kg/kmol):

$$u_{vc} = \sqrt{\frac{\gamma R T_{vc}}{M_w}} = \sqrt{\frac{R T_{st}}{M_w}\left(\frac{2\gamma}{1+\gamma}\right)} \tag{21}$$

[ix] FUTURE. The correct evaluation of the discharge coefficient C_d has not been checked, and ideally this should be attempted.

- Vena contracta vapour density (not output in ATEX, but can be verified in Phast):

$$\rho_{vc} = \frac{P_{vc} M_w}{R T_{vc}} = P_{st} \left(\frac{2}{1+\gamma} \right)^{1/(\gamma-1)} \frac{M_w}{R T_{st}} \quad \textbf{(22)}$$

- Vena contracta area and vena contracta diameter:

$$A_{vc} = C_d \, A_o = \frac{1}{4} \pi D_{vc}^{\ 2} \ , \ D_{vc} = C_d^{\ 0.5} D_o \quad \textbf{(23)}$$

- Choked ideal-gas flow rate

$$G = A_{vc} \rho_{vc} u_{vc} = C_d A_o P_{st} \sqrt{\frac{\gamma M_w}{R T_{st}} \left(\frac{2}{1+\gamma} \right)^{(\gamma+1)/(\gamma-1)}} \quad \textbf{(24)}$$

The following expressions apply for the specific heat C_p (J/K/kg) and the enthalpy change between vena contracta and final conditions:

$$C_p = \frac{\gamma M_w R}{\gamma - 1} \quad , \quad h_f - h_{vc} = C_p (T_f - T_{vc}) \quad \textbf{(25)}$$

Using Equation **(25)** and conservation of energy Equation **(9)**, the following equation can be derived:

$$\frac{T_f}{T_{vc}} = 1 + \frac{u_{vc}^{\ 2}}{2 C_p \, T_{vc}} \left[1 - \left(\frac{u_f}{u_{vc}} \right)^2 \right] = 1 + \frac{\gamma - 1}{2} \left[1 - \left(\frac{u_f}{u_{vc}} \right)^2 \right] \quad \textbf{(26)}$$

Subsequently the DISC/ATEX final data have been verified as follows:

- (case of conservation of momentum option)
  - Set final post-expansion velocity u_f for case of choked flow by using Equations **(19)**, **(21)**, **(22)** into conservation of momentum Equation **(12)**:

$$u_f = u_{vc} + \frac{P_{vc} - P_a}{\rho_{vc} u_{vc}} = u_{vc} \left\{ 1 + \frac{1}{\gamma} \left[1 - \frac{P_a}{P_{st}} \left(\frac{2}{1+\gamma} \right)^{-\gamma/(\gamma-1)} \right] \right\}, \text{ with } u_{vc} = \sqrt{\frac{R T_{st}}{M_w} \left(\frac{2\gamma}{1+\gamma} \right)} \quad \textbf{(27)}$$

    Note that the factor between brackets, [….], in the above equation equals 0 in case $P_{st} = P_{cr}^{sonic}$ and therefore at this value (as should be the case) $u_f = u_{vc}$.

  - Set final temperature T_f from conservation of energy Equation **(26)**
- (case of conservation of entropy option)
  - Set final temperature T_f from ideal-gas conservation-of-entropy Equation

$$\frac{T_f}{T_{vc}} = \left(\frac{P_a}{P_{vc}} \right)^{(\gamma-1)/\gamma} \quad \textbf{(28)}$$

  - Set final post-expansion velocity u_f from Equation **(26)**

$$u_f = u_{vc}\sqrt{1 + 2\frac{1 - T_f/T_{vc}}{\gamma - 1}} \quad \textbf{(29)}$$

- Set final vapour density from ideal-gas equation of state:

$$\rho_f = \frac{P_a M_w}{RT_f} \quad \textbf{(30)}$$

- Final post-expansion area A_f and diameter D_f:

$$A_f = \frac{G}{\rho_f u_f}, \quad D_f = \sqrt{\frac{4A_f}{\pi}} \quad \textbf{(31)}$$

By using Equations **(24)**, **(30)**, **(29)** into the above Equation **(31)** it follows for the case of conservation of momentum that:

$$\left(\frac{D_f}{D_o}\right)^2 = \frac{A_f}{A_o} = \frac{G}{A_o \rho_f u_f} = \frac{C_d \frac{P_{st}}{P_a}\frac{T_f}{T_{st}}\left(\frac{2}{1+\gamma}\right)^{1/(\gamma-1)}}{1 + \frac{1}{\gamma}\left[1 - \frac{P_a}{P_{st}}\left(\frac{2}{1+\gamma}\right)^{-\gamma/(\gamma-1)}\right]} \quad \textbf{(32)}$$

For $P_{st}/P_a >> P_{cr}^{sonic}/P_a$, the above equation approximates to

$$\left(\frac{D_f}{D_o}\right)^2 = \frac{C_d \frac{P_{st}}{P_a}\frac{T_f}{T_{st}}\left(\frac{2}{1+\gamma}\right)^{1/(\gamma-1)}}{1 + \frac{1}{\gamma}} \quad \textbf{(33)}$$

From the above equations it follows that the pressure, velocity, temperature, density are all independent of the discharge coefficient C_d at both vena contracta and final conditions; the diameter is proportional to $C_d^{0.5}$ at both vena contracta and final conditions.

4.2.2 Verification against Yüceil and Ötügen

Yüceil and Ötügen (2002)[/22/] also derive the above equation **(26)** for the final temperature and their model is fully in line with the ATEX conservation of momentum model for the case of a sonic jet (Mach number M_{vc} = 1). They also present analytical formulas for the final velocity, final density and the final diameter, again in line with our model.

In addition they also plot the diameter increase D_f/D_{vc} and the velocity increase u_f/u_{vc} during the atmospheric expansion as function of P_{vc}/P_a. Figure 4-1 includes ATEX predictions for these data using both the default SRK equation of state (EOS) and the ideal-gas EOS. It was confirmed that the ideal-gas EOS ATEX predictions were virtually identical to those presented by Figures 2 and 3 in the paper by Yüceil and Ötügen.

DISC simulations were carried out without application of velocity cap. Figure 4-2 plots DISC predictions of vena contracta pressure as function of the stagnation pressure. It is seen that real-gas law predicts higher pressure drops than the ideal-gas law. Figure 4-3 plots DISC predictions of vena contract and final data as a function of the stagnation pressure for both velocity and temperature. It is seen that the real-gas EOS produces lower temperatures and lower final velocities than the ideal-gas EOS. The figure also shows that the isentropic option results in significantly higher final velocities and lower final temperatures than the conservation-of-momentum option. Thus Phast selects as default the conservation of momentum option since this leads to minimum thermodynamic change.

Yüceil and Ötügen (2002) carried out dry air experiments (Mach number M_{vc} = 1) with a convergent nozzle (D_{vc} = 4.45mm). The settling chamber temperature varied between 293K and 283K corresponding with values of P_{vc}/P_a = 1, 2.5, 7.5 and 20.3. Immediately downstream of the orifice one has supersonic flow and the location of the Mach disk varied between x/D_{vc}=1 (P_{vc}/P_a = 2.5) and 3.8 (P_{vc}/P_a = 20.3). Subsonic compressible relations of isentropic flow were used to obtain the velocity from the total temperature measurements. Thus explicitly all flow rates were determined including Mach number, velocity, density and temperature.

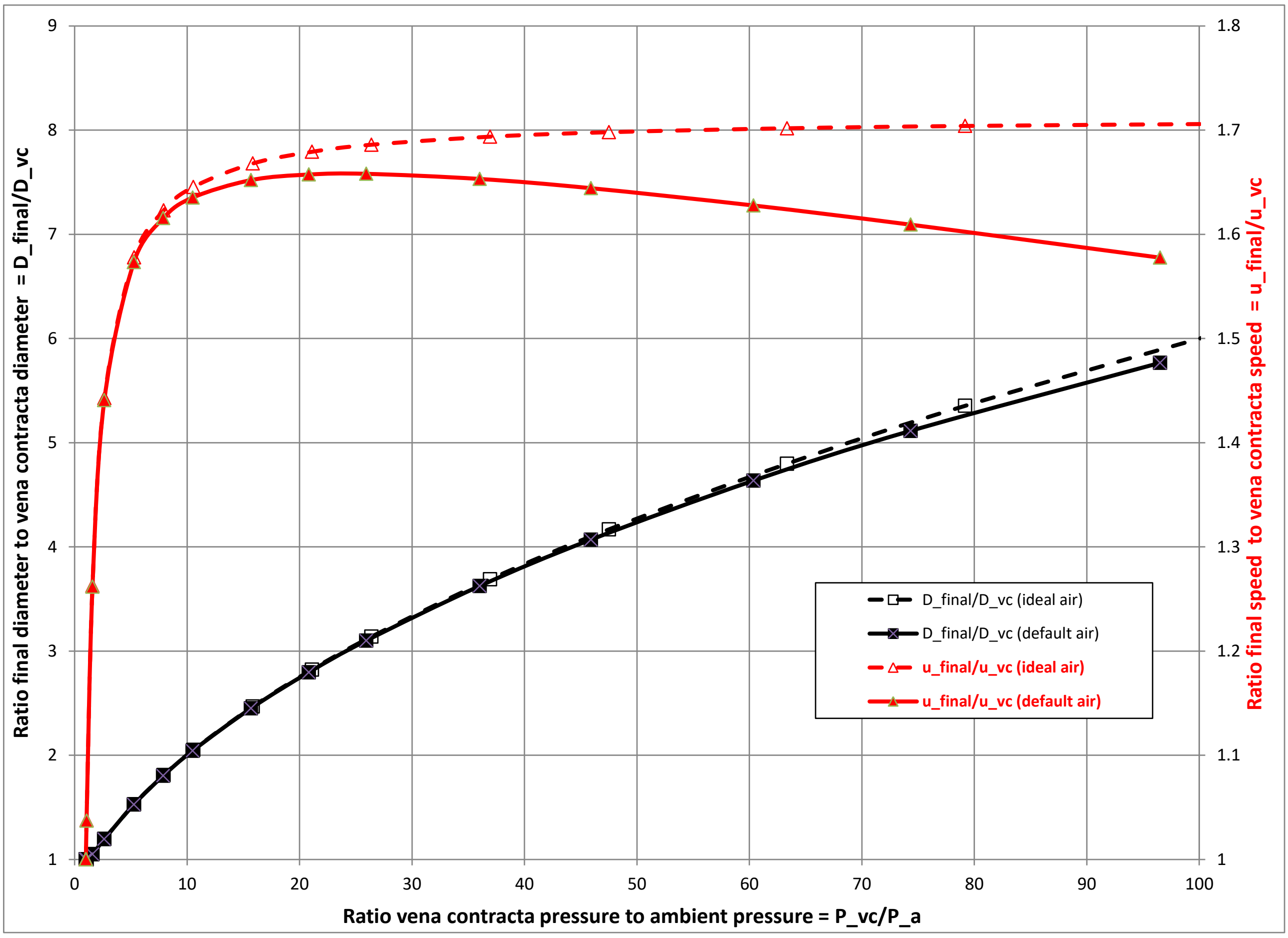

Figure 4-1 Air jets - variation of D_f/D_{vc} and u_f/u_{vc} with P_{vc}/P_a

Diameter data are given by black lines and velocity data by red lines; default ATEX predictions are given by solid lines and ideal-gas predictions by dashed lines.

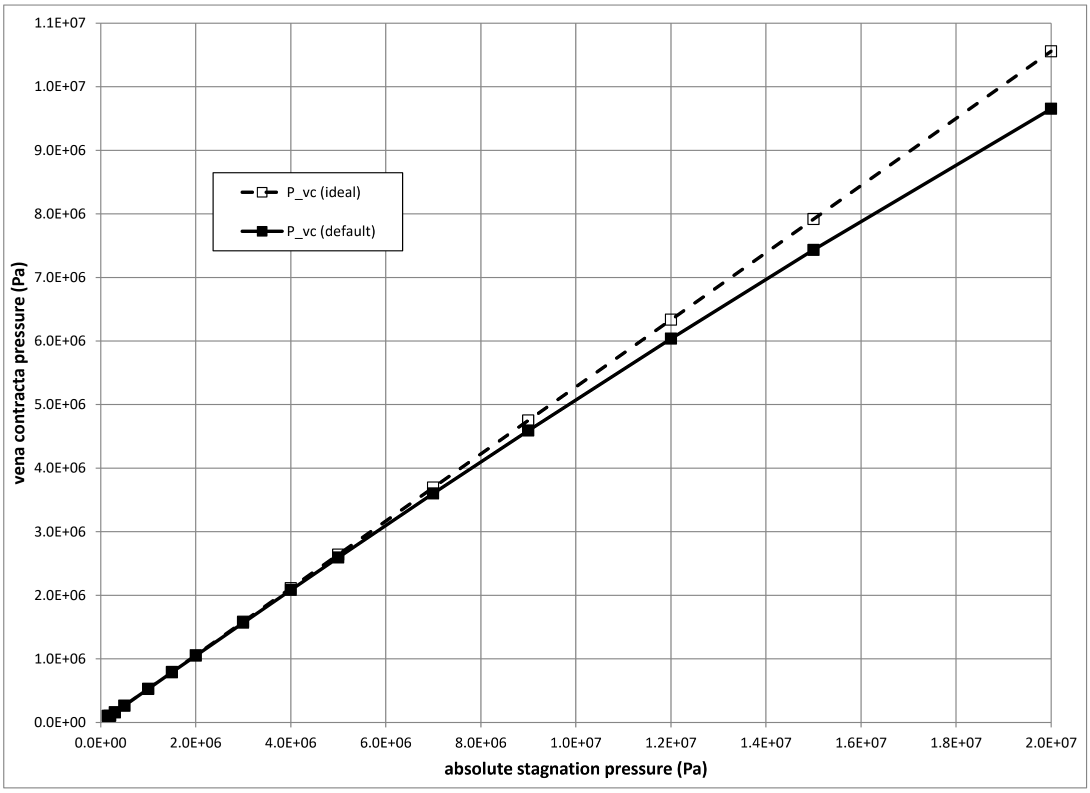

Figure 4-2 Air jets - vena-contracta versus stagnation pressure
Default EOS predictions are given by solid line and ideal-gas EOS predictions by dashed line.

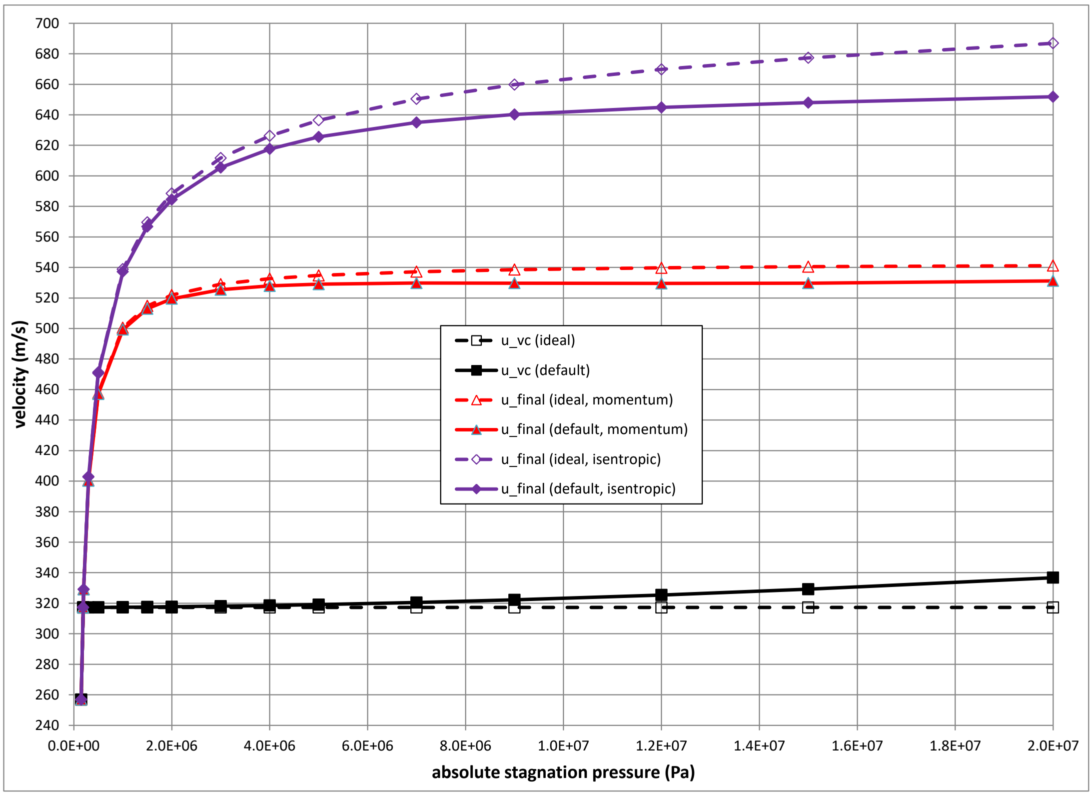

(b) velocity

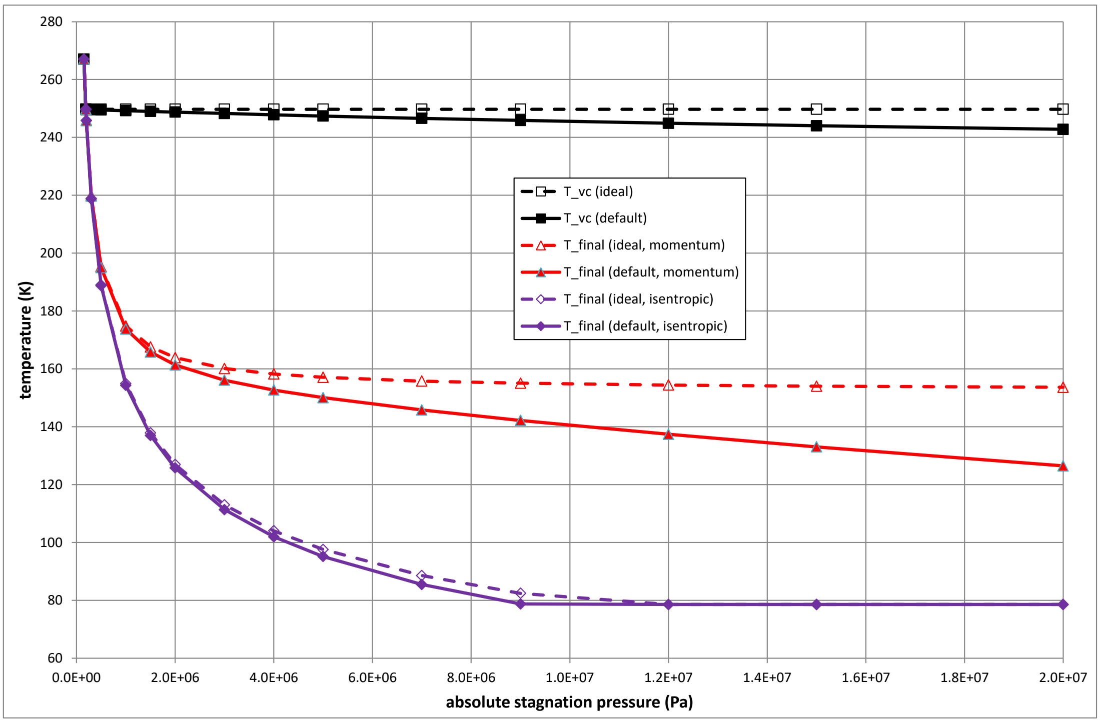

(c) temperature

Figure 4-3 Air jets - vena-contracta/final velocities/temperatures versus stagnation pressure
Vena contracta data are given by black lines, final data based on conservation of momentum by red lines, and final data based on conservation of entropy by purple lines; default EOS predictions are given by solid lines and ideal-gas EOS predictions by dashed lines.

5 LITERATURE REVIEW

5.1 Previous literature reviews

5.1.1 Phase I droplet modelling JIP (Witlox and Bowen)

Following a detailed assessment, revision and improvement of the Unified Dispersion Model UDM[/4/,/5/] amongst others carried out as part of the EU Project SMEDIS, further possible future improvements were identified for the pre-UDM atmospheric-expansion calculations in ATEX.

The ATEX expansion model is based on a set of assumptions and equations for the expansion zone (e.g. no air entrainment; conservation of mass, momentum or entropy, and energy, etc.). There is some uncertainty in the literature regarding the precise assumptions to be adopted for various aspects of the flashing (expansion) calculations. As a result a literature study (sponsored by HSE, Exxon-Mobil and ICI Eutech; Phase I of droplet modelling JIP) was carried out by Witlox and Bowen[/1/] to investigate these issues.

As far as ATEX is concerned, these issues primarily involve the assumption of isentropic versus isenthalpic versus constant-energy expansion; see e.g. Van den Akker et al.[/6/], Britter[/7/,/8/] , and the TNO yellow book[/9/].

5.1.2 EU Project FLADIS and USA DTRA project (Britter et al.; added ATEX comparison)

As part of EU funded work relating to the flashing ammonia releases (FLADIS experiments), Britter[/8/] compared a range of atmospheric-expansion formulations from the literature considering un-choked ideal-gas releases, choked gas releases (sonic jets), and flashing jet releases. He refers to the choked gas jet formulation by Birch (see Section 5.3.1), a formulation by Spicer (adiabatic irreversible expansion from exit plane to atmospheric pressure) and HGSYSTEM (assuming Bernoulli equation; assumptions in line with ATEX model; see Section **Error! Reference source not found.**4.1).

The recommendation by Britter et al.[/10/] (Sections 5.1, 5.2) and Britter[/7/] is to use always the constant-momentum expansion model as given by conservation equations **(7)**, **(8)** and **(9)**. Imposing the energy equation **(9)** is exact, while Britter indicates that the alternative assumptions of conservation of enthalpy [ignoring kinetic velocity term $½u^2$ in Equation **(9)**; applicable to Joule-Thomson expansion also known as Joule-Kelvin or Joule-Thomson effect] or entropy are both approximate. Here the isentropic approximation may be more accurate than the isenthalpic approximation.

Britter illustrates the above by a number of examples. In this section his results are compared with the ATEX results, where it is presumed that the ATEX velocity cap of 500 m/s has not been applied:

- Britter first considers the case of a sonic release of air, where the air is modelled as an ideal gas. Orifice data corresponded to p_o=1.1 or 2 or 10 bara, T_o=300K, speed of sound $u_o = (\gamma RT_o)^{1/2}$=347.6m/s. The orifice area A_o is not relevant to calculations and $h=C_pT$ for an ideal gas. Selected ambient pressure was 1bara. Both results from Britter and ATEX calculations are given in Table 5-1. Note that the Britter ‘isentropic’ formulation (conservation of mass, momentum and entropy) differs from the ATEX ‘isentropic’ formulation (conservation of mass, entropy and energy). The table is seen to give very close consistent predictions between the Britter’s analytical calculations and ATEX for the ‘conservation of energy’ case (‘conservation of momentum’ for ATEX) for both final velocity and temperature predictions as should be the case. Also close predictions are obtained for the temperature drop for the isentropic case. However significantly higher velocities are predicted for the isentropic case than for the conservation-of-momentum case.

- Secondly Britter considered the example of 100% saturated liquid propane at 10bara and 15C at the orifice state, with an orifice velocity of 50-100m/s and expansion to an atmospheric pressure of 1 bar. For all air cases in Table 5-1 it is seen that the minimum thermodynamic change (change in temperature) is applicable for the conservation of momentum case, and therefore this option corresponds to the default ATEX prediction. For the propane case the thermodynamic change is identical, and ATEX selects the isentropic case since the post-expansion liquid fraction is closer to the exit liquid fraction of 1 (metastable assumption). Note that the isentropic expansion method is consistent with the assumption for CCPS droplet size calculations.

Following the above, Britter concluded that for single-phase sonic gas releases velocity changes will be significant and if an exact solution (conservation of energy) is not used, an isentropic approximation is better than an isenthalpic approximation. For flashing jets which are all liquid at the exit plane the large density of the fluid at the exit plane reduces the velocity change and makes an isenthalpic approximation more acceptable. For flashing jets which are two-phase at the exit plane, the development will be between the all-gas and all-liquid scenarios. Either the exact result should be used or arguments presented as to why an isenthalpic or isentropic process is an acceptable approximation.

Expansion method	Air 1.1bar		Air 2bar		Air 10bar		Propane 10 bar	
	Britter	ATEX	Britter	ATEX	Britter	ATEX	Britter	ATEX
	Temperature rise T_f-T_o (K)							
Isenthalpic	0	n/a	0	n/a	0	n/a		n/a
Conservation of energy (Britter) or momentum (ATEX)	-8.09	-8.08	-50.87	-50.81	-102.7	-104.0		-57.4
Isentropic	-8.06	-8.09	-53.9	-54.17	-144.6	-145.7		-57.4
	Final velocity (m/s)							
Conservation of energy (Britter) or momentum (ATEX)	370.16	370.13	471.76	471.51	571.09	570.49		85.6
Isentropic	-	370.17	-	478.61	-	639.82		191.2
	Final liquid mass fraction (-)							
Isenthalpic	-	-	-	-	-	-	0.67	n/a
Conservation of energy (Britter) or momentum (ATEX)	-	-	-	-	-	-	0.67	0.68
Isentropic	-	-	-	-	-	-	0.71	0.71

Table 5-1 Atmospheric expansion for air (ideal gas) and saturated propane liquid

Britter always assumes conservation of mass and momentum, and imposes conservation of enthalpy, entropy or energy.
ATEX current always assumes conservation of mass and energy, and imposes either conservation of momentum or entropy

5.2 Liquid releases (Spicer and Paris; spherical final expansion surface)

Spicer et al.[13/,/14] presume the final surface to be part of a sphere with radius R_f (enclosing an angle of 2Φ, with final velocity u_f normal to final surface); see Figure 2-2b2. The idea of Spicer is that all points are equidistance from a single point (the sphere centre), and this assumption is quoted to be consistent of having no air entrainment upstream of 'f'. Spicer recommends to apply his model only to non-flashing and flashing liquid releases where the hole size is not too large. However at present he is not yet able to provide an indication of the upper limit of the hole size.

Spicer and Paris in fact consider expansion from pipe exit (o) to final 'spherical' conditions (f); see Figure 2-2b2. However below (in consistency with ATEX logic, and to simplify equations) expansion from vena contracta to final spherical conditions is considered (i.e. different control volume as indicated in Figure 2-2b1). Thus equations **(4)**, **(5)** and **(6)** reduce to:

$$\iint_{A_o+A_f} \rho(\underline{V}\bullet\underline{n})dS = -\rho_{vc}u_{vc}A_{vc} + \int_0^{\Phi}\rho_f u_f(2\pi R_f\sin\varphi)R_f d\varphi \quad \text{, mass}$$
$$= -\rho_{vc}u_{vc}A_{vc} + 2\pi R_f^{\,2}(1-\cos\varphi)\rho_f u_f = 0 \qquad \textbf{(34)}$$

$$\iint_S \{\rho V_{axial}(\underline{V}\bullet\underline{n}) + p\,n_{axial}\}dS = -\rho_{vc}u_{vc}^{\,2}A_{vc} + \int_0^{\Phi}\rho_f u_f^{\,2}\cos\phi(2\pi R_f\sin\varphi)R_f d\varphi + (P_f - P_{vc})A_{vc} \quad \text{, momentum}$$
$$= -\rho_{vc}u_{vc}^{\,2}A_{vc} + \pi R_f^{\,2}(1-\cos^2\varphi)\rho_f u_f^{\,2} + (P_f - P_{vc})A_{vc} = 0 \qquad \textbf{(35)}$$

$$\iint_S \rho\left(\frac{1}{2}V^2 + h\right)(\underline{V}\bullet\underline{n})dS = -\rho_{vc}u_{vc}A_{vc}(\frac{1}{2}u_{vc}^{\,2} + h_{vc}) + \int_0^{\Phi}\rho_f u_f(\frac{1}{2}u_f^{\,2} + h_f)(2\pi R_f\sin\varphi)R_f d\varphi \quad \text{, energy}$$
$$= -\rho_{vc}u_{vc}A_{vc}(\frac{1}{2}u_{vc}^{\,2} + h_{vc}) + 2\pi R_f^{\,2}(1-\cos\varphi)\,\rho_f u_f(\frac{1}{2}u_f^{\,2} + h_f) = 0 \qquad \textbf{(36)}$$

Using the mass equation **(34)** into momentum and energy equations **(35)** and **(36)**, the above equations can be simplified to

$$2\pi R_f^{\,2}(1-\cos\Phi)\rho_f u_f = \rho_{vc}u_{vc}A_{vc} = G \text{ , mass} \qquad \textbf{(37)}$$

$$\frac{1+\cos\Phi}{2}Gu_f = Gu_{vc} + (P_{vc} - P_f)A_{vc} \text{, momentum} \qquad \textbf{(38)}$$

$$\frac{1}{2}u_f^{\,2} + h_f = \frac{1}{2}u_{vc}^{\,2} + h_{vc} \text{ , energy} \qquad \textbf{(39)}$$

The overall algorithm is identical as indicated before (Chapter 1) except for the added factor *½(1+cosΦ)* in the momentum equation. Note that the post-expansion jet area $A_f = 2\pi R_f^2(1-\cos\Phi)$. So after A_f has been set, R_f can be determined.

The angle *Φ* is quoted by Spicer and Paris[13] to lie between 0 and 50 degrees based on photographic evidence from CCPS water tests, and therefore the factor ½(1+cosΦ) in Equation **(38)** varies between 1 to 0.82. However no equation is provided for this angle (e.g as function of material properties, storage pressure/temperature, etc.). In absence of this value Spicer suggests to use the conservative assumption *Φ*=0 which results in a smaller value of u_f and hence larger concentrations (less jet entrainment); *Φ*=0 reverts the above Spicer and Paris formulation to the ATEX equations **(7)**,**(8)**, **(9)** recommended by Britter et al.[7]

A value of *Φ*>0 will produce larger velocities and would therefore produce values between those currently given in ATEX for conservation of momentum and conservation of entropy. Also note that the starting conditions for the Phast dispersion model UDM presume a planar surface and therefore this is inconsistent with a value of *Φ*>0.

5.3 Gas releases

5.3.1 British Gas natural-gas, ethylene and air experiments (Birch et al.)

For high pressure gas jets (pressures between 2 and 70-75bar), British Gas carried out an experimental investigation of both concentration decay using gas chromatography (natural-gas and ethylene jets; Birch et al., 1984)[/17/] and velocity decay using hot film anemometry (air jets; Birch et al., 1987) [/21/]. The first paper[/17/] did erroneously not conserve momentum.

The second paper[/21/] provided an improved 'pseudo-source' definition based on conservation of both mass and momentum through control volume in line with the recommendations given earlier in this report. This model is also used in later work by British Gas (currently DNV, Loughborough, previously Advantica and GL Noble Denton), e.g. by Cleaver[/24/] as part of source modelling developed for the COOLTRANS project (involving crater modelling for buried CO_2 pipelines).

The results quoted by Birch for the 'orifice' data are fully in line with the ideal-gas analytical equations **(19)**, **(20)**, **(21)**, **(22)**, **(23)**, **(24)** of 'vena contracta' data presented in Section 4.2 for the case of C_d=1 (absence of vena contracta). However in case of C_d<1 his formulation is inconsistent with the ATEX formulation. Instead of Equation **(27)** for the final velocity (which is independent of the discharge coefficient), Birch imposes the following equation dependent on the discharge coefficient:

$$u_f = C_d u_o + \frac{P_o - P_a}{\rho_o u_o} = u_o \left\{ C_d + \frac{1}{\gamma C_d}\left[1 - \frac{P_a}{P_{st}}\left(\frac{2}{1+\gamma}\right)^{-\gamma/(\gamma-1)}\right]\right\}, \quad with\ u_o = \sqrt{\frac{RT_{st}}{M_w}\left(\frac{2\gamma}{1+\gamma}\right)} \tag{40}$$

The above also seems to imply that Birch considers a control volume for expansion from orifice (not vena contracta) to final conditions, with the speed of sound presumed at orifice and not vena contracta conditions.

Furthermore Birch does NOT impose the conservation of energy equation **(35)** for expansion between vena contracta and final conditions, but instead he quotes the final temperature to be close to the initial stagnation temperature, i.e. $T_f \approx T_{st}$. Thus this is inconsistent with the ATEX formulation, the formulation by Yüceil and Ötügen (2002)[/22/], and the recommendations from Britter et al[/10/]. Thus he derived the following modified equations for final expanded diameter, which differs from Equation **(32)**:

$$\left(\frac{D_f}{D_o}\right)^2 = C_d \frac{P_{st}}{P_a}\frac{u_o}{u_f}\left(\frac{2}{1+\gamma}\right)^{1/(\gamma-1)} = \frac{\frac{P_{st}}{P_a}\left(\frac{2}{1+\gamma}\right)^{1/(\gamma-1)}}{1 + \frac{1}{\gamma C_d^2}\left[1 - \frac{P_a}{P_{st}}\left(\frac{2}{1+\gamma}\right)^{-\gamma/(\gamma-1)}\right]} \tag{41}$$

For $P_{st}/P_a >> P_{cr}^{sonic}/P_a$ [see Equation **(18)** for definition of critical pressure P_{cr}^{sonic}] the term between square brackets [….] in the above equation approximates to unity, and the above equation becomes (again differing from the equivalent equation **(33)**; with same results only if both C_d = 1 and T_f=T_{st} assumed)[x]

$$\left(\frac{D_f}{D_o}\right)^2 = \frac{\frac{P_{st}}{P_a}\left(\frac{2}{1+\gamma}\right)^{1/(\gamma-1)}}{1 + \frac{1}{\gamma C_d^2}} \tag{42}$$

5.3.2 INERIS hydrogen and methane experiments (Ruffin et al., INERIS)

Ruffin et al. (1996)[/12/] carried out an experimental investigation of concentrations of elevated unsteady horizontal jets of methane and hydrogen (elevation height 5 m), corresponding to choked releases from a vessel (storage pressure 40 bar, storage temperature 288 K, volume 5 m^3) with orifice diameters of 25, 50, 75, 100 mm for hydrogen, and 25, 50, 75, 100, 150 mm for methane; see Figure 5-1. This work was carried out at INERIS as part of the EU project EMERGE (Extended

[x] Equation (9) in Birch et al. (1987) appears to be an incorrect approximation of Equation (7) in Birch et al., and this error in the approximation has been corrected in Equation **(42)**.

Modelling and Experimental Research into Gas Explosions). As shown in the figure, concentration sensors were placed in the subsonic part of the jet to measure the H_2 concentration in the subsonic part of the jet (Ma < 0.3).

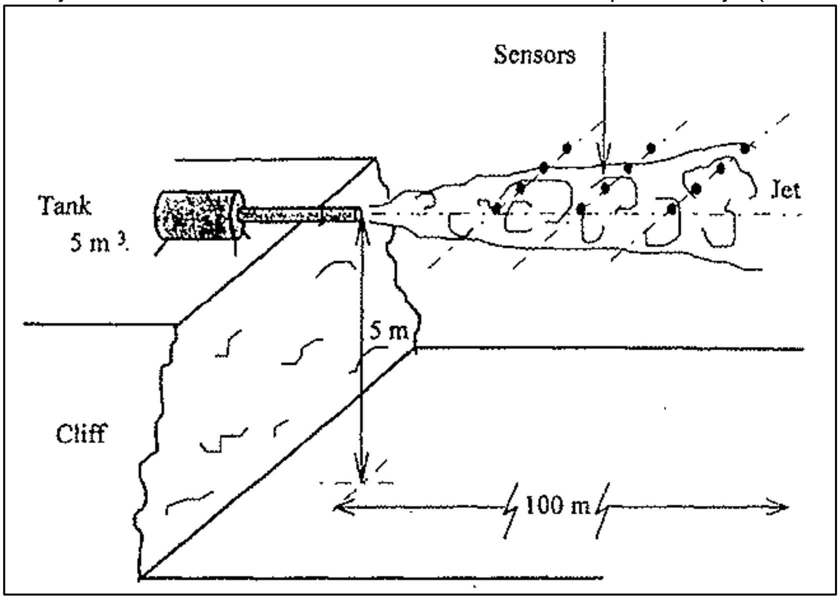

Figure 5-1 INERIS experimental rig – methane and hydrogen choked jet release

Ruffin et al. refer to the out-of-date paper by Birch et al. (1984)[/17/] which does NOT satisfy conservation of momentum and also remark that conservation of momentum should be used.

The issues of the current experiments are as follows:

- these experiments involved time-varying releases, where the stagnation pressure was not kept constant
- the mass flow rate was not measured, but derived from the measured time-varying stagnation pressure P_{st} presuming ideal-gas isentropic expansion between stagnation and orifice conditions

5.3.3 HSL hydrogen experiments (Roberts et al.; Phast, KFX & HGSYSTEM validation)

Commissioned by Shell Global solutions, HSL carried out experimental work relating to horizontal pressurised hydrogen orifice releases at 1.5m above the ground. Roberts et al. (2006)[/20/] discusses results of a set of 23 experiments for which the flow rate was unsatisfactorily not measured. For these experiments the hole diameter equals 3, 4, 6 or 12 mm, the temperature varies between 13 and 20C and the pressure varies between 10 barg and 129 barg. The paper compares predicted concentrations against the HGSYSTEM model AEROPLUME. The paper states that good results were obtained for 8 experiments which pointed close towards the wind direction (limited crosswind effects; Fig.7a in the paper; runs 6,7,8,9; 3mm or 4mm orifice size, temperature around 14C and pressure 92-118 barg). Presumably the conservation of momentum assumption is applied which the author believes is the option applied in HGSYSTEM, but this is not explicitly mentioned in the paper. The applied version of HGSYSTEM is an internal Shell version of the program (different from HGSYSTEM 3.0).

DNV Energy (Skottene and Holm, 2008) [/19/] carried out validation using both Phast and KFX against the hydrogen HSL experiments. They however also refer to an additional set of experiments with smaller orifice diameters for which the flow rate was measured, and for which the results are not reported in the paper by Roberts et al. (2006)[/20/]. It was also noted that distances to H_2 LEL clouds compared well between Phast and KFX. For runs 7, 9, 14 also comparisons are provided against Phast, and close results were obtained with the experimental data.

5.3.4 FLACS validation for hydrogen jets (Middha et al., Gexcon)

Middha et al.[/18/] validated the CFD software package FLACS for high-pressure hydrogen experiments by INERIS (experiments by Chaineaux, 1999; 0.5m nozzle through a tank upto 200 bar pressures), the HSL experiments referred to in Section 5.3.3 (Roberts et al. [/20/]). They point out that the pseudo source approach has limitations for the case of very small nozzles. However this may also be caused by issues of crosswind effects which would be less relevant in the near field for larger nozzles.

5.3.5 Phast 6.2 application to hydrogen and methane jets (Air Liquide)

Jallais and Morainville (2007)[/11/] compared predictions of Phast for sonic releases of hydrogen and methane. The ideal-gas sonic release velocity is quoted to be $(\gamma RT/M_w)^{1/2}$, with γ the isentropic coefficient, R the gas constant (8,314 kJ/kmol/K), T the temperature (K) and M_w the molecular weight (kg/kmole). At 288 K, the sonic velocities are quoted to be 1290 m/s and 450 m/s for hydrogen and methane, respectively.

Prior to Phast 6.53 the orifice velocity was erroneously capped. Therefore the release rate was erroneously reduced when the cap was applied as illustrated by Jallais and Morain Ville. However from Phast 6.53 this cap is no longer applied to the orifice velocity and therefore this is no longer more an issue. This was reconfirmed by additional Phast runs.

5.4 Multi-component liquid releases: comparison Phast MC and Chemcad (DNV, Paris)

Gouzy-Hugelmeier (2013)[/23/] carried out a comparison between Phast MC and Chemcad for a hydrocarbon mixture, where she considered two scenarios (16” line rupture with pipe length of 10 m and leak of 65 mm; metastable liquid assumption):

- Stagnation temperature (30C), vary stagnation pressure between 2 bar and 250 bar
- Stagnation pressure 15 bar, vary stagnation temperature between -150C and 110C

Results of Chemcad (based on isenthalpic flash) were compared against Phast for final temperature. Here the isentropic option of Phast was shown to result in too much cooling.

6 DISC/ATEX/UDM MODEL VALIDATION

This chapter discusses the validation of the Phast discharge model DISC (including ATEX model) and the Phast dispersion model UDM. A range of atmospheric expansion options has been applied, and the effect of these options on the accuracy of the discharge predictions (flow rate) and dispersion predictions has been investigated.

Section 6.1 discusses discharge and dispersion results for two-phase flashing jets, while Section 6.2 and Section 6.3 discuss results for gas jets.

6.1 Flashing 2-phase jets (ammonia, propane, HF and CO_2)

This section details the results of discharge and dispersion calculations associated with two-phase jets, i.e. the FLADIS ammonia, Desert Tortoise ammonia, EEC propane, Goldfish HF experiments, and CO2PIPETRANS CO_2 experiments (BP and Shell tests).

Input data for these calculations as well as additional input required for the dispersion calculations were obtained from the SMEDIS project for FLADIS, Desert Tortoise and EEC. For the Goldfish HF experiments, input data were obtained from Chapter 9 of the HGSYSTEM 1.0 Technical Reference Manual[/26/]. Note that these input data for Goldfish differ from those used in the MDA by Hanna et al.[/27/], while the SMEDIS Desert Tortoise data are in line with the values in the MDA.

The data provided for the FLADIS experiments are in line with those presented by Nielsen and Ott[/28/]. The data for the CO_2 simulation have been obtained from the CO2PIPETRANS JIP.

See the UDM validation manual[/16/] for further details on the input data.

6.1.1 Discharge

The discharge calculations have been carried out using the leak scenario of the Phast discharge model DISC (version 7.1; see Chapter 1 for further details):

- The DISC model has two methods for modelling the expansion from stagnation conditions to orifice conditions, i.e.
  - the metastable liquid assumption: non-equilibrium at the orifice, liquid remains liquid at the orifice, orifice pressure = ambient pressure
  - flashing liquid assumption: equilibrium at the orifice, flashing may occur upstream of the orifice

- The DISC model has also the following three options for performing the expansion from the choke point in the orifice to the atmospheric pressure, namely:
  - Isentropic
  - Conservation of momentum
  - (default option) One of the two options above, with the option selected which results in minimum thermodynamic change between orifice conditions and final conditions. For all current sets of experiments, it was found that this default option corresponded with the isentropic option. This is with the exception of three hot CO_2 release (BP tests 8, 8R and Shell test 14).

Table 6-1 summarises the DISC input data and results for the case of the default assumption of metastable liquid assumption in conjunction with conservation of momentum for the FLADIS, EEC, DT and GF experiments.

Table 6-2 summarises the key experimental data required as DISC and/or UDM input for the BP and Shell CO_2 tests; see the UDM validation manual for further details.

<u>Flow rates and post-expansion data (FLADIS, EEC, Desert Tortoise and Goldfish)</u>

Table 6-3 first compares observed flow rates (reported by SMEDIS for the FLADIS, EEC experiments and by Hanna for the DT, GF experiments) against DISC predictions for both cases of 'metastable liquid' and 'flashing':

- It is concluded that the Goldfish predictions are virtually identical for both cases with very close agreement with the data.

- Predictions for EEC and DT presuming ‘flashing’ are seen to provide considerably improved predictions compared to the ‘metastable liquid’ assumption. On the other hand, FLADIS results are best presuming ‘metastable liquid’, with significant under-prediction presuming ‘flashing’. Overall the ‘metastable liquid’ is seen to provide conservative results, with an over-prediction of the observed flow rates.

Note there is an inherent inaccuracy in the measured flow rates with e.g. an accuracy of 18% quoted by Nielsen and Ott[/28/] for the case of the FLADIS experiments.

The results given in Table 6-3 are obtained by quick DISC simulations, and more accurate estimate of the input as well more accurate method of modelling may be able to be obtained by means of a more thorough analysis of the experimental data sets. However this was not part of scope of the current work.

Table 6-3 secondly compares predictions of post-expansion data (liquid fraction, velocity and SMD droplet size) using the range of model assumptions as described above. It also compares these predictions against values of liquid fraction and velocity provided as part of the SMEDIS project. The following can be stated regarding this table:

- Liquid fraction
    - The data provided by SMEDIS are seen to be in close agreement with the DISC predictions
- Velocity
    - DISC predictions of final post-expansion velocity presuming metastable liquid assumption are lower than presuming ‘flashing’ upstream of the orifice. DISC predictions of velocities presuming conservation of entropy result in significant larger velocities than presuming conservation of momentum.
    - For the case of the FLADIS experiments, SMEDIS values for velocity are closest to the DISC predictions presuming metastable liquid and conservation of momentum. On the other hand, for the EEC and Desert Tortoise experiments, the SMEDIS values are closest to the DISC predictions presuming flashing and conservation of momentum. Using the isentropic approach, DISC predicts post flash velocities which are much higher than those provided as part of the SMEDIS project.
- Droplet size (SMD – Sauter Mean Diameter)
    - The default modified CCPS correlation was applied to set the droplet size (SMD). For these cases (superheated releases), it should use the CCPS flashing correlation, but for the conservation of momentum method in conjunction with metastable liquid assumption in fact it uses the mechanical correlation[xi] and thus SMD values may be less accurate. However in case rainout would not occur, the precise value of the SMD is not expected to significantly affect the dispersion calculations.

Flow rates and post-expansion data (BP and Shell CO_2)

Table 6-4 compares first compares observer flow rates for the BP and Shell CO_2 tests:

- Given observed data for flow rate correspond to averaged values over first 20 s for BP tests and initial rate for Shell tests; DISC values correspond to initial rate; see UDM validation manual for TVDI averaged values for first 20s for BP tests.
- Discharge calculations for the BP tests presume default density (SRK EOS if vapour, ideal saturated if liquid) while simulations for Shell tests presume Peng-Robinson EOS. For the Shell tests more accurate results were obtained using PR EOS. see UDM validation document for furhter detailed discussion.
- Flashing (non-default Phast) or non-flashing (default Phast; metastable liquid assumption)
    - Using Peng-Robinson density (Shell tests), this was seen to affect results very little. Using the saturated density (BP tests), the default non-flashing option provides conservative results while the non-default flashing assumption produces significantly more accurate results.
    - The application of the metastable assumption to the hot vapour tests may not be appropriate; it leads to a fatal error for Shell tests 16.

Table 6-4 secondly compares predictions of post-expansion data (liquid fraction, velocity and SMD droplet size) for the CO_2 tests using the range of model assumptions:

- Close results are seen between all post-expansion data between the metastable liquid and flashing assumptions
- Compared to the conservation-of-momentum option, the isentropic option results in considerably larger velocities, larger liquid fractions and significantly smaller SMD.

[xi] Due to calculated partial expansion energy being < 0 (warning ATEX 1010)

Disc_2_Phase_Cons_Momentum.xls: Two-phase pressurised releases (FLADIS, EEC, Desert Tortoise) - Conservation of Momentum																
Input Description	**Units**	**FLADIS9**	**FLADIS16**	**FLADIS24**	**EEC170**	**EEC360**	**EEC550**	**EEC560**	**DT1**	**DT2**	**DT3**	**DT4**	**GF1**	**GF2**	**GF3**	**Comments** [Refs. SMEDIS emails, MDA data in Hanna (1991), Table 3.1 TNER.90.015 for GF, FLADIS report http://w w w .risoe.dk/rispubl/VEA/veapdf/ris-r-898.pdf - Table 2]
Material																
Stream name	-	Ammonia	Ammonia	Ammonia	Propane	Propane	Propane	Propane	Ammonia	Ammonia	Ammonia	Ammonia	Hydrogen F	Hydrogen F	Hydrogen Fluoride	
Storage state																
Specification flag (0 = P&T&LF, 1 = P&T, 2 = Tbub, 3 = Pbub, 4 = Tdew, 5 = Pdew, 6 = P&LF, 7 = T&LF)	-	6	1	6	1	1	1	1	1	1	1	1	1	1	1	6 (saturated liquid), 1 (pressurised non-saturated liquid)
Gauge pressure	Pa	5.91E+05	6.96E+05	4.69E+05	8.40E+05	6.70E+05	9.10E+05	9.23E+05	9.22E+05	1.02E+06	1.05E+06	1.09E+06	7.66E+05	7.93E+05	8.07E+05	SMEDIS for FLADIS/EEC; Hanna (1991) for DT; TNER.90.015 for GF - lower values in Hanna
Temperature	K	286.85	290.25	282.6	284.05	286.15	286.45	286.65	294.7	293.3	295.3	297.3	313.15	310.95	312.55	SMEDIS for FLADIS/EEC; Hanna (1991) for DT; TNER.90.015 for GF
Liquid fraction (MOLE basis)	mol/mol	1														
Vessel data																
Orifice diameter	m	0.0063	0.004	0.0063	0.0155	0.004	0.0155	0.0155	0.081	0.0945	0.0945	0.0945	0.0419	0.0242	0.0242	not affects final post-expansion data; SMEDIS for FLADIS,EEC; Hanna (1991) for DT,GF
Atmospheric expansion data																
Atmospheric pressure	Pa	102000	102000	101300	100000	100000	102500	100000	90888	90990	90586	90280	101325	101325	101325	SMEDIS for FLADIS/EEC; Hanna (1991) for DT; TNER.90.015 for GF (Hanna more accurate!)
Atmospheric temperature	K	288.7	290	291	288.15	289	282.9	285	302	304	307.05	306.9	310.4	309.38	310	SMEDIS for FLADIS/EEC; Hanna (1991) for DT; TNER.90.015 for GF
Atmospheric humidity	-	0.86	0.62	0.536	0.55	0.7	0.99	1	0.132	0.175	0.148	0.213	0.0562	0.126	0.35	SMEDIS for FLADIS/EEC; Hanna (1991) for DT; TNER.90.015 for GF
PARAMETERS (values to be changed by expert users only)																
Flashing allowed to orifice?	-	FALSE														Metastable liquid assumption (frozen liquid) **or (nondefault) flashing**
Use Bernoulli model for metastable liquid releases?		FALSE														use default compressible model
Orifice L/D ratio	-	1														
ATEX expansion method (0 = min thrm change, 1 = isentropic, 2 = cons moment)	-	2														**Nondefault: conservation of momentum**
Droplet correlation (0=original CCPS, 1= JIPII, 2=TNO, 3=Tilton, 4= Melhem, 5=JIPIII, 6=modified CCPS, 7=modified CCPS excl. 2PH pipe)	-	6														Modfied CPPS droplet size calculation (default)
													27.13	10.16	10.07	Observed flow rate for GF from Table 3.1 in TNER.90.015 (used for UDM calcs.)
Description	Observ	0.4	0.27	0.46	2.9	0.11	3	3	79.7	111.5	130.7	96.7	27.67	10.46	10.27	Observed flow rate: from Hanna for DT/GF, from SMEDIS for FLADIS,EEC
	Predict	1.426133	0.920825	1.111064	1.19118	1.863356	1.195527	1.203554	1.464976	1.505258	1.294841	1.780888	1.111402	1.001237	1.025875	for FLADIS metastable better results; for EEC, DT flashing better; GF almost same
ERROR STATUS		***WARN***	***WARN***	***WARN***	***WARN***	***WARN***	***WARN***	***WARN***	***WARN***	***WARN***	***WARN***	***WARN***	***OK***	***OK***	***OK***	
Release state																
Pressure	Pa	693000	798000	570000	940000	769500	1012500	1022625	1012500	1115775	1137038	1178550	867342	894699.8	907872	
Temperature	K	286.7446	290.25	281.0403	284.05	286.15	286.45	286.65	294.7	293.3	295.3	297.3	313.15	310.95	312.55	
Liquid fraction (MASS basis)	kg/kg	1	1	1	1	1	1	1	1	1	1	1	1	1	1	
Orifice state																
Pressure	Pa	102000	102000	101300	100000	100000	102500	100000	90888	90990	90586	90280	101325	101325	101325	
Temperature	kg/kg	286.5729	290.0382	280.9139	283.3719	285.5879	285.6882	285.8753	294.4025	292.9758	294.9598	296.9364	312.8714	310.6659	312.2579	
Liquid fraction (MASS basis)	-	1.00E+00	1	1	1	1	1	1	1	1	1	1	1	1	1	
Velocity	m/s	49.27421	53.70876	43.57772	59.3913	53.25518	62.07802	62.52898	62.16053	65.41988	66.28532	67.78113	41.13356	41.73085	42.17135	
Vena contracta diameter	m	4.88E-03	3.10E-03	4.88E-03	1.20E-02	3.10E-03	1.20E-02	1.20E-02	6.27E-02	7.32E-02	7.32E-02	7.32E-02	3.25E-02	1.87E-02	1.87E-02	
Final (post-expansion) state																
Temperature	K	239.8804	239.8804	239.7426	230.7823	230.7823	231.3409	230.7823	237.5967	237.6186	237.5315	237.4653	292.7764	292.7764	292.7764	
Liquid fraction (MASS basis)	kg/kg	0.840029	8.28E-01	0.85978	0.702604	0.688616	0.690474	0.686789	0.804972	0.810237	0.802746	0.795301	0.857297	0.873391	0.861785	
Velocity	m/s	49.27421	53.70876	43.57772	59.3913	53.25518	62.07802	62.52898	62.16053	65.41988	66.28532	67.78113	41.13356	41.73085	42.17135	
ATEX outputs																
Droplet diameter	m	1.44E-04	1.22E-04	1.87E-04	4.54E-05	5.67E-05	3.97E-05	4.06E-05	1.08E-04	9.78E-05	9.67E-05	9.29E-05	3.60E-04	3.54E-04	3.54E-04	
Flashing or mechanical (1 = mechanical, 2 = flash, 3 = transition)	-	1	1	1	1	1	1	1	1	1	1	1	2	2	2	
ATEX expansion method (1 = isentropic, 2 = cons momentum)	-	2	2	2	2	2	2	2	2	2	2	2	2	2	2	
Expanded diameter	m	5.18E-02	3.40E-02	4.90E-02	9.68E-02	2.55E-02	9.73E-02	0.098936	0.768146	0.885142	0.90201	0.917972	0.220967	0.120745	0.125752	
Partial expansion energy	J/kg	-9.55E+02	-1069.59	-747.668	-521.6	-1014.24	-555.684	-556.245	-1139.79	-838.102	-993.043	-1125.03	629.7134	685.458	681.7128	
Other data																
Discharge coefficient	-	0.6	0.6	0.6	0.6	0.6	0.6	0.6	0.6	0.6	0.6	0.6	0.6	0.6	0.6	
Mass release rate	kg/s	5.70E-01	0.248623	0.511089	3.454422	0.204969	3.586581	3.610661	116.7585	167.8362	169.2357	172.2119	30.75249	10.47294	10.53573	
Release duration	s	3600	3600	3600	3600	3600	3600	3600	3600	3600	3600	3600	3600	3600	3600	

Table 6-1 DISC input spreadsheet for FLADIS, EEC, Desert Tortoise and Goldfish experiments

[The spreadsheet applies the assumptions of metastable liquid and ATEX conservation-of-momentum]

Input	Test1	Test2	Test3	Test5	Test6	Test11	Test8	Test8R	Test9	Input for models
Discharge data										
steady-state/transient	steady	steady	steady	steady	steady	steady	trans.	trans.	trans.	-
storage phase	liquid	liquid	liquid	liquid	liquid	liquid	vapour	vapour	vapour	DISC
storage pressure (barg)	103.4	155.5	133.5	157.68	156.7	82.03	157.76	148.7	154.16	DISC
storage temperature (ºC)	5	7.84	11.02	9.12	9.48	17.44	147.12	149.37	69.17	DISC
orifice diameter (mm)	11.94	11.94	11.94	25.62	6.46	11.94	11.94	11.94	11.94	DISC
Ambient data										
ambient temperature (ºC)	14.2	7.5	10.6	5.8	6.1	11.6	11.19	11.1	8.2	DISC, UDM
ambient pressure (mbara)	999.4	958.2	972.5	985.4	938.4	960.2	957.99	957.1	958.9	DISC, UDM
relative humidity (%)	74.4	96	95.8	96.7	1	94	100	100	99.9	DISC, UDM
wind direction (degrees)	322.4	265.6	288.8	278.6	299	270.8	269.3	270	270.7	UDM uses 270º
wind speed (m/s)	4	3.44	3.37	5.13	2.20	5.99	4.71	0.76	4.04	UDM

(a) BP CO_2 tests

Input	Test3	Test5	Test11	Test1	Test2	Test4	Test14	Test16	Input for models
Discharge data									
steady-state/transient	steady	steady	steady	trans.	trans.	trans.	trans.	trans.	-
storage phase	liquid	liquid	liquid	Liquid	liquid	liquid	vapour	Vapour	DISC
nozzle pressure (barg)	144.8	126.4	80.3	143	118	148.2	147.7	146.0	DISC
nozzle temperature (ºC)	8.2	13.7	-1.4	23	18	20.1	65.0	31.7	DISC
vessel volume (m^3)	-	-	-	6.3	6.3	6.3	6.3	6.3	DISC
orifice diameter (mm)	12.7	25.4	12.7	12.7	25.4	6.3	12.7	12.7	DISC
Ambient data									
ambient temperature (ºC)	11.2	9	3.6	14.7	10.3	13.8	0	-2.9	DISC, UDM
ambient pressure (mbara)	1017	905	995	1006	1005	975.5	1005	997	DISC, UDM
relative humidity (%)	66	91	78	83	77	77	88	88	DISC, UDM
wind direction (degrees)	267	213	261	263	250	215	303	292	UDM uses 270º
wind speed (m/s)	4.05	1.30	2.76	3.93	5.43	1.98	1.34	1.48	UDM

(b) Shell CO_2 tests

Table 6-2 Experimental conditions for BP and Shell CO_2 tests (DISC and UDM input)

	FLAD 9	*FLAD 16*	*FLAD 24*	EEC170[xii]	*EEC360*	*EEC550*	*EEC560*	*DT1*	*DT2*	*DT3*	*DT4*	*GF1*	*GF2*	*GF3*
FLOW RATE														
Observed, kg/s	0.4	0.27	0.46	2.9	0.11	3	3	79.7	111.5	130.7	96.7	27.67	10.46	10.27
Predicted (metastable)	0.57	0.25	0.51	3.45	0.20	3.59	3.61	116.8	167.8	169.2	172.2	30.75	10.47	10.54
Predicted (flashing)	0.15	0.08	0.13	2.78	0.11	2.89	2.92	63.0	116.1	110.9	108.2	30.69	10.46	10.52
Pred./Obs. (metastable)	**1.43**	**0.92**	**1.11**	1.19	1.86	1.20	1.20	1.46	1.51	1.29	1.78	1.11	1.00	1.03
Pred./Obs. (flashing)	0.38	0.28	0.29	**0.96**	**0.99**	**0.96**	**0.97**	**0.79**	**1.04**	**0.85**	**1.12**	1.11	1.00	1.02
SMEDIS														
Liquid Fraction	0.84	0.83	0.83	0.72	0.71	0.70	0.70	0.82	0.82	-	-	-	-	-
Velocity (m/s)	65.17	67.85	55.87	85.21	84.2	68.5	89.03	90.3	72.7	-	-	-	-	-
DISC (conservation of momentum; metast.)														
Liquid Fraction	**0.84**	**0.83**	**0.86**	0.70	0.69	0.69	0.69	0.80	0.81	0.80	0.80	0.86	0.87	0.86
Velocity (m/s)	**49.3**	**53.7**	**43.6**	59.4	53.3	62.1	62.5	62.2	65.4	66.3	67.8	41.1	41.7	42.2
SMD (µm)	**144**	**122**	**187**	45	57	40	41	108	98	97	93	360	354	354
DISC (conservation of momentum; flashing)														
Liquid Fraction	0.84	0.83	0.86	**0.70**	**0.69**	**0.69**	**0.69**	**0.81**	**0.81**	**0.80**	**0.80**	0.86	0.87	0.86
Velocity (m/s)	122.7	119.4	113.1	**65.6**	**82.2**	**68.3**	**68.7**	**82.2**	**71.1**	**75.0**	**79.2**	41.3	41.8	42.3
SMD (µm)	23	25	28	**325**	**268**	**319**	**318**	**275**	**316**	**304**	**293**	348	344	343
DISC (Isentropic; metastable)														
Liquid Fraction	0.85	0.84	0.87	0.73	0.72	0.72	0.72	0.82	0.83	0.82	0.82	0.86	0.88	0.87
Velocity (m/s)	201.8	216.9	178.1	172.0	176.5	178.0	180.4	246.0	241.0	249.5	258.1	70.7	66.0	69.9
SMD (µm)	113	102	131	141	137	136	134	84	87	82	77	265	275	267

Table 6-3 Flow-rate and post-expansion data predictions (FLADIS, EEC, Desert Tortoise, Goldfish)

[xii] Previously SMD was presumed 40 micrometer, but now it has been calculated as 45 micrometer. Given the small difference, the original value of 40 micrometer has been obtained.

	Cold liquid tests						Supercritical hot tests			Steady state liquid tests			Transient liquid tests			Transient hot tests	
	BP1	***BP2***	***BP3***	***BP5***	***BP6***	***BP11***	***BP8***	***BP8R***	***BP9***	***SHL3***	***SHL5***	***SHL11***	***SHL1***	***SHL2***	***SHL4***	***SHL14***	***SHL16***
FLOW RATE																	
Observed, kg/s	8.2	11.41	9.972	41.17	3.50	7.12	4.07	3.80	6.05	12.4	44.7	8.9	10.55	38	3.17	7.37	10.5
Predicted (ms)	10.19	12.44	11.53	57.61	3.65	9.28	4.19	3.90	6.71	12.16	43.92	9.29	11.12	41.15	2.85	7.71	Error
Predicted (fl)	8.84	10.98	9.99	50.75	3.21	7.03	4.19	3.90	6.86	12.37	44.36	9.10	11.38	41.26	2.92	7.67	10.88
DISC (conservation of momentum; metastable)																	
Liquid Fraction	0.397	0.403	0.384	0.400	0.397	0.329	0.000	0.000	0.158	0.399	0.370	0.415	0.342	0.351	0.355	0.164	Error
Velocity (m/s)	157.92	191.36	180.95	193.34	193.05	152.16	466.49	472.77	295.93	174.98	168.47	129.14	185.10	166.99	185.26	276.64	Error
SMD (µm)	9.21E-6	6.42E-6	7.15E-6	6.05E-6	6.43E-6	1.03E-5	0	0	2.69E-6	7.27E-6	8.89E-6	1.33E-5	6.67E-6	8.06E-6	6.87E-6	2.83E-6	Error
DISC (conservation of momentum; flashing)																	
Liquid Fraction	0.397	0.403	0.384	0.399	0.397	0.330	0.000	0.000	0.154	0.400	0.371	0.416	0.343	0.352	0.356	0.165	0.308
Velocity (m/s)	156.72	189.76	179.16	191.67	191.35	154.20	466.49	472.77	289.00	176.25	170.94	132.22	187.93	170.79	187.48	277.54	199.61
SMD (µm)	9.35E-6	6.53E-6	7.29E-6	6.16E-6	6.54E-6	1.00E-5	0	0	2.82E-6	7.16E-6	8.64E-6	1.27E-5	6.47E-6	7.71E-6	6.71E-6	2.81E-6	5.42E-6
DISC (Isentropic; metastable)																	
Liquid Fraction	0.480	0.486	0.472	0.483	0.482	0.433	0.161	0.152	0.305	0.482	0.464	0.494	0.440	0.447	0.451	0.308	Error
Velocity (m/s)	347.78	363.78	365.68	364.91	368.14	377.49	500	500	500	353.41	368.84	327.08	383.83	371.54	379.72	491.88	Error
SMD (µm)	1.90E-6	1.78E-6	1.75E-6	1.70E-6	1.77E-6	1.67E-6	9.54E-7	9.55E-7	9.43E-7	1.78E-6	1.86E-6	2.07E-6	1.55E-6	1.63E-6	1.64E-6	8.94E-7	Error

Table 6-4 Flow-rate and post-expansion data predictions (BP and Shell CO_2 tests)

6.1.2 Dispersion

This section reports results of UDM dispersion calculations based on the source-term data as described in the previous section. The following four cases are considered for selection of the source terms (flow rate; post-expansion liquid fraction, velocity and SMD):

(1) Conservation of momentum and metastable liquid
(2) Conservation of momentum and flashing at the orifice
(3) Isentropic and metastable liquid
(4) SMEDIS input data

UDM rainout predictions

No rainout was predicted for the FLADIS and Goldfish experiments. Furthermore the UDM calculations applied for the CO_2 tests presume a two-phase (solid/vapour) equilibrium model without solid deposition, which is in line with the experimental observations.

Table 6-5 includes results of predicted rainout fractions for the EEC and Desert Tortoise experiments:

- Isentropic assumption: never rainout is seen to be predicted
- conservation-of-momentum assumption:
    - For the Desert Tortoise experiments. the lower post-expansion velocity results in rainout. The large SMD using the flashing assumption results in a further increased amount of rainout.
    - For the EEC experiments, the larger SMD using the flashing assumption results in rainout

Rainout fraction (fraction)	Conservation of momentum; metastable liquid	Conservation of momentum; flashing at the orifice	Isentropic; metastable liquid	Smedis
EEC170	-	0.32	-	-
EEC360	-	0.15	-	-
EEC550	-	0.31	-	-
EEC560	-	0.29	-	-
DT1	0.44	0.57	-	0.32
DT2	0.44	0.62	-	0.42
DT3	0.44	0.60	-	0.44
DT4	0.40	0.58	-	0.40

Table 6-5 Predicted rainout fractions for EEC and Desert Tortoise experiments

UDM concentration and width predictions[13]

The following figures compare the UDM concentration and widths predicted for two-phase jet releases under the various DISC model assumptions:

(1) Conservation of momentum and metastable liquid (labelled in figures by MM)
(2) Conservation of momentum and flashing at the orifice (labelled in figures by MF)
(3) Isentropic and metastable liquid (labelled in figures by E)

One representative test has been selected for each of set of experiments:

- Desert Tortoise - Test 03
- EEC – Test 550
- Fladis – Test 24

[13] UPDATE. Concentration versus distance plots are provided in the UDM validation manual for BP tests 9,11 and Shell tests 11, 16,1 in the UDM validation manual for the case of conservation of momentum and flashing. Thus for reasons of completeness, it may be considered to include in this section also the steady-state liquid CO2 tests (BP test 11 and/or Shell test 11)

The results are given in Figure 6-1, Figure 6-2 and Figure 6-3, respectively. For the concentrations plots, the centreline concentration and the maximum concentration at the measurement height are shown. For the width plots, the cloud width according to the cloud width definition, Smedis or Hanna[14], is shown. The following conclusions can be drawn:

- Figure 6-1 (DT03) and Figure 6-2 (EEC550) illustrate the discontinuity of the observer centre-line concentration at the point of rainout. After rainout, the centre-line concentrations observed by the different observers are different because of the time-varying pool data. It is seen that at a distance sufficient far downwind the maximum value of the centre-line concentrations (over all observers) closely matches the maximum concentration, which should be the case since no AWD effects were applied.
- From Figure 6-1 to Figure 6-3 it can be observed that the assumption of conservation of momentum for atmospheric expansion gives the closest agreement to the experiments. In general, the assumption of metastable liquid for the expansion from stagnation to orifice conditions shows slightly better agreement. The isentropic option results in too large concentrations for Desert Tortoise 3 (caused by absence of rainout due to smaller SMD), while it is resulting in too low concentrations for EEC550 (caused by larger jet entrainment due to larger post-expansion velocity).

For the Goldfish set of experiments, very little difference was found in the DISC model predictions for the assumptions listed above (see Table 6-3), thus resulting in similar behaviour in the UDM predicted concentrations and widths. Given this, Goldfish Test 01 was investigated for the effects of along wind diffusion given that it is a short duration release (125 s) and experimental arc measurements were reported for downwind distances of up to 3 km. Figure 6-4 compares for this Goldfish test the predicted concentration and width with and without along–wind diffusion effects assuming conservation of momentum and metastable liquid. From the figure it can be observed that the effects of along wind diffusion are not significant up to the distance of the last arc measurement (3000 m).

[14] Refer to UDM validation document for cloud width definition formulae

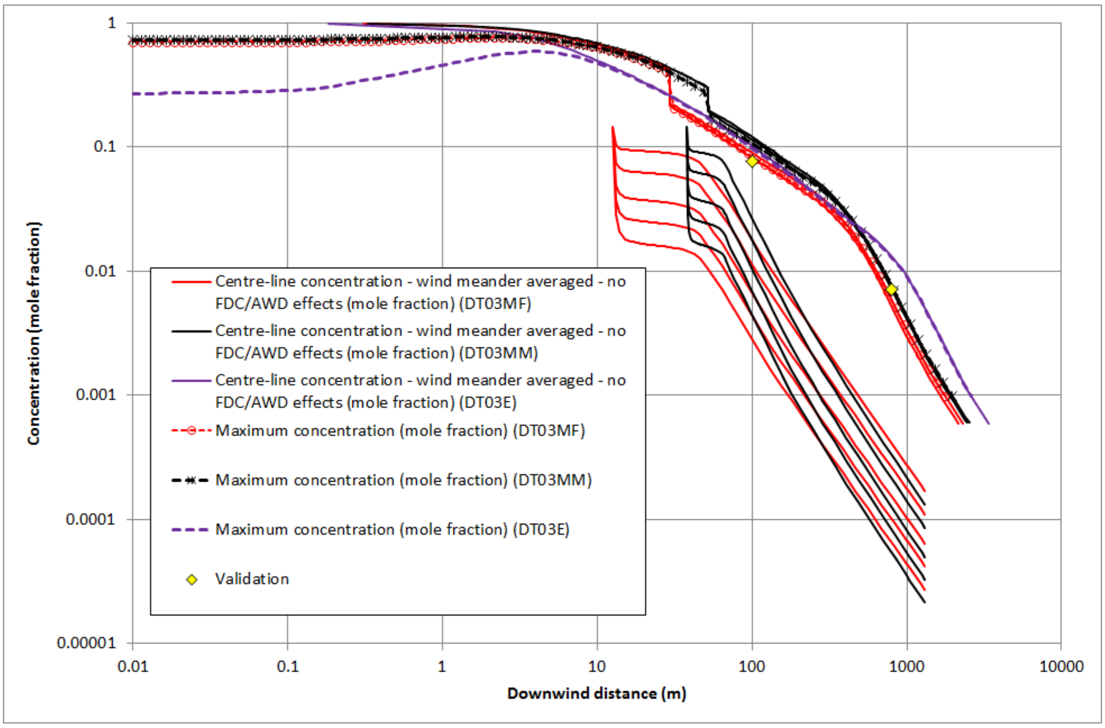

(a) Concentration

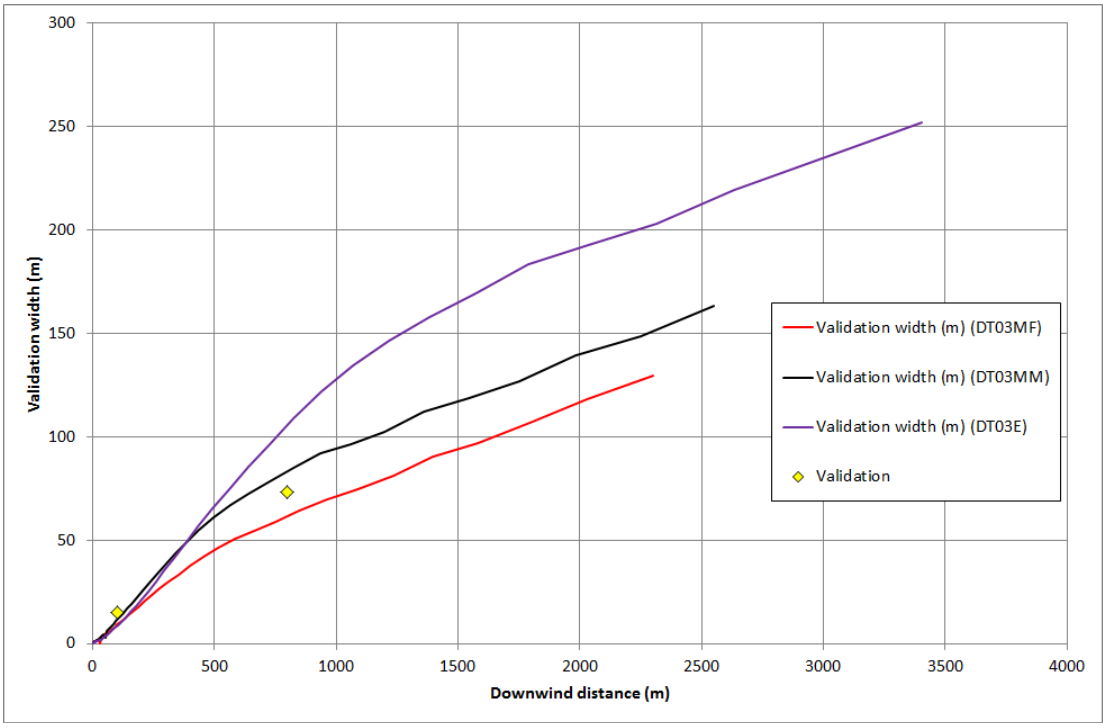

(b) Width

Figure 6-1 Desert Tortoise 03 - concentration and width validation – vary DISC/ATEX options
Conservation of momentum with flashing at the orifice predictions are given in red lines; conservation of momentum with metastable liquid predictions, in black; and, isentropic with metastable liquid, in purple. Experimental data points are shown as yellow markers

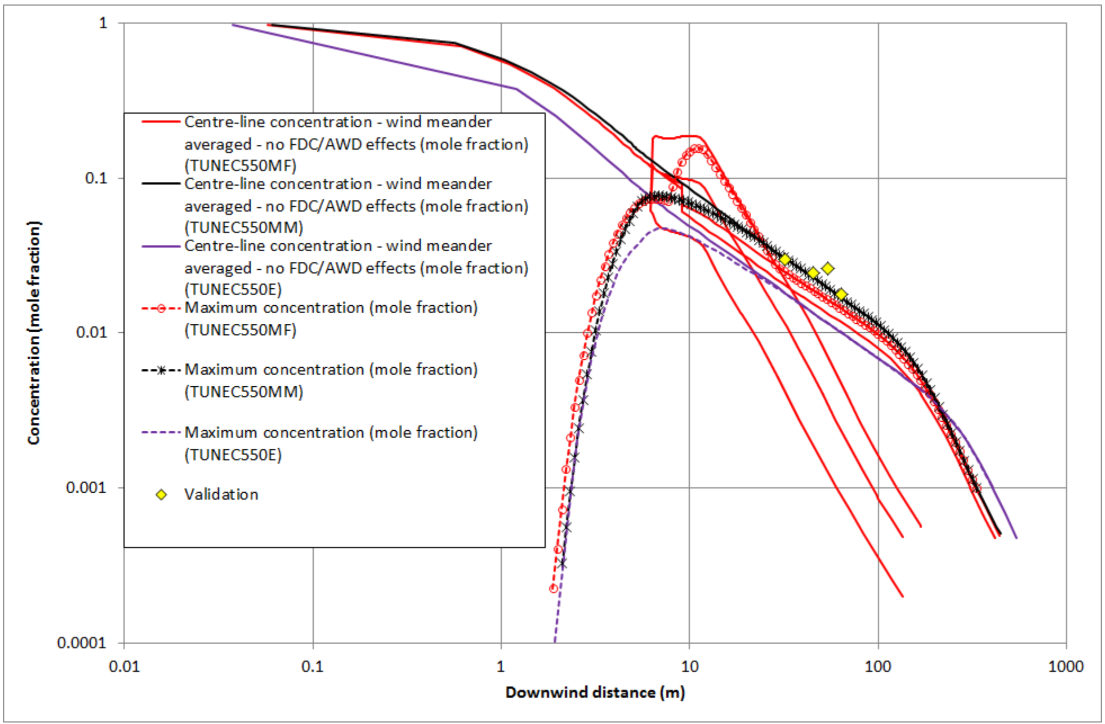

(a) Concentration

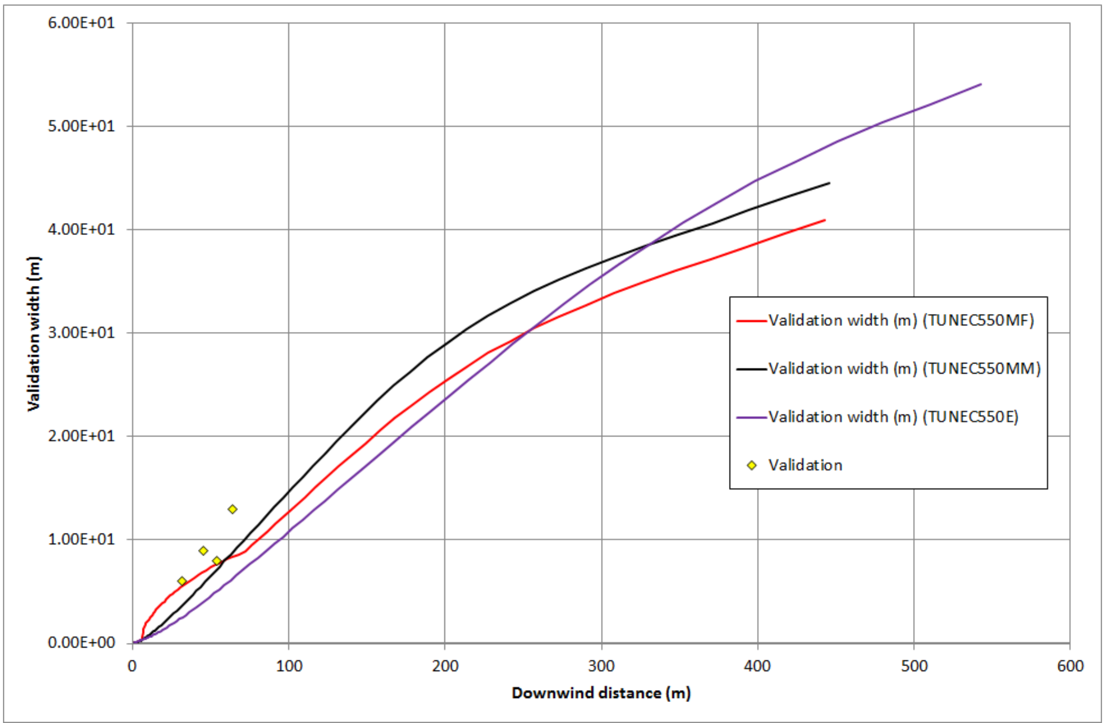

(b) width

Figure 6-2 EEC 550 - concentration and width validation – vary DISC/ATEX options
Conservation of momentum with flashing at the orifice predictions are given in red lines; conservation of momentum with metastable liquid predictions, in black; and, isentropic with metastable liquid, in purple. Experimental data points are shown as yellow markers

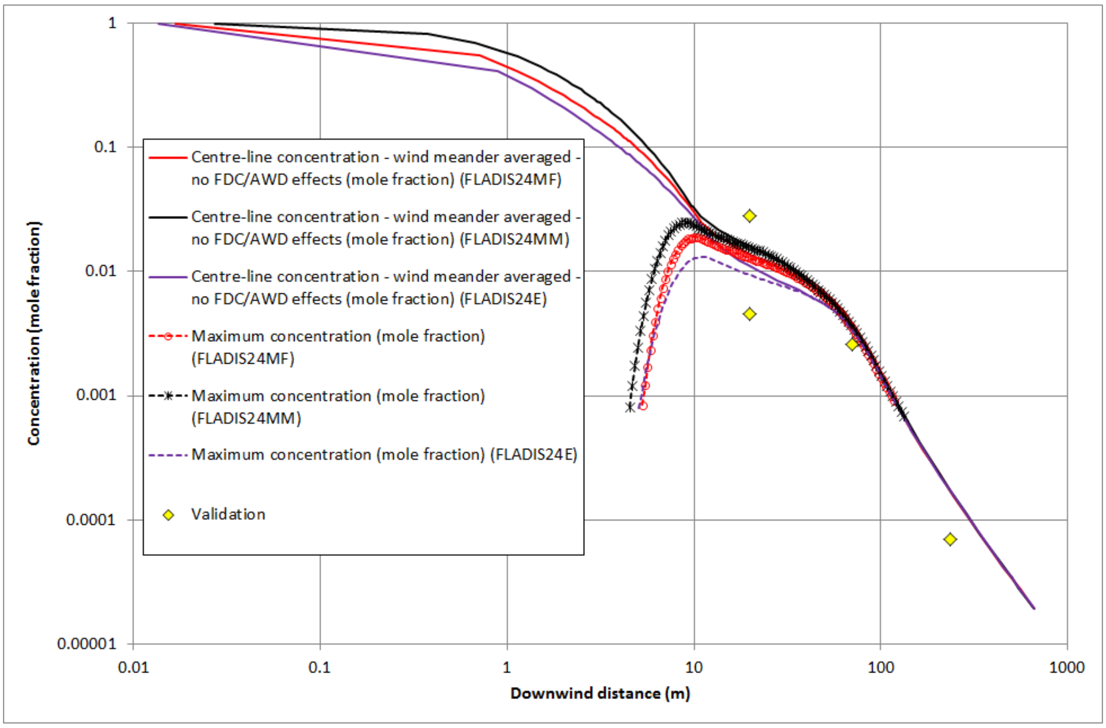

(a) Concentration

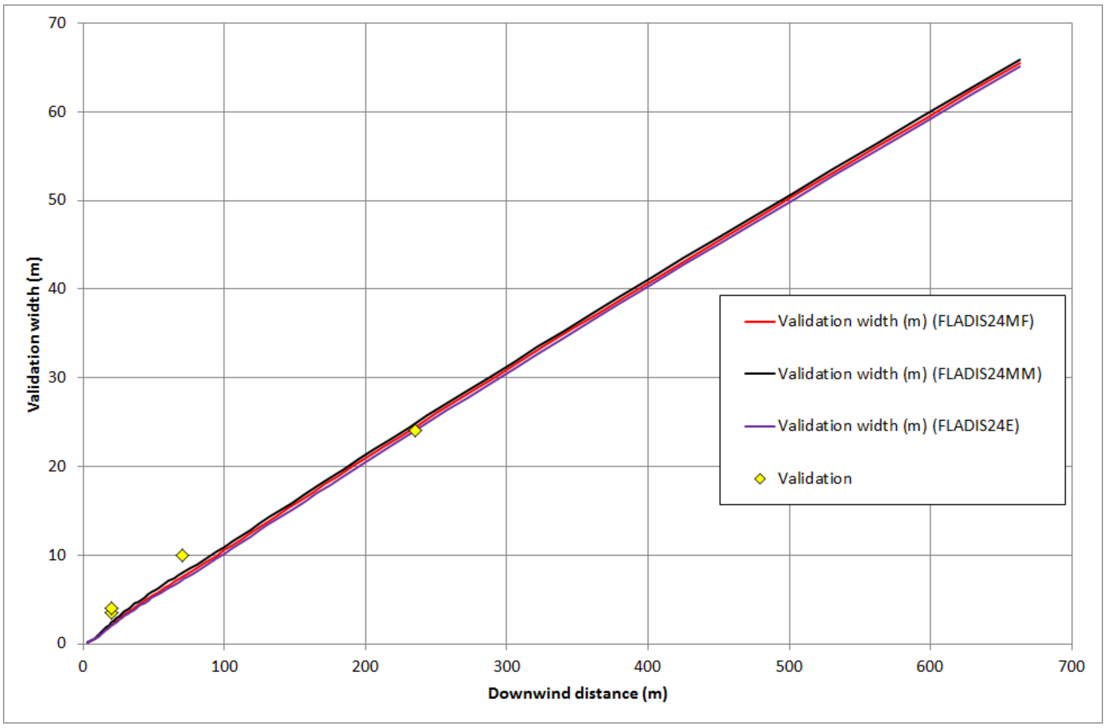

(b) Width

Figure 6-3 FLADIS 24 - concentration and width validation – vary DISC/ATEX options
Conservation of momentum with flashing at the orifice predictions are given in red lines; conservation of momentum with metastable liquid predictions, in black; and, isentropic with metastable liquid, in purple. Experimental data points are shown as yellow markers

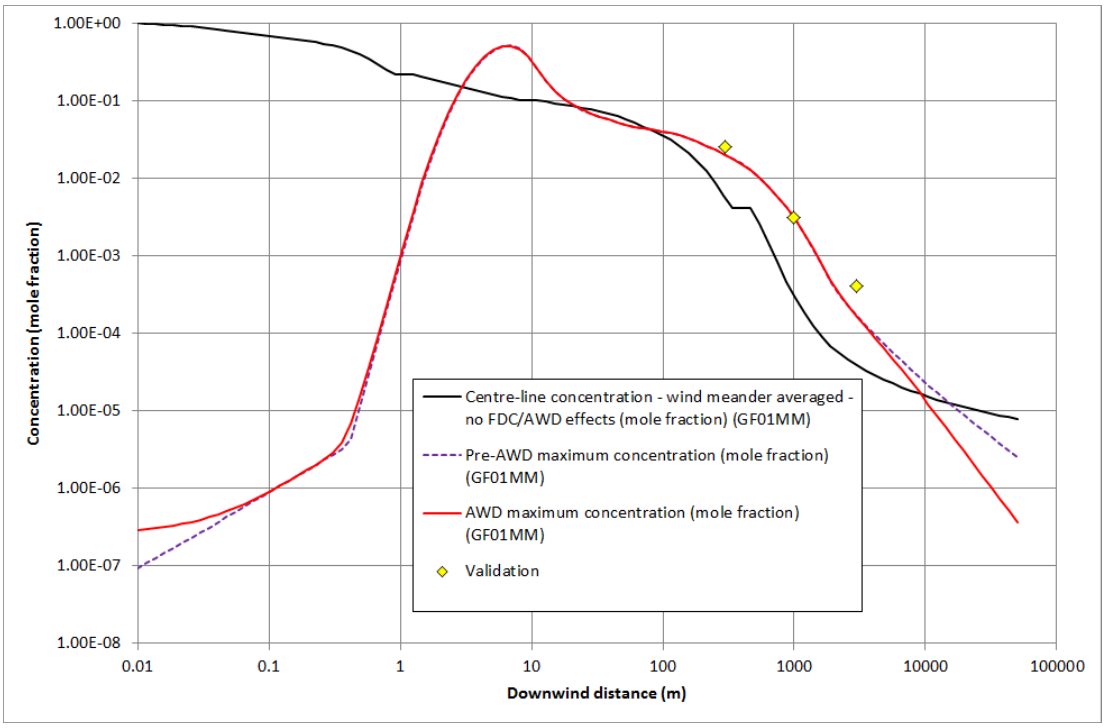

(a) Concentration

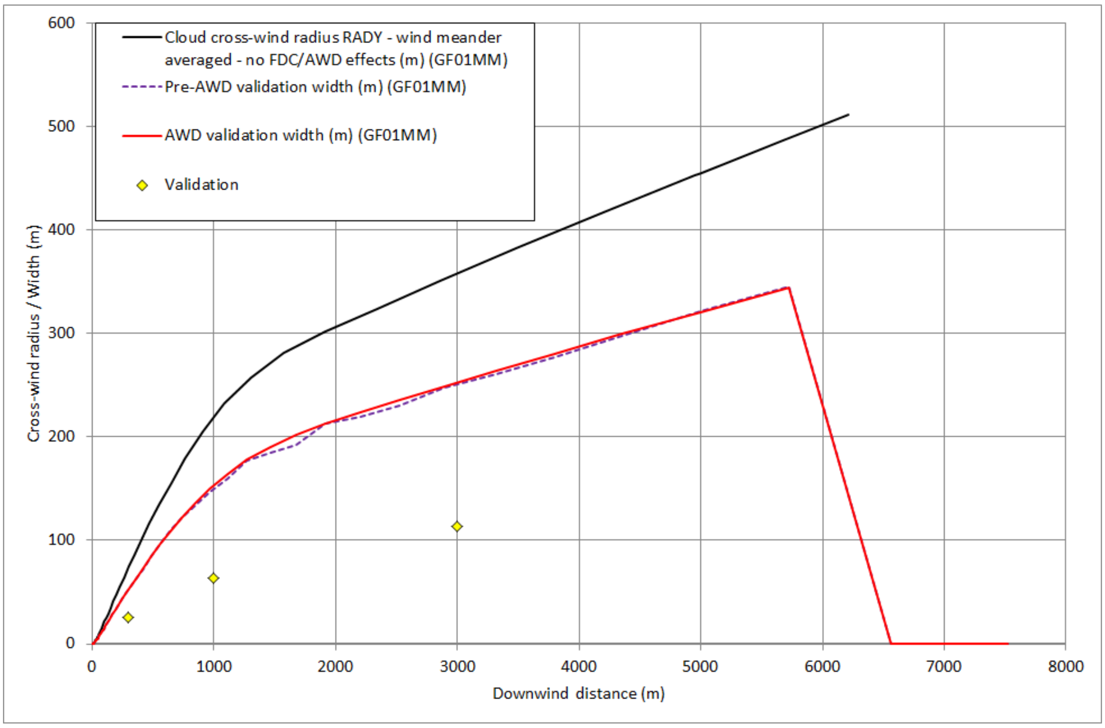

(b) Width

Figure 6-4 Goldfish 01 – concentration and width validation – AWD effects

Comparison of AWD effects on Goldfish 01 (short duration release) with conservation of momentum and metastable liquid ATEX options

UDM MG/VG concentration and width validation statistics

Figure 6-5 and Figure 6-6 show the summary MG/VG plot for concentration and widths predictions for two-phase jet releases of propane (EEC) , HF (Goldfish), ammonia (FLADIS and Desert Tortoise) and CO_2 (BP and Shell). The figures compare the accuracy of the various expansion methods for predicting concentration and cloud width, and it's been colour coded for easier comparison:

- Conservation of momentum and metastable liquid predictions are shown with black markers
- Conservation of momentum and flashing at the orifice, in red markers
- SMEDIS input data, in blue markers
- Isentropic and metastable liquid, with green markers

In general, it can be seen that applying conservation of momentum with metastable liquid yields more accurate MG/VG values.

The overall results can be summarised as follows:

- Desert Tortoise, EEC and CO_2 BP and Shell sets of tests show very good accuracy
- Desert Tortoise results show the better agreement for conservation of momentum and metastable liquid method. Applying isentropic and metastable liquid results in the higher concentrations, which is due to the absence of rainout. Results for conservation of momentum and metastable liquid correspond well with results obtained using SMEDIS data. Conservation of momentum and flashing at the orifice predict lower concentrations than SMEDIS or metastable liquid due to the larger rainout fraction predicted by the flashing assumption
- For EEC, rainout was predicted only for conservation of momentum and flashing at the orifice. Thus lower concentrations are obtained for flashing than for metastable liquid when applying conservation of momentum. However, the higher final velocities predicted by the isentropic expansion results in the lower concentrations predictions at a given height. The better agreement for concentration predictions was observed when applying conservation of momentum and metastable liquid assumption. Conversely, for the widths, applying conservation of momentum with flashing yield better agreement.
- CO_2 BP and Shell results show a similar trend as EEC. Applying isentropic expansion with metastable liquid assumption results in lower predicted concentrations due to the higher final velocities. Results for conservation of momentum with flashing and metastable liquid assumptions produce very similar results
- Fladis predictions of concentration show larger values for the geometric variance. The better agreement was observed for conservation of momentum and metastable liquid.
- Goldfish results show accurate prediction of the maximum concentration and an under-prediction of the cloud width. Very little difference was found between the predictions for conservation of momentum or isentropic and flashing at the orifice or metastable liquid assumptions.

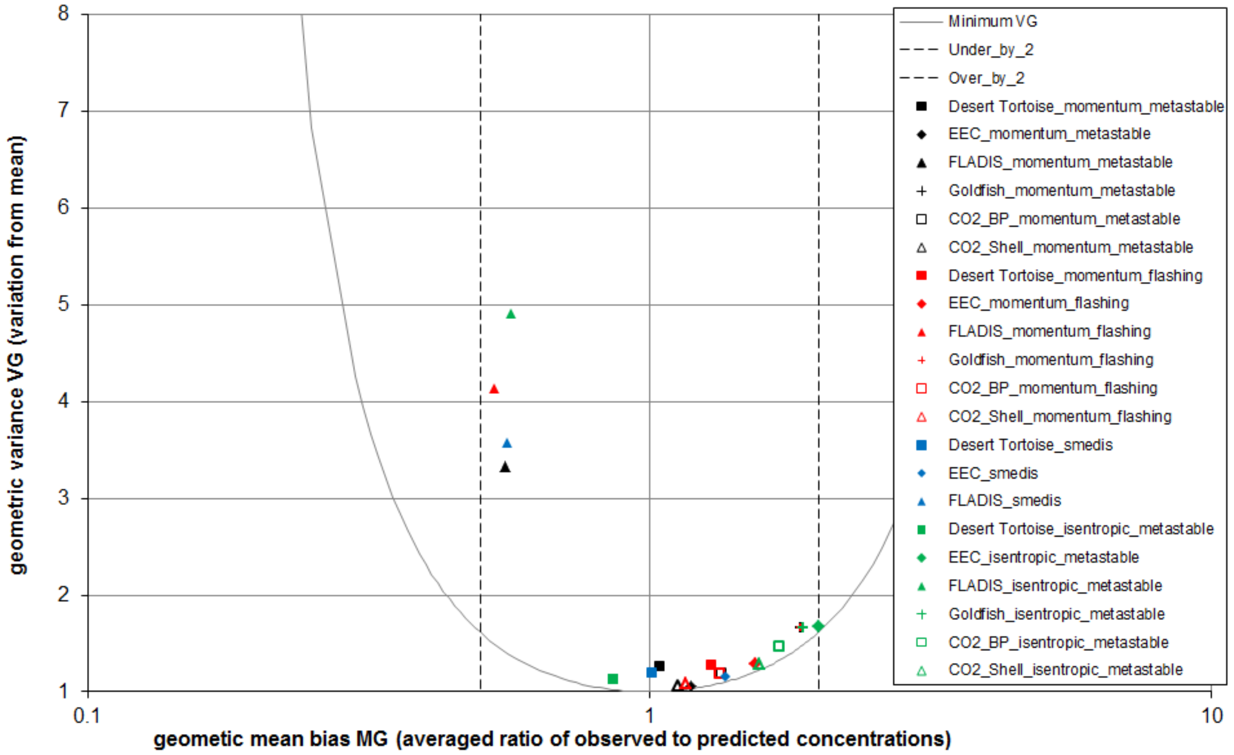

Figure 6-5 MG/VG concentration plot (flashing two-phase jets ; vary DISC/ATEX options)[15]

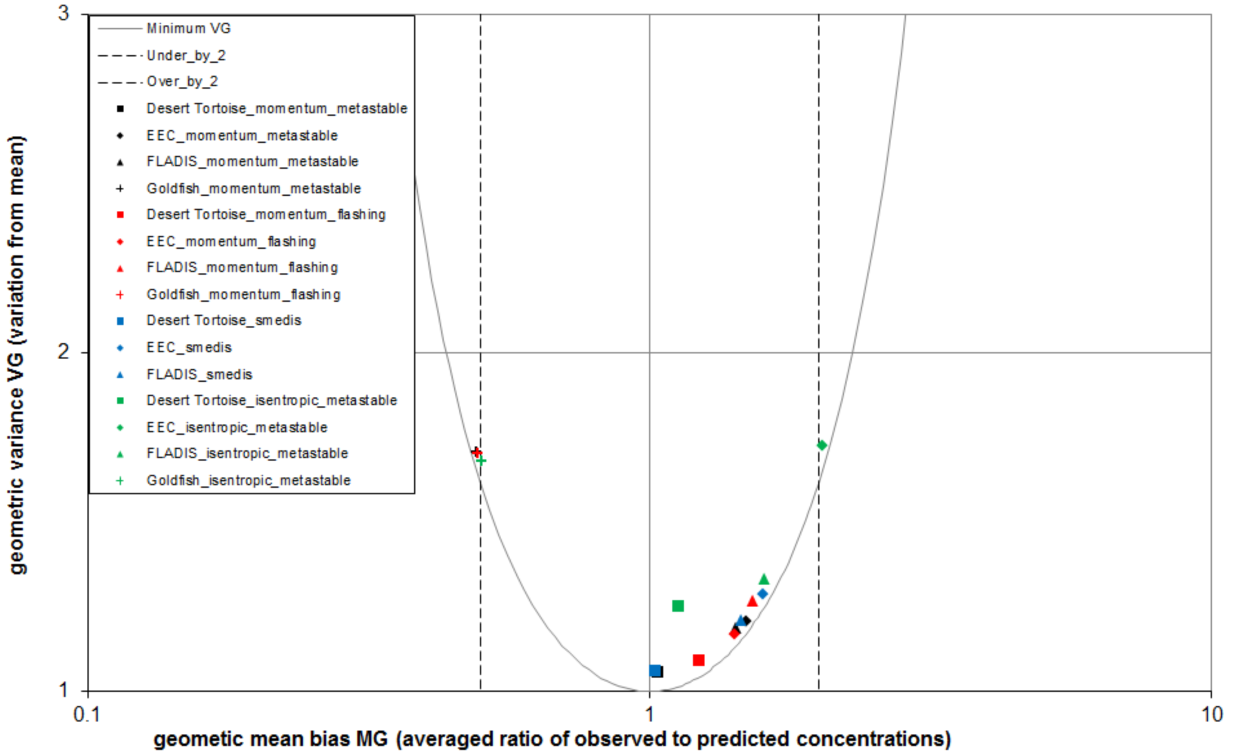

Figure 6-6 MG/VG width plot (flashing two-phase jets; vary DISC/ATEX options)

[15] CO_2 Shell Test 16 is not included in the overall MG/VG values for the metastable liquid runs, either with conservation of momentum or conservation of entropy. Test 16 is a hot vapour release, using the DISC option metastable liquid is not appropriate for this test and consequently it fails as entropy is not conserved in the calculation of chocked flow.

6.1.3 Conclusions regarding selection of model assumptions

As indicated in Section 6.1.1 regarding accuracy of flow-rate predictions and agreement of final post-expansion velocity with SMEDIS data, it could be considered to apply the 'flashing' assumption for the Desert Tortoise and EEC experiments. However it was found in 6.1.2 that the metastable liquid assumption generates overall more accurate predictions (improved MG,VG values) using the metastable liquid assumption for all sets of experiments (FLADIS, Desert Tortoise, EEC), except for the CO_2 tests.

Thus it is recommended that UDM validation datasets which require as input post flash data (liquid fraction, velocity, SMD), would obtain all these data using the Phast discharge model, adopting the conservation of momentum approach in conjunction with the metastable liquid assumption for evaluation of the flow rate. [16].

[16] Thus it is may be considered to further update the UDM validation manual to no longer use the SMEDIS input data for the SMEDIS validation sets, and to use for these the same approach as for the non-SMEDIS validation datasets. However as indicated in this report, the SMEDIS input data are generally close to the input data associated with our recommended approach.

6.2 High-pressure hydrogen vapour jets (Shell HSL experiments)

6.2.1 Introduction

Commissioned by Shell Global solutions, HSL carried out experimental work relating to horizontal pressurised hydrogen orifice releases at 1.5 m above the ground:

- Roberts et al. (2006)[/20/] discusses results of a set of 23 experiments for which the flow rate was unsatisfactorily not measured. For these experiments the hole diameter equals 3, 4, 6 or 12 mm, the stagnation temperature varies between 13 and 20C and the stagnation pressure varies between 10 barg and 129 barg. The paper compares predicted concentrations against the HGSYSTEM model AEROPLUME. The paper states that good results were obtained for 8 experiments which pointed close towards the wind direction (limited crosswind effects; Fig.7a in the paper; runs 6, 7, 8, 9, 10, 11, 14, 16; 3 mm or 4 mm orifice size, stagnation temperature around 14C and stagnation pressure 50-118barg). Presumably the conservation of momentum assumption is applied which the author believes is the option applied in HGSYSTEM, but this is not explicitly mentioned in the paper. The applied version of HGSYSTEM is an internal Shell version HGSYSTEM 5 of the program, which differs from the previously public version HGSYSTEM 3.0.
- DNV (Skottene and Holm, 2008) [/19/] carried out validation using both Phast and KFX against the hydrogen HSL experiments. They however also refer to an additional set of experiments with smaller orifice diameters (0.25, 0.75 and 1 mm) for which the flow rate was measured, and for which the results are not reported in the paper by Roberts et al. (2006)[/20/]. Skottene and Holm also note that distances to H2 LEL clouds compared well between Phast and KFX. For runs 7, 9, 14 (3 or 4 mm orifice size) also comparisons are provided against Phast, and close results were obtained with the experimental data.

In Section 6.2.2 results by the DISC orifice discharge model (version Phast 7.1) are provided for the small orifice sizes (0.25, 0.75 and 1 mm), for which experimental measurements of the flow rate are available. Identical results have been confirmed as those reported by Skottene and Holm [/19/] using an earlier version of Phast.

In Section 6.2.3 DISC simulations are carried out for the larger orifice diameters 3 and 4 mm, for which no experimental measurements of the flow rate are available. For these experiments flow rate predictions are compared with results of the HGSYSTEM model AEROPLUME reported by Roberts et al. (2006)[/20/]. Furthermore the UDM dispersion model has been validated for runs 7, 9 and 14 (3 or 4 mm orifice size).

6.2.2 Small orifice (0.25, 0.75 and 1 mm; with flow rate measurements)

First nine tests are considered corresponding to small orifice diameters (0.25, 0.75 and 1 mm). For these tests flow rate measurements are available, while concentration measurements are not available.

Table 6-6 summarises the associated input and output data for the Phast discharge model DISC using the Phast orifice (leak) scenario:

- The column for HD 31 contains all input data for this experiment, while deviations to these input data are given only in the subsequent columns for experiments HD 32, HD 33, HD 34, HDH3, HD 22, HD 23, HD 24 and HDH13. It is seen that the storage temperature is taken as 14.5C and the pressures varies between 92.6 barg and 207 barg.
- At the bottom of the table the DISC results are compared with the observer flow rate. It is seen that DISC accurately predicts the data, with an under-prediction of the flow rate of between 6.5% and 8.3%.
- The comments column at the right of the table also includes a description of the verification of the DISC orifice pressure/temperature data (choked flow) against those obtained by the process simulation package Hysis (as quoted by Skottene and Holm[/19/]). Note that both packages apply the Soave-Redlich-Kwong (SRK) Equation of State. However the Hysis calculations appear to have adopted as reservoir temperature 20C and not 14.5C. Therefore accounting for this, the Hysis predicted orifice temperature of about 243 K (based on isentropic expansion from storage to orifice conditions) is very close to the Phast predicted temperature of 235.9-237.1 K. In addition the predicted ratio of orifice to stagnation pressure is very close between the Hysis value (52.6%) to the values predicted by Phast (range 50.5-51.5%)

Inputs	DISC orifice model validation against Shell hydrogen experiments (Roberts et al.)													
Input Index	Description	Units	Limits		1-HD31	1-HD32	1-HD33	1-HD34	2-HDH3	3-HD22	3-HD23	3-HD24	4-HDH13	Comments
			Lower	Upper										
	Material													
N	Stream name	-			Hydrogen									
	Storage state													
3	Gauge pressure	Pa	0		9.68E+06	9.71E+06	9.76E+06	9.26E+06	2.07E+07	1.62E+07	1.59E+07	1.61E+07	1.95E+07	converted from given pressures in bara (reduced with 1 bar)
4	Temperature	K	10	1000	287.65									
	Vessel data													
7	Orifice diameter	m	1.00E-04	50	1.00E-03				7.50E-04	2.50E-04	2.50E-04	2.50E-04		0.25, 0.75 or 1 mm; min. allowable input reduced from 1 to 0.1mm
8	Liquid head	m	0		0									not used
	Atmospheric expansion data													
9	Atmospheric pressure	Pa	50000	120000	101325									presumed value
10	Atmospheric temperature	K	10		287.65									presumed value = reservoir temperature
11	Atmospheric humidity	-	0	1	0.7									presumed value; not relevant
12	Wind speed	m/s	0		0									not relevant for dischargte
	PARAMETERS (values to be changed by expert users only)													
19	Is discharge coefficient specified? TRUE = Specified	-			FALSE									
21	Input discharge coefficient	-	0	1	1									
22	ATEX expansion method (0 = min thrm change, 1 = isentropic, 2 = cons moment)	-	0	2	2									
26	Maximum velocity capping method (0 = user input, 1 = sonic velocity)	-	0	1	0									
26	Maximum velocity	m/s	10	1000	500									
Outputs														
Output Index	**Description**													
	ERROR STATUS				***WARN***	***WARN***	***WARN***	***WARN***	***WARN***	***WARN***	***WARN***	***WARN***	***WARN***	
	Release state													
1	Pressure	Pa			9781325	9811325	9861325	9361325	20831325	16281325	16041325	16211325	19641325	
2	Temperature	K			287.65	287.65	287.65	287.65	287.65	287.65	287.65	287.65	287.65	
3	Liquid fraction (MASS basis)	kg/kg			0	0	0	0	0	0	0	0	0	
	Orifice state													
5	Pressure	Pa			5037560	5052702	5077936	4825375	10495935	8276670	8158533	8242224	9919214	
6	Temperature	kg/kg			237.1267	237.1227	237.1162	237.1815	235.7492	236.3017	236.3314	236.3104	235.8919	DISC SRK range 235.9-237.1K; Hysis SRK value about 243K
7	Liquid fraction (MASS basis)	-			0.00E+00	0	0	0	0	0	0	0	0	
8	Velocity	m/s			1229.984	1230.137	1230.391	1227.846	1285.632	1262.865	1261.658	1262.513	1279.698	
9	Vena contracta diameter	m			9.29E-04	9.29E-04	9.29E-04	9.29E-04	6.95E-04	2.32E-04	2.32E-04	2.32E-04	9.27E-04	
	Final (post-expansion) state													
10	Temperature	K			283.765	283.7807	283.8067	283.5465	289.6667	287.2042	287.0755	287.1666	289.0187	
11	Liquid fraction (MASS basis)	kg/kg			0	0.00E+00	0	0	0	0	0	0	0	
12	Velocity	m/s			500	500	500	500	500	500	500	500	500	
	ATEX outputs													
16	ATEX expansion method (1 = isentropic, 2 = cons momentum)	-			2	2	2	2	2	2	2	2	2	
17	Expanded diameter	m			1.10E-02	1.10E-02	1.11E-02	1.08E-02	1.20E-02	3.55E-03	3.52E-03	3.54E-03	1.56E-02	
18	Expansion energy	J/kg			Undefined	Undefined	Undefined	Undefined	Undefined	Undefined	Undefined	Undefined	Undefined	
19	Partial expansion energy	J/kg			Undefined	Undefined	Undefined	Undefined	Undefined	Undefined	Undefined	Undefined	Undefined	
	Other data													
20	Discharge coefficient	-			0.86309	0.863081	0.863067	0.863208	0.85923	0.860903	0.86099	0.860929	0.859671	
21	Mass release rate	kg/s			4.12E-03	4.13E-03	4.15E-03	3.95E-03	4.83E-03	4.23E-04	4.17E-04	4.22E-04	8.12E-03	calculated values match those quoted in DNV report 2008-0073
	MANUALLY ADDED CALCULATIONS/COMPARISONS													
	Observed mass release rate	kg/s			4.41E-03	4.42E-03	4.45E-03	4.22E-03	5.28E-03	4.60E-04	4.50E-04	4.60E-04	8.85E-03	from DNVE report 2008-0073
	Relative deviation Phast predicted/observed	%			-6.6%	-6.5%	-6.7%	-6.5%	-8.5%	-8.0%	-7.3%	-8.4%	-8.3%	calculated values very close to those quoted in DNV report 2008-0073
	Ratio orifice pressure to stagnation pressure	-			51.5%	51.5%	51.5%	51.5%	50.4%	50.8%	50.9%	50.8%	50.5%	Range 50.5-51.5% compared with Hysis value 52.6% for hydrogen

Table 6-6 Shell hydrogen experiments (0.25, 0.75 and 1 mm) - DISC input and validation

Inputs	"DISC orifice" validation (Shell HSL H2 experiments; Roberts et al.)					<....Default runs ----------->							<no CAP, CD=1 ---------------------------->			
Input Index	Description	Units	Limits Lower	Upper	RUN6	RUN7	RUN8	RUN9	RUN10	RUN11	RUN14	RUN16	RUN7NCD1	RUN9NCD1	RUN14NCD1	Comments
	Material															
N	Stream name	-			Hydrogen											
	Storage state															
3	Gauge pressure	Pa	0		1.18E+07	9.90E+06	9.80E+06	9.20E+06	9.30E+06	7.60E+06	4.90E+06	5.00E+06	9.90E+06	9.20E+06	4.90E+06	Table 1 Roberts - converted from given pressures in bara (reduced with 1 bar)
4	Temperature	K	10	1000	288.15	287.15	287.15	286.65	286.15	286.15	285.65	287.65	287.15	286.65	285.65	Table 1 Roberts - convert from Celsius to Kelvin
	Vessel data															
7	Orifice diameter	m	1.00E-04	50	3.00E-03			4.00E-03	4.00E-03	4.00E-03		4.00E-03		4.00E-03		Table 1 Roberts - 3mm or 4mm orifice (27mm thick stainless plug with drilled hole)
8	Liquid head	m	0		0											not used
	Atmospheric expansion data															
9	Atmospheric pressure	Pa	50000	120000	101325											presumed value
10	Atmospheric temperature	K	10		288.15	287.15	287.15	286.65	286.15	286.15	285.65	287.65	287.15	286.65	285.65	presumed value = reservoir temperature
11	Atmospheric humidity	-	0	1	0.7											presumed value; not relevant
12	Wind speed	m/s	0		0											not relevant for discharge
	PARAMETERS (values to be changed by expe	**Ratio orifice/stagn. pres.**			5.13E-01	5.15E-01	5.15E-01	5.15E-01	5.15E-01	5.17E-01	5.20E-01	5.20E-01	5.15E-01	5.15E-01	5.20E-01	Range 51.5-52% close to Hysis value of 52.6% for hydrogen
19	Is discharge coefficient specified? TRUE = Specified	-			FALSE								TRUE	TRUE	TRUE	TRUE --> more in line with AEROPLUME (expected to overpredict flowrate)
21	Input discharge coefficient	-	0	1	1								1	1	1	
22	ATEX expansion method (0 = min thrm change, 1 = isentropic, 2 = cons moment)	-	0	2	2											
26	Maximum velocity capping method (0 = user input, 1 = sonic velocity)	-	0	1	0											
26	Maximum velocity	m/s	10	2500	500								2500	2500	2500	
Outputs		**Flow rate DISC**			4.49E-02	3.79E-02	3.75E-02	6.28E-02	6.36E-02	5.22E-02	1.92E-02	3.46E-02	4.39E-02	7.28E-02	2.22E-02	From DISC calculations below
Output Index	**Description**	**Flow rate AEROPLUME**			0.053	0.045	0.044	0.074	0.0075	0.061	0.022	0.04	0.045	0.074	0.022	From AEROPLUME results in Table 1 Roberts (presuming discharge coefficient Cd=1?)
		Ratio DISC/AEROPLUME			8.47E-01	8.43E-01	8.53E-01	8.49E-01	8.47E+00	8.56E-01	8.72E-01	8.66E-01	9.76E-01	9.84E-01	1.01E+00	Close to value of DISC discharge coefficient!!
	ERROR STATUS				***WARN***	***WARN***	***WARN***	***WARN***	***WARN***	***WARN***	***WARN***	***WARN***	***OK***	***OK***	***OK***	
	Release state															
1	Pressure	Pa			11901325	10001325	9901325	9301325	9401325	7701325	5001325	5101325	10001325	9301325	5001325	
2	Temperature	K			288.15	287.15	287.15	286.65	286.15	286.15	285.65	287.65	287.15	286.65	285.65	
3	Liquid fraction (MASS basis)	kg/kg			0	0	0	0	0	0	0	0	0	0	0	
	Orifice state															
5	Pressure	Pa			6103583	5148242	5097804	4794464	4844728	3982572	2600750	2652651	5148242.439	4794463.802	2600749.673	
6	Temperature	kg/kg			237.2747	236.676	236.689	236.3455	235.9105	236.1348	236.0768	237.7503	236.6760092	236.3454942	236.0768237	
7	Liquid fraction (MASS basis)	-			0.00E+00	0	0	0	0	0	0	0	0	0	0	
8	Velocity	m/s			1241.723	1230.125	1229.616	1225.577	1225.104	1216.417	1201.572	1206.078	1230.12495	1225.577268	1201.57229	
9	Vena contracta diameter	m			2.79E-03	2.79E-03	2.79E-03	3.72E-03	3.72E-03	3.72E-03	2.79E-03	3.72E-03	3.00E-03	4.00E-03	3.00E-03	
	Final (post-expansion) state															
10	Temperature	K			285.3833	283.3728	283.3207	282.502	282.0472	281.1699	279.29	281.3579	143.0877983	143.107301	145.408693	
11	Liquid fraction (MASS basis)	kg/kg			0	0.00E+00	0	0	0	0	0	0	0.00E+00	0	0	
12	Velocity	m/s			500	500	500	500	500	500	500	500	2041.995611	2035.788458	1997.439016	
	ATEX outputs															
16	ATEX expansion method (1 = isentropic, 2 = cons momentum)	-			2	2	2	2	2	2	2	2	2	2	2	
17	Expanded diameter	m			3.65E-02	3.34E-02	3.32E-02	4.29E-02	4.31E-02	3.90E-02	2.36E-02	3.18E-02	1.26E-02	1.63E-02	9.16E-03	
18	Expansion energy	J/kg			Undefined	Undefined	Undefined	Undefined	Undefined	Undefined	Undefined	Undefined	Undefined	Undefined	Undefined	
19	Partial expansion energy	J/kg			Undefined	Undefined	Undefined	Undefined	Undefined	Undefined	Undefined	Undefined	Undefined	Undefined	Undefined	
	Other data															
20	Discharge coefficient	-			0.862445	0.863014	0.863043	0.863201	0.863161	0.863584	0.863815	0.863859	1	1	1	
21	Mass release rate	kg/s			4.49E-02	3.79E-02	3.75E-02	6.28E-02	6.36E-02	5.22E-02	1.92E-02	3.46E-02	4.39E-02	7.28E-02	2.22E-02	

Table 6-7 Shell hydrogen experiments (3, 4 mm) – DISC input and verification against AEROPLUME

UDM validation (Shell HSL H2 experiments; Roberts et al.)	DNV MODEL UDM			<Default (with cap, CD calc.>			<--- with cap, CD=1 ------->			< no cap, CD calculated -->			<no velocity cap, CD=1 ------------->			
Description	Units	Limits		RUN7	RUN9	RUN14	RUN7CD1	RUN9CD1	RUN14CD1	RUN7NC	RUN9NC	RUN14NC	RUN7NCD1	RUN9NCD1	RUN14NCD1	COMMENTS
		Lower	Upper													
RELEASE DATA																
General inputs																
Flag: release type (instantaneous =1, continuous (old) = 2, time-varying =3)		1	3	2												steady-state release
Released material name (from material database)				Hydrogen												
Number of observers = number of source term points (time varying only)		2	161	2												
Release observer arrays																
Observer release time (time-varying) or duration (cont. old)	s	0		60												60s travel time beyond furthest data point of 11m
flowrate at observer time (non-instantaneous only)	kg/s	1.00E-06	1.00E+05	3.79E-02	6.28E-02	1.92E-02	4.39E-02	7.28E-02	2.22E-02	3.79E-02	6.28E-02	1.92E-02	4.39E-02	7.28E-02	2.22E-02	From DISC (default Cd or Cd=1)
Initial mass flowrate of air mixed in (non-instantaneous only)	kg/s	0	1.00E+05	0												
State flag (1 - temperature, 6 = liquid fraction)		1	6	1												
Temperature of release component	K	10	900	283.4	282.5	279.3	283.4	282.5	279.3	143.1	143.1	145.4	143.1	143.1	145.4	From ATEX (with or without cap)
Release velocity (non-instantaneous only)	m/s	0	2500	500.00						2042	2036	1997	2042	2036	1997	From ATEX (with or without cap)
Radius for pool source (≤ 0 not a pool source)	m		1000	0												
Release height, angle and impingement																
Release height	m	0		1.5												Roberts paper page2, 1.5m above test pad
Release angle [0 = horizontal, pi/2 = vertical upwards; cont.only]	radians	-1.571	1.571	0												Roberts paper page2, horizontal release
Impingement flag (0 -horizontal, 1 - angled, 2 - vertical, 3 - along ground, 4 - impinged, 5 - angled fron		0	5	1												
AMBIENT DATA																
Pasquill stability class (1-A,2-A/B,3-B,4-B/C,5-C,6-C/D,7-D,8-E,9-F,10-G); 0 = use																
Monin-Obukhov length	-	1	10	7												Presumed
Monin-Obukhov length (stable > 0, unstable <0, neutral = 1E+05)	m	-1.00E+05	1.00E+05	1.00E+05												Not yet used
Wind speed at reference height	m/s	0.1	50	1	3	3		3	3		3	3		3	3	Table 5-1 DNVE paper, for RUN7 Roberts Fig4b
Reference height for windspeed	m	0.1	100	1.5												Roberts page 2 (1.5m high, 12.5m from orifice)
Temperature at reference height	K	200	350	287.15	286.65	285.65		286.65	285.65		286.65	285.65		286.65	285.65	Presume equal to release temperature
Pressure at reference height	N/m2	50000	120000	101325												presumed value
Reference height for temperature and pressure	m	0	100	0												presumed value
Atmospheric humidity (fraction)	-	0	1	0.7												presumed value
SUBSTRATE DATA																
Surface roughness length	m	0.0001	3	0.01												PRESUMED VALUE
Dispersing surface type (1-land,2-water)		1	2	1												
Temperature of dispersing surface	K	200	500	287.15	286.65	285.65		286.65	285.65		286.65	285.65		286.65	285.65	Presume equal to ambient temperature
AVERAGING TIME																
Averaging time	s	1	3600	18.75												

Table 6-8 Shell hydrogen experiments (3, 4 mm) – UDM input

6.2.3 Large orifice (3 and 4 mm; with concentration measurements)

Secondly eight tests (tests 6-11, 14 and 16) are considered corresponding to larger orifice diameters (3 or 4 mm) and for which the horizontal release direction is closely aligned with the wind direction (no crosswind release). Concentration measurements are available, but flow rate measurements are not available. For these tests the stagnation pressure varies between 49 barg and 118 barg, while the temperature is in the range 12.5-15C.

Discharge

Table 6-7 includes DISC input and output data (orifice scenario) for the above tests:

- The column RUN6 contains all input data for test 6, while deviations to these input data are given only in the subsequent columns. The first 8 data columns include results for tests 6-11, 14 and 16 for which the default Phast DISC assumptions are applied, i.e. the ATEX post-expansion velocity cap of 500 m/s is applied and the discharge coefficient C_d is calculated. The last three columns of the table include results for tests 7, 9 and 14 for which the discharge coefficient C_d is prescribed and no ATEX velocity cap is applied. In this aspect note that the ATEX velocity cap only affects the post-expansion data after expansion to atmospheric pressure (temperature and velocity), while the discharge coefficient C_d only affects the flow rate and not the post-expansion data.

- Removal of the velocity cap, causes the predicted post-expansion velocity to increase from 500 m/s to around 2000 m/s, while the post-expansion temperature decreases from around 280 K to around 145K. Thus removal of the velocity cap results in considerably larger post-expansion velocity and substantial more cooling (presuming conservation of mass, momentum and energy).

- The green-coloured cells in Table 6-7 include a verification of the predicted flow rate by DISC against the predicted value of the HGSYSTEM model AEROPLUME as reported by Roberts et al. (2006)[/20/]. It is seen that very close agreement with AEROPLUME is obtained assuming C_d=1, while using the default calculated C_d (approximately 0.86) the DISC flow rate is about 14% lower. Thus it appears that the AEROPLUME model applies the conservative value C_d = 1.

Dispersion

For tests 7, 9, 14 the experimental measurements of the concentrations have been approximated from Figure 3.1 contained in the paper of Skottene and Holm[/19/]. These measurements are taken along the release axis (i.e. at 1.5 m height) and distances 3, 4, 5, 6, 7, 8, 9, 10, 11 m from the release orifice.

Table 6-8 includes UDM input corresponding to tests 7, 9, 14:

- Input data for the flow rate, post-expansion velocity and post-expansion diameter are obtained from the above DISC runs (with or without velocity cap, discharge coefficient C_d calculated or C_d=1).
- No information is found regarding the stability and the surface roughness; neutral conditions (stability class D) and the surface roughness 0.01 m is presumed.[17] It was confirmed that the concentration decrease with increasing surface roughness (as expected), and that this already slightly affects the results at the measurement locations further downwind. However, without further information, the value of 0.01 m appears to be a reasonable value (corresponding to a relative low value of the surface roughness).
- See the last column of Table 6-8 for further justification of the UDM input data.

Figure 6-7, Figure 6-8 and Figure 6-9 include UDM predictions for tests 7, 9 and 14, respectively. For each of the DISC model assumptions (without and with velocity cap, C_d =1 or calculated) results are given for the centre-line height and concentration as function of downwind distance. UDM results with a velocity cap are given by the blue curves (calculated C_d) and red curves (C_d=1), while results without a velocity cap are given by the green curves (calculated C_d) and purple curves (C_d=1).

The concentration plots include results for both the off-centre line concentration (at the measurement height of 1.5m and zero crosswind distance; indicated by solid lines) and the centre-line concentration (indicated by dashed lines). The concentration plot also includes the observed experimental data at 1.5 m height.

The following is concluded from the figures:

[17] FUTURE. Ideally the original data should be checked (rather than the wind speeds and concentration measurements quoted by the DNV report). In addition dispersion simulations could be carried out for all experiments 6-11, 14, 16 if all input data and concentration measurements could be traced.

- Plume rise
  - Without the velocity cap, the UDM input initial velocity (ATEX post-expansion velocity) is considerably larger and the UDM input initial temperature (ATEX post-expansion temperature) is considerably colder. The faster speed (more initial horizontal momentum) and as well as the colder plume (less buoyancy) result in considerable less plume rise. The larger wind speed (3 m/s versus 1 m/s) results in less plume rise for test 9 than test 7.
  - The smaller flow rate (0.022 versus 0.073 kg/s) results in less plume rise for test 14 than test 9.
  - Also the slightly smaller flow rate (smaller concentrations) results in slightly less plume rise for the runs with calculated C_d than the runs with C_d=1.

- Concentrations
  - Without the velocity cap, the larger initial velocity causes significant larger amount of jet entrainment and therefore significantly smaller concentrations in the near field. For the larger distances the effects of plume rise result in the concentrations at 1.5 m height to be smaller as the centre-line concentrations. For the larger distances the effect of reduced plume rise (and consequently smaller axial distances and less crosswind entrainment) result in the concentrations without cap to be larger as those with cap.
  - The slightly smaller flow rate results in slightly lower concentration for the runs with calculated C_d than the runs with C_d=1.
  - Along the range of experimental data, no significant difference is seen between the centre-line and off-centreline concentrations for the cases without a velocity cap but significant lower off-centreline concentrations (particularly for test 7) are seen at 1.5 m height for the cases without a velocity cap. It is seen from the figure that the model accuracy is improved considerably in the near-field while removing the velocity cap, particularly for tests 7 and 9. Thus removal of the velocity cap improves the predictions.
  - Skottene and Holm (2008) [/19/] do not detail the precise assumptions they have taken for their Phast simulations, and also do not indicate the Phast version they have adopted. Their Phast results (figures 5-2, 5-3, 5-4 in their paper) only slightly differ to our Phast results without a velocity cap.

Table 6-9 includes results of MG and VG values for the hydrogen experiments.

Test	with cap, C_d calc.		with cap, C_d=1		no cap, C_d calc.		no cap, C_d=1	
	MG	VG	MG	VG	MG	VG	MG	VG
7	1.26	1.35	1.13	1.26	1.11	1.01	1.03	1.00
9	1.02	1.06	0.93	1.06	1.23	1.05	1.14	1.02
14	1.13	1.07	1.03	1.05	1.28	1.07	1.17	1.03

Table 6-9 Shell hydrogen experiments (3, 4 mm) - UDM values of MG and VG

Also note that in case the isenthalpic or isothermal option would have been applied for the ATEX expansion, this would have resulted in a higher temperature, consequently more plume rise and therefore smaller concentrations at 1.5 m height. Thus this would have resulted in an increased under-prediction of the results.

Thus the conservation of momentum option in conjunction with removal of the cap results in the most accurate predictions in the near-field and this is in line with our recommendations.

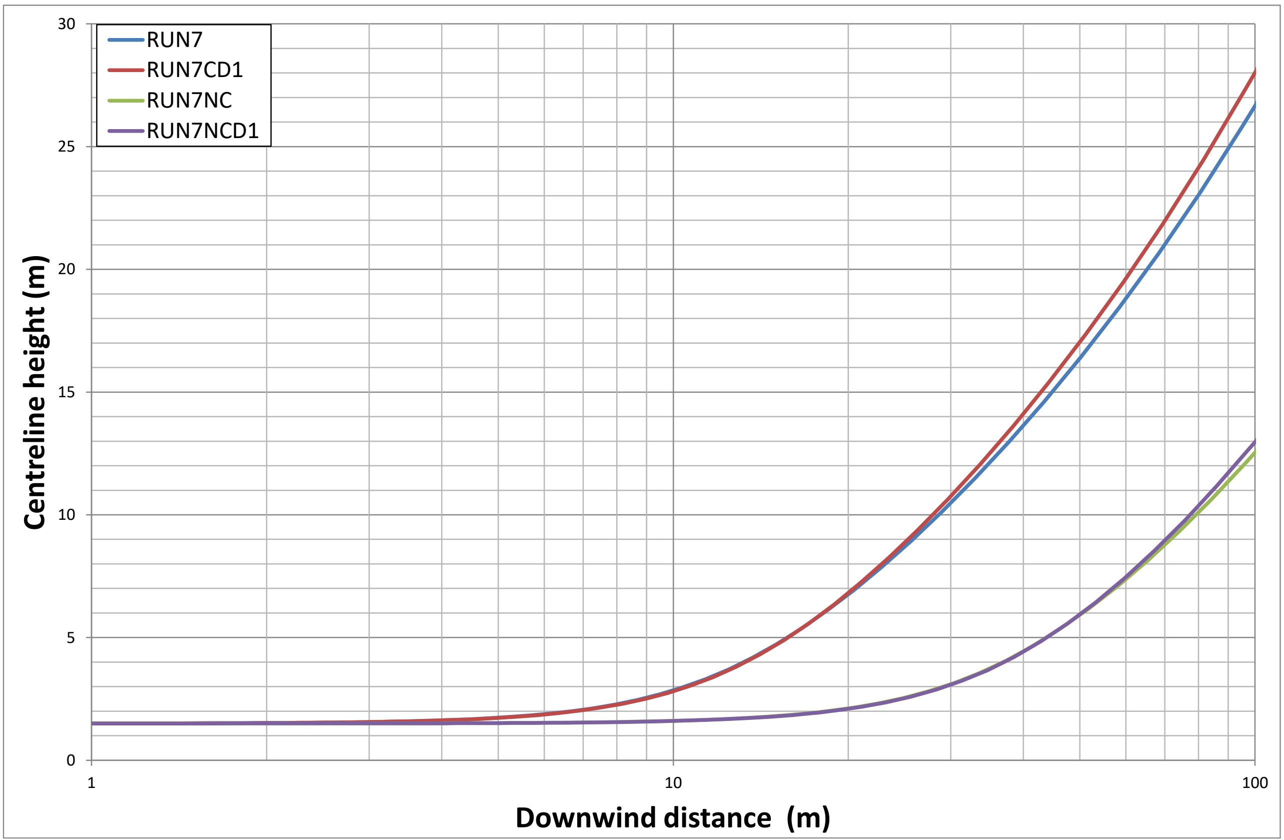

(a) Cloud centre-line height (with or without cap, C_d=1 or calculated)

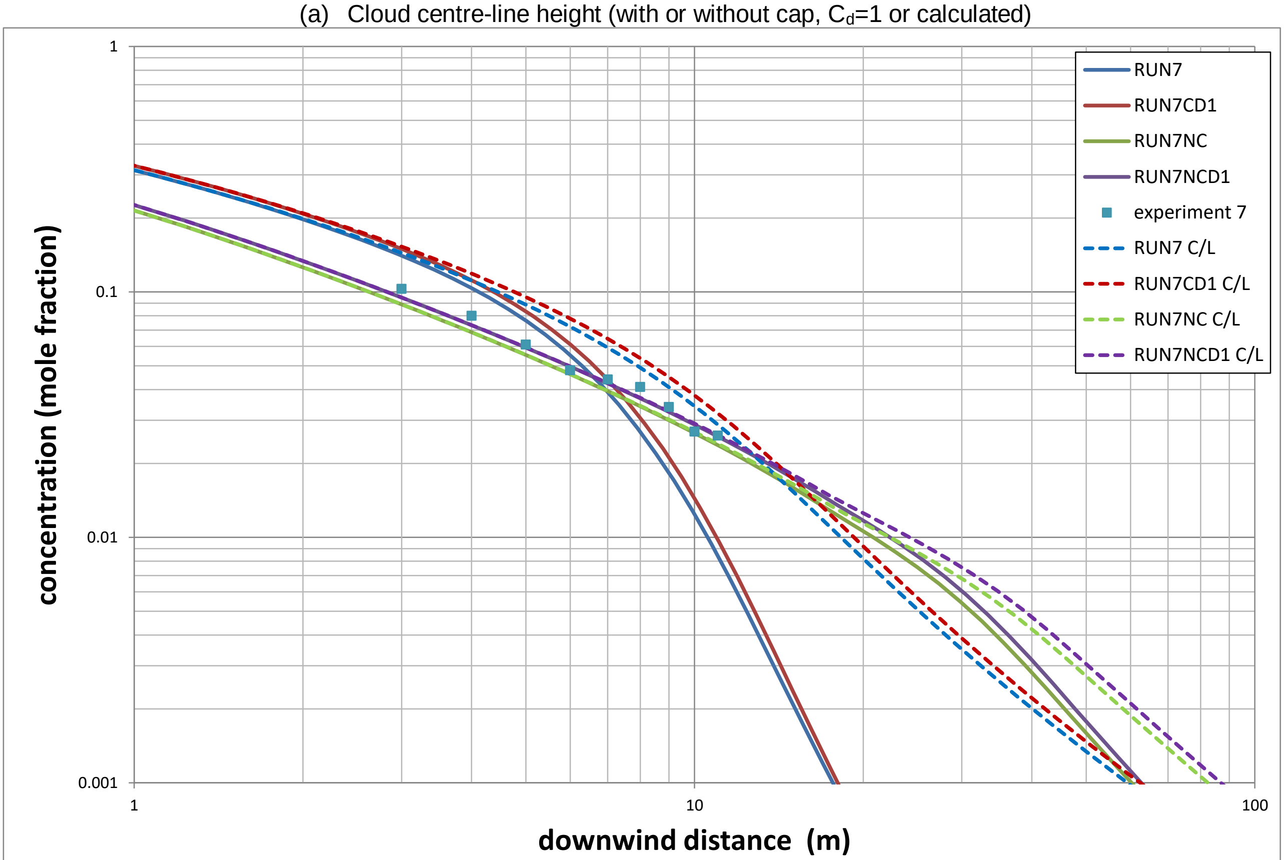

(b) Concentration (with/without cap, C_d=1 or calculated, at 1.5 m height or C/L, measured at 1.5 m)

Figure 6-7 UDM validation against H_2 test 7 (3 mm, 99 barg)

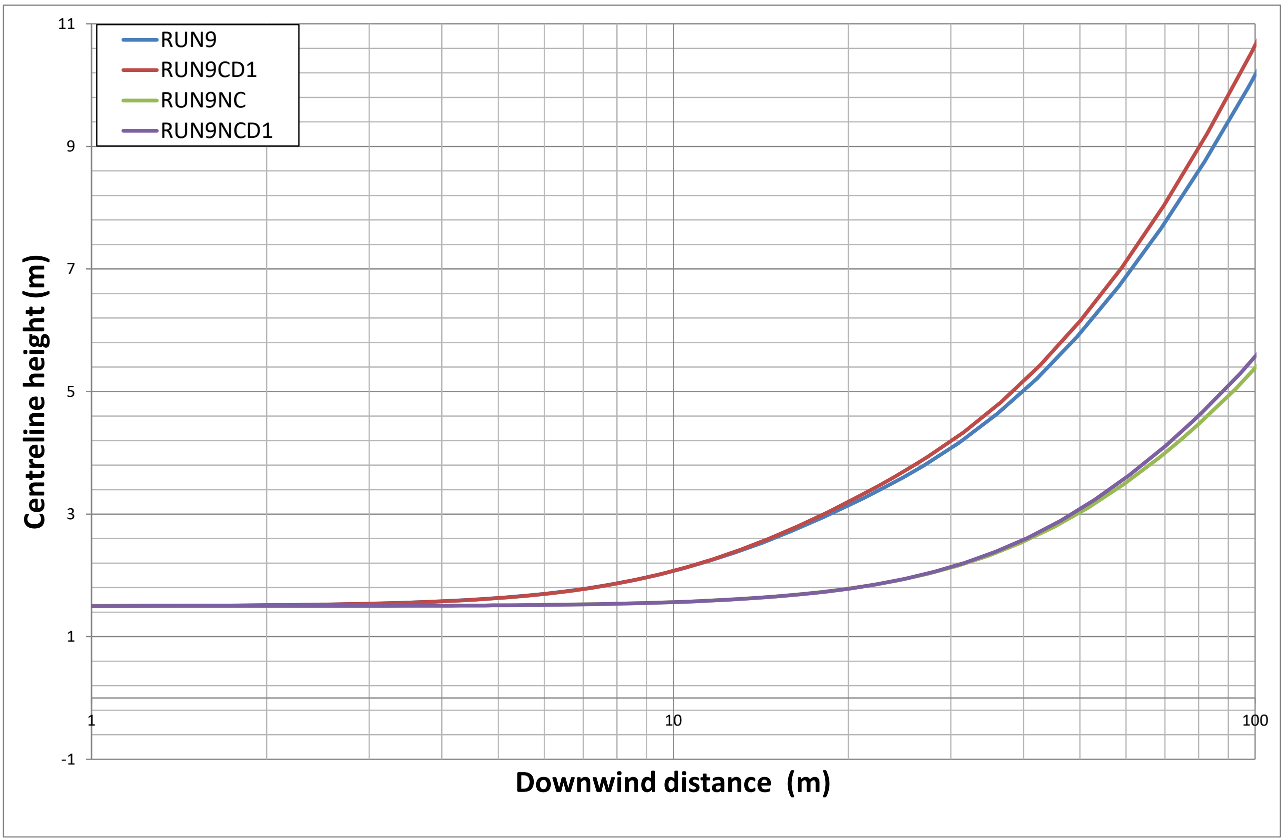

(a) Cloud centre-line height (with or without cap, C_d=1 or calculated)

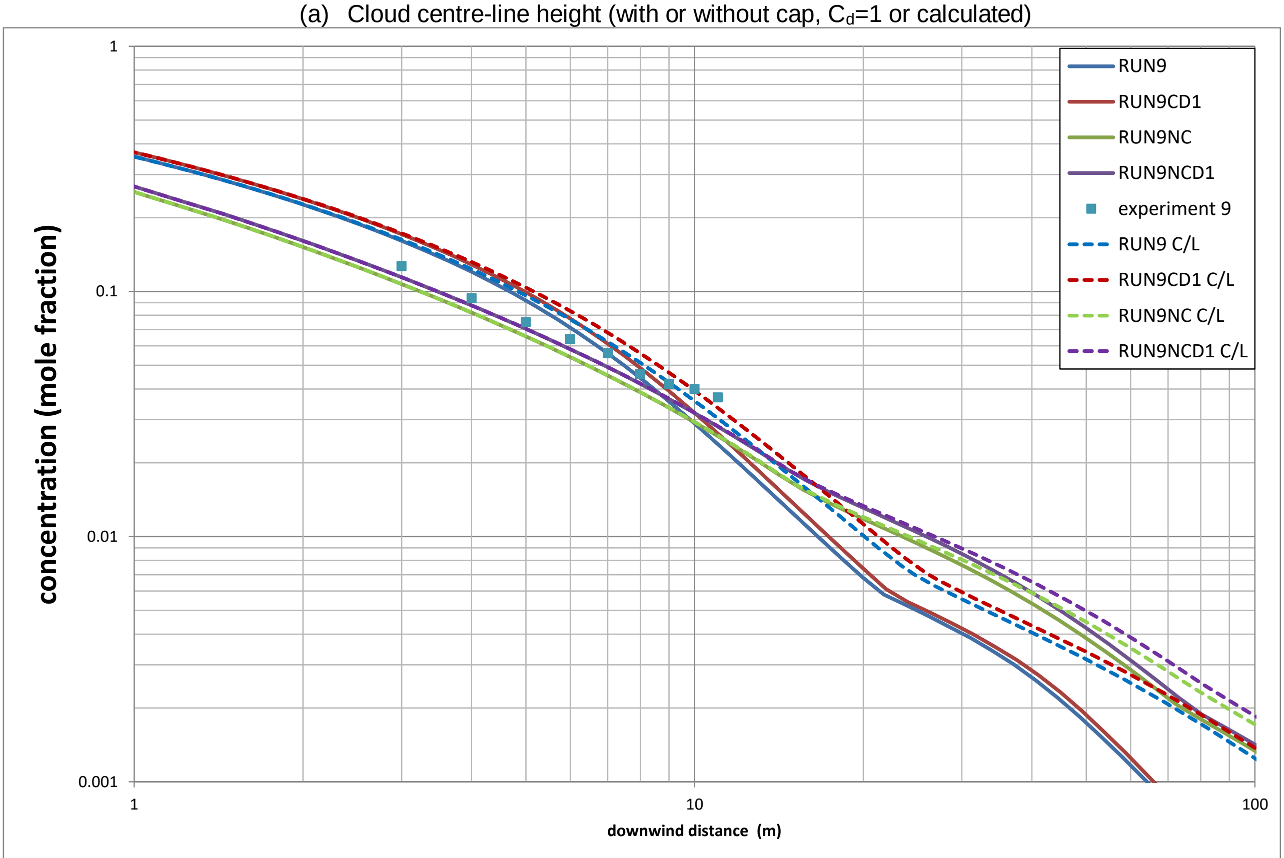

(b) Concentration (with/without cap, C_d=1 or calculated, at 1.5 m height or C/L, measured at 1.5 m)

Figure 6-8 UDM validation against H_2 test 9 (4 mm, 92 barg)

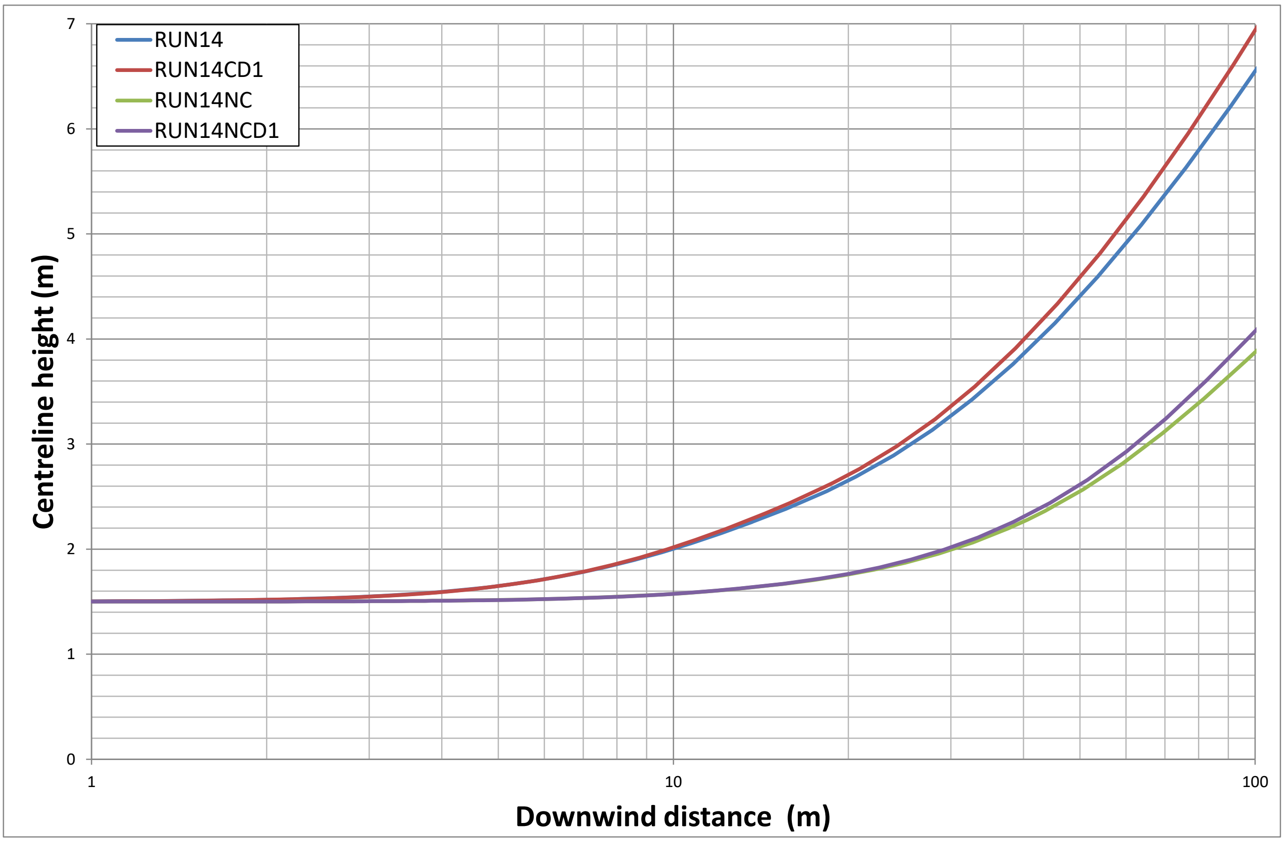

(a) Cloud centre-line height (with or without cap, C_d=1 or calculated)

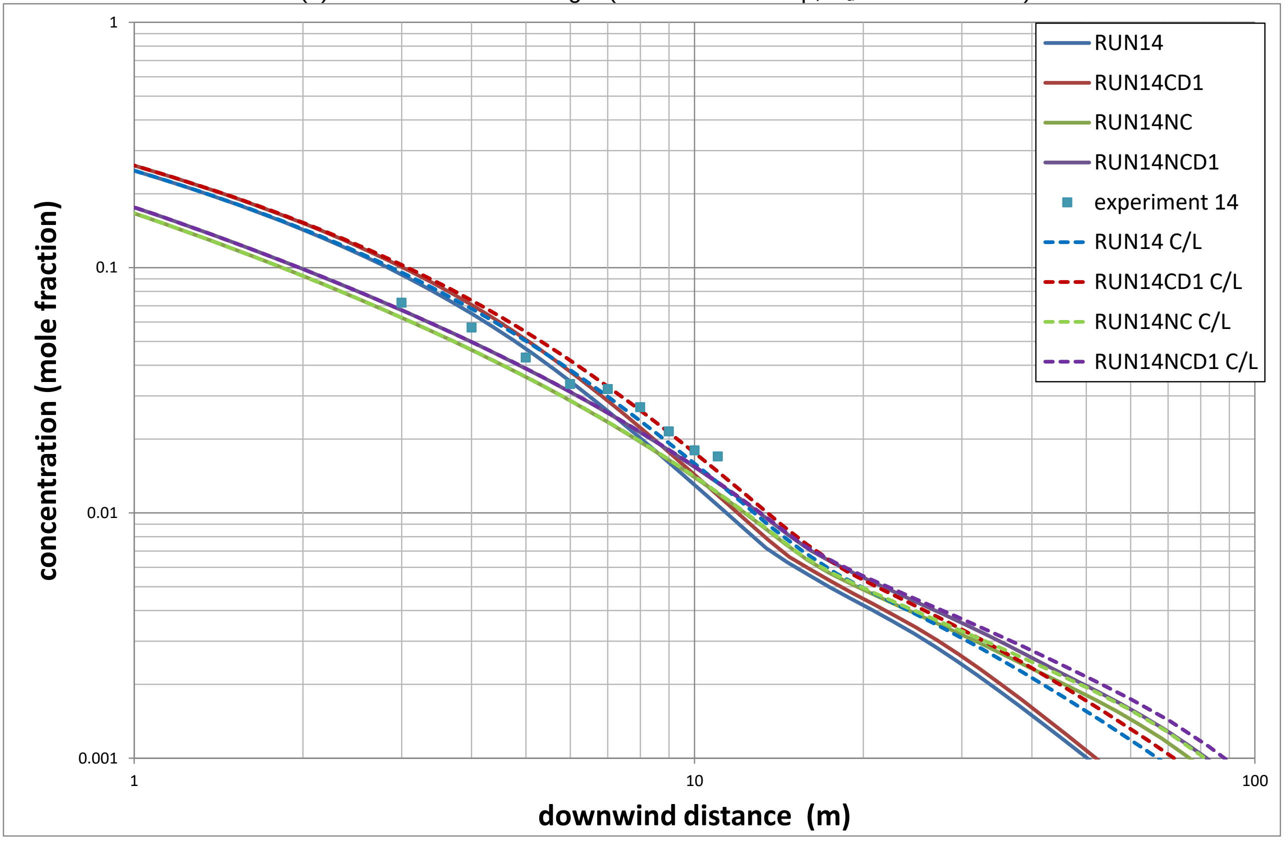

(b) Concentration (with/without cap, C_d=1 or calculated, at 1.5 m height or C/L, measured at 1.5 m)

Figure 6-9 UDM validation against H_2 test 14 (4 mm, 49 barg)

6.3 High-pressure natural-gas and ethylene jets (BG experiments)

See also Section 5.3.1 for a discussion. British Gas carried out experiments for natural-gas and ethylene jets (Birch et al., 1984)[/17/]. The gas jet was released from a nozzle with internal diameter d_o=2.7 mm. The natural gas used was quoted to have a methane content of between 92.0 and 92.4% and a mean molecular weight of 17.32 kg/kmol. In the experiments the gas was sampled continuously from the jet centre-line, and mean concentrations were measured using a rapid chromatograph.

The natural gas was modelled as a mixture of methane and ethane, with a composition such that the mole weight equals 17.32 kg/kmol. This results in a composition of 90.9 mole% CH_4 and 9.1% C_2H_6, i.e. reasonably close to the specified value of 92% of methane content. At 15C and 1 atm., the resulting sonic speed (as output by Phast 6.7) was 422 m/s (versus 421 m/s reported by Birch) and the ratio of specific heats γ=1.29 (versus γ=1.35 reported by Birch et al.).

<u>Discharge</u>

Table 6-10 summarises the associated input and output data for the Phast discharge model DISC using the Phast orifice (leak) scenario. Results are given for natural-gas experiments with stagnation pressures of 3.5, 6, 16, 46 and 71 bara using either a final-velocity cap of 500 m/s (Phast default) or no velocity cap. Also validation results are given for the ethylene experiment with a stagnation pressure of 8 bara.

- It is seen that with increasing stagnation pressure, the vena-contracta pressure increases, the vena contracta temperature decreases, and the vena-contracta velocity slightly decreases. The discharge coefficient C_D increases from 0.83 to 0.87. This is in line with the value of 0.85 stated in Birch (1984). The flow rate increases with increasing pressure.
- The final post-expansion temperature T_f decreases with increasing stagnation pressure. For the natural gas cases the final velocity u_f (without cap of 500 m/s applied) initially increases from 536 m/s to 654 m/s and subsequently decreases to 627 m/s. For the ethylene case the final velocity is less than 500 m/s, and therefore the velocity cap is not applicable.

<u>Dispersion</u>

Table 6-11 includes UDM input data corresponding to the above experiments:

- Input data for the flow rate, post-expansion velocity and post-expansion diameter are obtained from the above DISC runs (with or without velocity cap).
- No information is found regarding the stability and the surface roughness; neutral conditions (stability class D with low wind-speed of 0.1m/s) and the surface roughness 0.01m is presumed
- See the last column of Table 6-11 for further justification of the UDM input data.

For the natural gas experiments, Birch (1984) plotted the reciprocal concentration (1/c, with c being volume fraction of natural-gas) against the scaled axial distance $x/[d_oP^{1/2}]$ and his experimental data could closely be fitted by a straight line. Figure 6-10 includes this experimental fit as well as predictions from the above UDM runs. It is seen that the reciprocal concentration 1/c is slightly over-predicted, and therefore the concentration is under-predicted. The latter under-prediction could also be (partly) caused by under-prediction of the flow rate. The under-prediction is slightly larger for those cases without a cap than with a cap. Also note that the experiment fitted curve (while extrapolating to x=0m) appears to cross the point x=0,c=0 while it SHOULD cross the point x=0,c=1 (100% concentration at the release location). Thus this may indicate some inaccuracy in the concentration measurements. Therefore taking the above into account, it is concluded that close agreement is obtained with the experimental data for both with and without a cap. The effect of the cap is very much smaller for the natural gas experiments than for the hydrogen experiments, since the final velocities are now not very significantly exceeding the cap.

Birch (1984) also plotted the reciprocal concentration (1/c) versus the scaled axial distance $x/[d_oP^{1/2}]$ for the ethylene experiment. Figure 6-11 includes the experimental data as well as predictions from the above UDM runs. It is again seen that the reciprocal concentration 1/c is slightly over-predicted, and therefore the concentration is slightly under-predicted.

Inputs	"DISC orifice" validation (BG gas jet experiments; Birch et al. 1984)				<NG default runs, with cap ----------->						<NG, no CAP ----------------------------->						ethylene	
Input Index	Description	Units	Limits Lower	Upper	3.5bara	6bara	16bara	31bara	46bara	71bara	3.5baraNC	6baraNC	16baraNC	31baraNC	46baraNC	71baraNC	8bar_eth	Comments
	Material																	
N	Stream name	-			NG_Birch												ethylene	natural gas = 90.9%CH4,9.1%C2H6-> mole weight 17.32 from Birch (1984)
	Storage state																	
3	Gauge pressure	Pa	0		2.49E+05	4.99E+05	1.50E+06	3.00E+06	4.50E+06	7.00E+06	2.49E+05	4.99E+05	1.50E+06	3.00E+06	4.50E+06	7.00E+06	6.80E+05	absolute pressures form Figure 5 Birch(1984) reduced with ambient pressu
4	Temperature	K	10	1000	288.15													presumed (since NG&ethylene data evaluated at 15C and 1atm)
	Vessel data																	
7	Orifice diameter	m	1.00E-04	50	2.70E-03													2.7mm - internal nozzle diameter (Birch, 1984)
8	Liquid head	m	0		0													not used
	Atmospheric expansion data																	
9	Atmospheric pressure	Pa	50000	120000	101325													presumed value
10	Atmospheric temperature	K	10		288.15													presumed value = reservoir temperature
11	Atmospheric humidity	-	0	1	0.7													presumed value; not relevant
12	Wind speed	m/s	0		0													not relevant for discharge
	PARAMETERS (values to be changed by expert users only)																	
19	Is discharge coefficient specified? TRUE = Specified	-			FALSE													
21	Input discharge coefficient	-	0	1	1													
22	ATEX expansion method (0 = min thrm change, 1 = isentropic, 2 = cons moment)	-	0	2	2													
26	Maximum velocity capping method (0 = user input, 1 = sonic velocity)	-	0	1	0													
26	Maximum velocity	m/s	10	2500	500						2500	2500	2500	2500	2500	2500		
Outputs																		
Output Index	**Description**	**Units**																
	ERROR STATUS				***WARN***	***WARN***	***WARN***	***WARN***	***WARN***	***WARN***	***OK***	***OK***	***OK***	***OK***	***OK***	***OK***	***OK***	
	Release state																	
1	Pressure	Pa			350000	600000	1600000	3100000	4600000	7100000	350000	600000	1600000	3100000	4600000	7100000	781325	
2	Temperature	K			288.15	288.15	288.15	288.15	288.15	288.15	288.15	288.15	288.15	288.15	288.15	288.15	288.15	
3	Liquid fraction (MASS basis)	kg/kg			0	0	0	0	0	0	0	0	0	0	0	0	0	
	Orifice state																	
5	Pressure	Pa			190459	326467.8	870294.6	1683724	2491478	3810374	190458.9968	326467.7532	870294.6102	1683724	2491478	3810374	431563.69	
6	Temperature	kg/kg			250.0789	249.8542	248.9818	247.7086	246.5202	244.8194	250.0789235	249.8541891	248.9817605	247.7086	246.5202	244.8194	253.46203	
7	Liquid fraction (MASS basis)	-			0.00E+00	0	0	0	0	0	0	0	0	0	0	0	0	
8	Velocity	m/s			394.7264	393.5542	388.7927	381.7916	375.0483	365.1214	394.7264186	393.5541847	388.7927198	381.7916	375.0483	365.1214	301.34416	
9	Vena contracta diameter	m			2.45E-03	2.49E-03	2.51E-03	2.52E-03	2.52E-03	2.52E-03	2.45E-03	2.49E-03	2.51E-03	2.52E-03	2.52E-03	2.52E-03	2.50E-03	
	Final (post-expansion) state																	
10	Temperature	K			226.2818	224.8091	218.8261	209.5875	200.074	183.8607	217.0186452	197.0586232	175.2681784	164.7936	157.8802	147.9377	193.99678	
11	Liquid fraction (MASS basis)	kg/kg			0	0.00E+00	0	0	0	0	0.00E+00	0.00E+00	0	0	0	0	0	
12	Velocity	m/s			500	500	500	500	500	500	536.0286289	601.1010634	651.1753858	654.6792	646.5661	626.8884	484.21122	
	ATEX outputs																	
16	ATEX expansion method (1 = isentropic, 2 = cons momentum)	-			2	2	2	2	2	2	2	2	2	2	2	2	2	
17	Expanded diameter	m			2.85E-03	3.77E-03	6.18E-03	8.52E-03	1.03E-02	1.24E-02	2.69E-03	3.22E-03	4.83E-03	6.58E-03	7.98E-03	9.93E-03	3.61E-03	
18	Expansion energy	J/kg			Undefined	Undefined	Undefined	Undefined	Undefined	Undefined	Undefined	Undefined	Undefined	Undefined	Undefined	Undefined	Undefined	
19	Partial expansion energy	J/kg			Undefined	Undefined	Undefined	Undefined	Undefined	Undefined	Undefined	Undefined	Undefined	Undefined	Undefined	Undefined	Undefined	
	Other data																	
20	Discharge coefficient	-			0.826128	0.850424	0.866651	0.870255	0.870749	0.869123	0.826127827	0.850423574	0.866650879	0.870255	0.870749	0.869123	0.8604714	
21	Mass release rate	kg/s			2.98E-03	5.28E-03	1.45E-02	2.89E-02	4.39E-02	7.05E-02	2.98E-03	5.28E-03	1.45E-02	2.89E-02	4.39E-02	7.05E-02	8.90E-03	

Table 6-10 BG natural gas and ethylene experiments (2.7 mm) - DISC input and results

UDM validation (BG natural gas experiments; Birch et al. 1984)	DNV MODEL UDM				<....Default runs (with cap) ----------->						<no CAP ---------------------------->							
Description	Units	Dim	Limits		3.5bara	6bara	16bara	31bara	46bara	71bara	3.5baraNC	6baraNC	16baraNC	31baraNC	46baraNC	71baraNC	8bar_eth	Comments
		3	Lower	Upper														
RELEASE DATA																		
General inputs																		
Flag: release type (instantaneous =1, continuous (old) = 2, time-varying =3)			1	3	2													steady-state release
Released material name (from material database)					NG_Birch												ethylene	NG mixture (90.9%CH4,9.1%C2H6)
Number of observers = number of source term points (time varying only)			2	161	2													
Release observer arrays																		
Observer release time (time-varying) or duration (cont. old)	s		0		60													60s travel time well beyond furthest data point 0.5m
flowrate at observer time (non-instantaneous only)	kg/s		1.00E-06	1.00E+05	2.98E-03	5.28E-03	1.45E-02	2.89E-02	4.39E-02	7.05E-02	2.98E-03	5.28E-03	1.45E-02	2.89E-02	4.39E-02	7.05E-02	8.90E-03	From DISC (cap does not affect results)
Initial mass flowrate of air mixed in (non-instantaneous only)	kg/s		0	1.00E+05	0													
State flag (1 - temperature, 6 = liquid fraction)			1	6	1													
Temperature of release component	K		10	900	226.28176	224.80911	218.82615	209.5875	200.074	183.86065	217.01865	197.05862	175.26818	164.79362	157.8802	147.9377	193.9968	From ATEX (with or without cap)
Release velocity (non-instantaneous only)	m/s		0	2500	500	500	500	500	500	500	536.02863	601.10106	651.17539	654.67918	646.5661	626.8884	484.2112	From ATEX (with or without cap)
Radius for pool source (≤ 0 not a pool source)	m			1000	0													
Instantaneous only																		
release mass (instantaneous only)	kg		1.00E-04	1.00E+09	80													
mass of air (instantaneous only)	kg		0	1.00E+09	0													
Expansion energy (instantaneous only)	(J/kg)		0	12500	0													
Release height, angle and impingement																		
Release height	m		0		1													presumed (1m)
Release angle [0 = horizontal, pi/2 = vertical upwards; cont.only]	radians		-1.571	1.571	0													horizontal flow
Impingement flag (0 -horizontal, 1 - angled, 2 - vertical, 3 - along ground, 4 - impinged, 5 - angled from hori			0	5	1													
AMBIENT DATA																		
Pasquill stability class (1-A,2-A/B,3-B,4-B/C,5-C,6-C/D,7-D,8-E,9-F,10-G); 0 = use Monin-Obukhov length	-		1	10	7													Presumed
Wind speed at reference height	m/s		0.1	50	0.1													Preusmed low value (should not affect near-field result
Reference height for windspeed	m		0.1	100	1													presumed value (show nor affect near-field)
Temperature at reference height	K		200	350	288.15													Presume equal to release temperature
Pressure at reference height	N/m2		50000	120000	101325													presumed value
Reference height for temperature and pressure	m		0	100	0													presumed value
Atmospheric humidity (fraction)	-		0	1	0.7													presumed value
SUBSTRATE DATA																		
Surface roughness length	m		0.0001	3	0.01													PRESUMED VALUE
Dispersing surface type (1-land,2-water)			1	2	1													
Temperature of dispersing surface	K		200	500	288.15													Presume equal to ambient temperature
AVERAGING TIME																		
Averaging time	s		1	3600	18.75													

Table 6-11 BG natural gas and ethylene experiments (2.7 mm) - UDM input

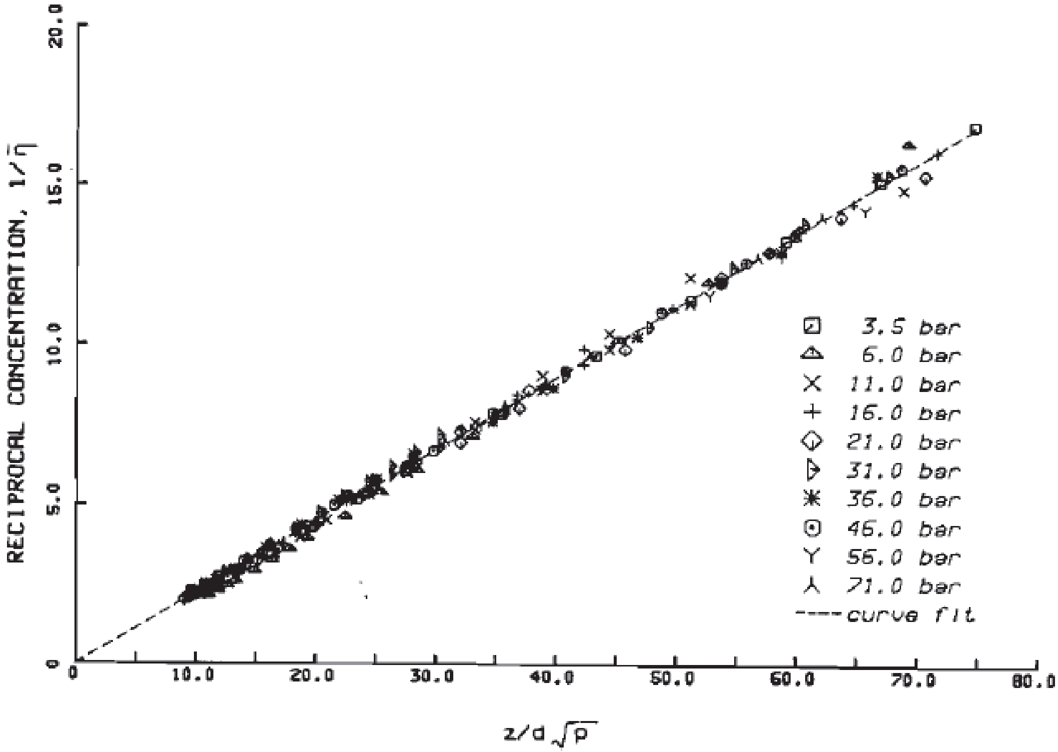

(a) Curve fit of experimental data (Figure from Birch, 1984)

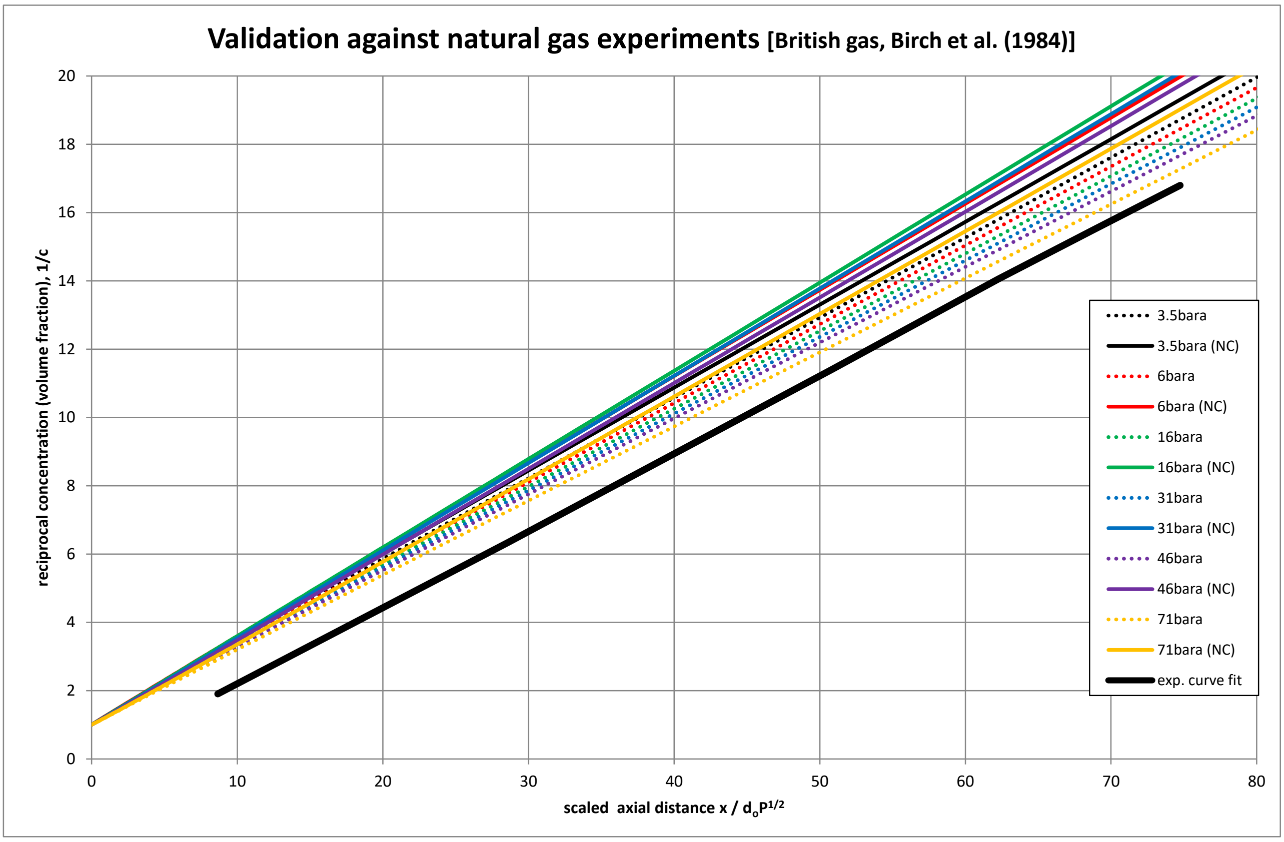

(b) UDM model validation

Figure 6-10 UDM validation against BG natural-gas experiments (pressures P=3.5-71bara)

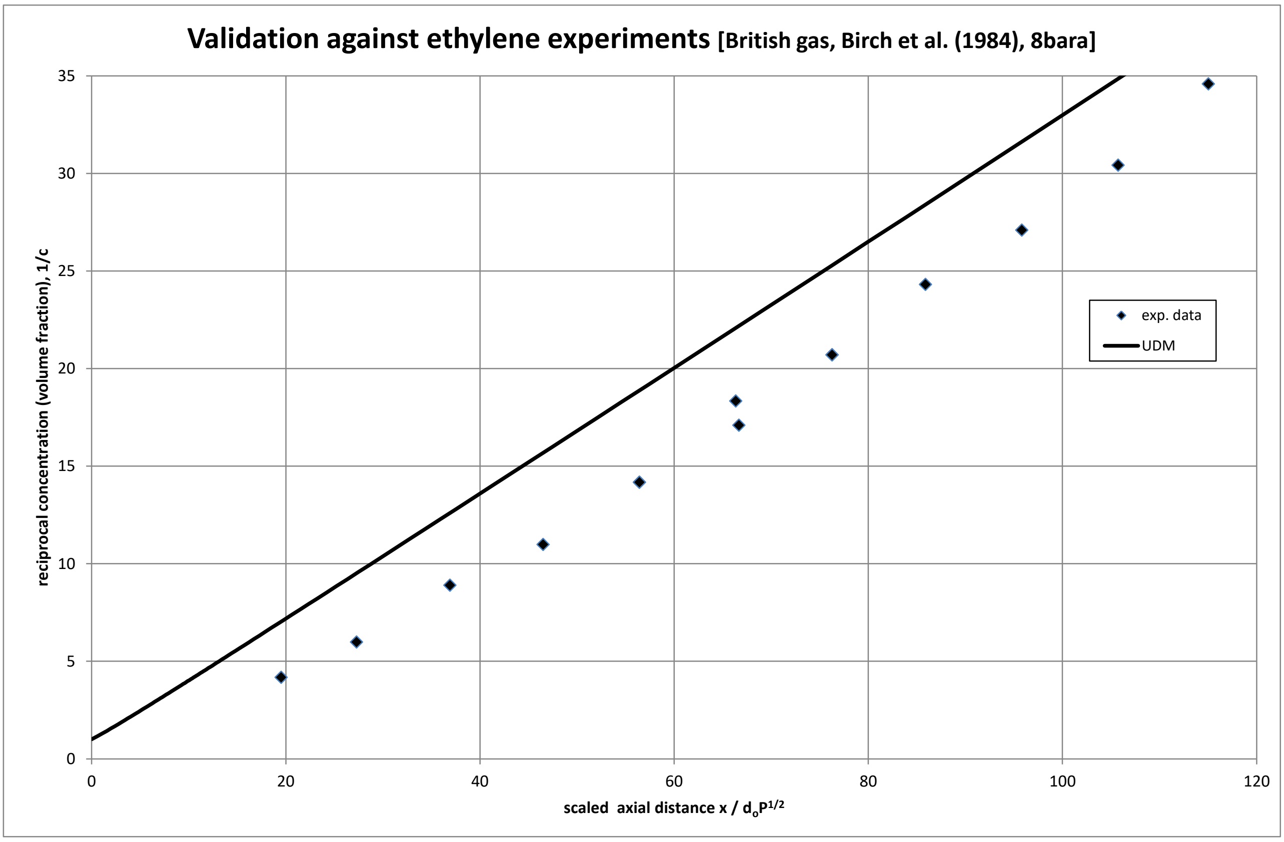

Figure 6-11 UDM validation against BG ethylene experiment (pressure P=8bara)

7 DISCUSSION

The following range of expansion methods can be considered:

1. Britter[7] indicates that the model imposing conservation of mass, momentum and energy should always be used. Subject to the initial reduction of the problem (1-dimensional, homogeneous flow and thermal equilibrium), no further approximations have been introduced, and therefore the Equations **(7)**,**(8)**,**(9)** may be referred to as the *exact* equations. This model corresponds to the HGSYSTEM model, the 'conservation of momentum' model in Phast, and the model described in the TNO Yellow Book[9]. It is also in agreement with recommended logic by Yüceil and Ötügen (2002)[22] applied to sonic air jets. In Phast the vapour enthalpy, liquid enthalpy and density calculations [see Equations **(10)** and **(11)**] are carried out 'exact' using a DIPPR material property database.

   However there is confusion whether the control volume should apply to the expansion from vena contracta to ambient conditions (as presuming in DISC/ATEX) or whether to the expansion from orifice to ambient conditions, which is relevant in case $C_d < 1$ (for leak scenario; not for line rupture and long pipelines). Note that the speed of sound is imposed by DISC/ATEX of a sonic jet at the vena contracta and not at the orifice.

2. The isenthalpic formulation relies on the change in the kinetic energy being small (hence ignored) compared with the change in enthalpy, in which case the energy equation **(9)** reduces to conservation of enthalpy across the flashing zone. Clearly a weakness exists if the change in kinetic energy across the flashing zone – which is known unambiguously from equation **(8)** - is significant.

3. The 'isentropic' formulation as referred to by Britter, replaces the energy equation **(9)** with an isentropic assumption. Thus it applies conservation of mass, momentum and entropy. The 'isentropic' formulation as referred to as an additional option in Phast, replaces the momentum equation **(8)** with the isentropic assumption **(14)**. Thus it applies conservation of mass, entropy and energy.

4. Birch et al. (1987)[21] considers conservation of mass and momentum. However their equations differ from ATEX since they appear to consider a control volume between orifice and final conditions, with e.g. speed of sound imposed at the orifice and not the vena contracta. Furthermore they do not impose conservation of energy or entropy, but simplistically presume for gas jets that the final temperature is close to the initial stagnation temperature which they quote is based on experimental evidence. Thus this contradicts the above approaches.

5. Regarding the choice of the appropriate expansion model for non-instantaneous releases the following is noted:

   - The application of the above equations (conservation of mass, momentum, energy) may lead to excessive post-expansion velocities for cases where turbulence becomes important (possible occurrence of supersonic speeds and shock waves). To avoid these excessive velocities, Phast adopts a rather arbitrary cut-off value for the velocity. Ideally the formulation should be extended to include the effects of turbulence. Moreover, the thermodynamic path may need to include non-equilibrium effects and/or slip. The authors are however not aware of a published and validated formulation, which takes these effects into account. As a result, the above formulation is recommended (with a possible cut-off for post-expansion velocity) until an improved formulation becomes available.

   - For most situations, the 'conservation of momentum' model results in lower post-expansion velocities than the 'isentropic model'.

   - It is also recommended that the near-field dispersion model includes the kinetic energy term. However the current Phast model UDM applies an isenthalpic term instead of a kinetic energy term and this may result in inaccuracies of concentrations in the near field.

   - However in Phast the expansion model applies not only to pipe and orifice models, but also to relief valve and disc rupture calculations. For the latter cases, the 'conservation of momentum' equation produced extremely high results (thousands of m/s)[18], and the 'isentropic' model is giving more reasonable results. On the other hand, the use of the forced liquid leak discharge scenario (metastable liquid) results in un-choked liquid at the orifice, and therefore $u_f = u_o$. As a result a further investigation is required by e.g. a sensitivity analysis. Instead of the isentropic model, also the 'conservation of momentum' model could be considered to be used with a cut-off value for the post-expansion velocity. Note that currently the default in Phast is to use the 'minimum thermodynamic change' option whereby the method with the closest temperature or liquid fraction to the exit is used.

[18] CHECK (JS). To confirm this conclusion by runs for relief valve and disc rupture, and subsequently explain?

- There are weaknesses in the thermodynamic property model which sometimes cause the isentropic model to predict a very low temperature at the end of the expansion.[19]

[19] CHECK (JS). Is this still applicable? Do we have example cases?

8 CONCLUSIONS AND FUTURE WORK

1. For flashing liquid orifice releases, the metastable liquid assumption provides most accurate predictions of the flow rate for most of the available experimental data for orifice releases and this option is also in line with recommendations from the literature (for orifice lengths <0.1m). Furthermore it is conservative compared to the assumption of allowing flashing upstream of the orifice. Thus this option is recommended to be retained as the default Phast assumption.

2. The conservation-of-momentum option in conjunction with the absence of a velocity cap for final post-expansion velocity overall provides the most accurate predictions for near-field concentrations.

    2.1. For liquid releases the velocity cap of 500 m/s is not applicable. For gas releases, the velocity cap is mostly relevant for those gases where the speed of sound is very large, i.e. in particular for hydrogen and up to a lesser extent for natural gas (methane). Thus removal of the velocity cap was shown to significantly increase the accuracy of near-field concentration predictions for hydrogen releases, while there was only a small difference for natural-gas releases. In both cases there is a slight under-prediction of the experimental data.

    2.2. For gas releases, the conservation-of-momentum option is normally selected (using the option of minimum thermodynamic change), since the isentropic option results in larger final post-expansion velocities and hence smaller temperatures. In addition, also isenthalpic or isothermal options are expected to reduce the accuracy for the validation against the hydrogen experiments.

    2.3. For liquid releases, the isentropic option is normally selected using the option of minimum thermodynamic change. In case of rainout, this option is currently recommended to retain to be selected since the Phast rainout correlation for superheated flashing jets is based on a best fit against experimental data using this isentropic option (Witlox and Harper, 2013)[/15/]. However for releases without rainout, the conservation-of-momentum is recommended to be selected. Thus as part of potential future work the Phast rainout correlation for superheated flashing jets is recommended to be modified to provide a best fit against experimental data in conjunction with the conservation-of-momentum option.

3. The UDM dispersion model is currently based on isenthalpic mixing between the released pollutant and the ambient moist air. Thus it does not account for the initial kinetic energy of the released pollutant (velocity uf), and therefore it is inconsistent with the ATEX conservation-of-energy equation **(9)**. Thus the UDM could be considered to be modified with the addition of a kinetic-energy term in conjunction with redoing the UDM model validation. Alternatively ATEX could be modified to impose conservation of enthalpy instead of conservation of energy.

9 REFERENCES

/1/ Witlox, H.W.M. and Bowen, P., "Flashing liquid jets and two-phase dispersion - A review", Work carried out by DNV for HSE, Exxon-Mobil and ICI Eutech, HSE Books, Contract research report 403/2002 (2002)

/2/ Witlox, H.W.M., Harper, M. and Stene, J., "ATEX theory document", Provided as part of Phast/Safeti 6.7 Technical Documentation, DNV, London, May 2011

/3/ Witlox, H.W.M, Harper, M. and Oke, A., "Droplet size theory document", Provided as part of Phast/Safeti 6.7 Technical Documentation (following completion of Phase IV of droplet modelling JIP; including extensive validation results), DNV, London, May 2011

/4/ Witlox, H.W.M., and Holt, A., "A unified model for jet, heavy and passive dispersion including droplet rainout and re-evaporation", International Conference and Workshop on Modelling the Consequences of Accidental Releases of Hazardous Materials, CCPS, San Francisco, California, September 28 – October 1, pp. 315-344 (1999)

/5/ Witlox, H.W.M., Harper, M., and Holt, A., "UDM Technical Reference Manual", Part of Phast 6.7 Technical Documentation, DNV (2011)

/6/ Van den Akker, H.E.A., Snoey, H., and Spoelstra, H., "Discharges of pressurised liquefied gases through apertures and pipes", IchemE Symposium Series 80, pp. E23-E31 (1983)

/7/ Britter, R.E., "Dispersion of two-phase flashing releases - FLADIS field experiments", Report FM89/3 by CERC for EEC Commission DGXII (1995)

/8/ Britter, R.E., 'Dispersion of two-phase flashing releases - FLADIS field experiments; the modelling of pseudo-source for complex releases', Report FM89/2 by CERC for EEC Commission DGXII (1994)

/9/ van den Bosch, C.J.H., and Duijm, N.J., "Methods for calculating physical effects", TNO Yellow Book, Ch. 2, pp. 2.105-2.112 (1997): isentropic versus isenthalpic flash (pp. 2.42,2.106), initial droplet size (2.43,2.56,2.107)

/10/ Britter, R., Weil, J., Leung, J., and Hanna, S., "Toxic Industrial Chemical (TIC) source emissions model improvements for pressurised liquefied gases", Atmospheric Environment 45, pp. 1-25 (2011)

/11/ Jallais, S., and Morainville, A., "Phast limitations and comparison with Explojet", Doc. Ref. No. 118, Air Liquide, Confidential report, 3 December 2007 (2007)

/12/ Ruffin, E., Mouilleau, Y. and Chaineaux, J., "Large scale characterisation of the concentration field of supercritical jets of hydrogen and methane", J. Loss Prev. Process Ind. 9, pp. 279-284 (1996)

/13/ Paris, A., Spicer, T., and Havens, J., "Modeling the initial conditions of two-phase jet flow through an orifice after depressurisation", Mary Kay O'Connor Process Safety Center Symposium, Texas A&M University, College Station (2005)

/14/ Paris, A., "Implementing an experimental program for model validation of initial velocity in aerosol jets", PhD thesis, UMI number 3329179, University of Arkansas (2008)

/15/ Witlox, H.W.M. and Harper, M., "Two-phase jet releases, droplet dispersion and rainout , I. Overview and model Validation, Journal of Loss Prevention in the Process Industries 26, pp. 453-461 (2013).

/16/ Witlox, H.W.M., Harper, M., and Fernandez, M., "UDM validation document", UDM Technical Reference Manual, DNV (2015)

/17/ Birch, A.D., Brown, D.R., Dodson, M.G., and Swaffield, F., "The structure and concentration decay of high pressure jets of natural gas", Combustion Science Technology 36, pp. 249-261 (1984)

/18/ Middha, P., Hansen, O.R., and Storvik, I.E., "Validation of CFD model for hydrogen dispersion", Journal of Loss Prevention in the Process Industires 22, pp. 1034-1038 (2009)

/19/ Skottene, M. and Holm, A., "H2 release and jet dispersion – validation of Phast and KFX", Report 2008-0073 for DNV CTI910, 24 January 2008 (2008)

/20/ Roberts, P.T., Shirvill, L.C., Roberts, T.A., Butler, C.J. and Royle, M., "Dispersion of hydrogen from high-pressure sources", Proceedings of Hazards XIX conference, Manchester, UK, March 27-30 (2006)

/21/ Birch, A.D., Hughes, D.J., and Swaffield, F., "Velocity decay of high pressure jets", Combustion Science Technology 52, pp. 161-171 (1987)

/22/ Yüceil, K.B. and Ötügen, M.V., "Scaling parameters for underexpanded supersonic jets", Physics of Fluids (14) 12, pp. 4206-4215 (2002)

/23/ Gouzy-Hugelmeir, K., "Diphasic release modelling PHAST", Engineer internship report, DNV, Paris, 5 August 2013 (2013)

/24/ Cleaver, R.P., "Source modelling developed for the COOLTRANS Programme", Confidential report for National Grid, DNV, Loughborough, March 2014 (2014)

/25/ Wareing, C.J., Fairweather, M., Peakall, J., Keevil, G., Falle, S.A.E.G., and Woolley, R.M., "Numerical modelling of particle-laden sonic CO_2 jets with experimental validaton", AIP Conference Proceedings 1558, pp. 92-102, Rhodes, Greece, September 2013 (2013)

/26/ McFarlane, K., Prothero, A., Puttock, J.S., Roberts, P.T., and Witlox, H.W.M., "Development and validation of atmospheric dispersion models for ideal gases and hydrogen fluoride", Part I: Technical Reference Manual, Shell Report TNER.90.015, Thornton Research Centre (1990)

/27/ Hanna, S.R., D.G.Strimaitis, and J.C.Chang, "Hazard response modelling uncertainty (A quantitative method)", Sigma Research Corp. report, Westford, MA for the API (1991)

/28/ Nielsen, M. and Ott, S., "FLADIS field experiments", Final report Risø-R-898(EN), Risø National Laboratory, Roskilde, Denmark, July 1996 (1996)

APPENDIX A. GUIDANCE ON USING THE ATEX MODEL

A.1 Orifice model input and output data

A list of the orifice model inputs and outputs (taken from the model's MDE Generic Spreadsheet) is illustrated in

Table 0-1 ATEX model input and output
For each input a brief description of its meaning is given, its unit, and its lower and upper limits. Columns N contains a complete list of input data corresponding to case ATEX A, a metastable (superheated) liquid ammonia at ambient pressure.

Columns to the right indicate those values that need to be changed from column N to model the following continuous releases:

B. Methane pressurised vapour leak (column O)
C. Subcooled water at ambient pressure (column P)
D. Pressurised liquid chlorine (column Q)

Inputs	MDE_Test_ATEX: Atmospheric Expansion Testbed							
Input Index	Description	Units	Limits Lower	Limits Upper	AtexA	AtexB	AtexC	AtexD
	Material							
N	Stream name	-			Ammonia	Methane	Water	Chlorine
	Storage state (only used for flash							
2	Specification flag (0 - P&T&LF, 1 - P&T, 6 - P&LF, 7 - T&LF)	-	0	7	0	1	1	6
3	Pressure	Pa			1.01E+05	1.00E+06	1.01E+05	5.00E+06
4	Temperature	K			260	170	300	275
5	Liquid fraction (MOLE basis)	mol/mol			1			
	Exit state							
6	Specification flag (0 - P&T&LF, 1 - P&T, 6 - P&LF, 7 - T&LF)	-	0	7	0	1	1	6
7	Pressure	Pa			1.01E+05	1.00E+06	1.01E+05	5.00E+06
8	Temperature	K			260	170	300	275
9	Liquid fraction	-			1			
10	Is Exit flowrate supplied as input or exit velocity? TRUE - Exit Flowrate supplied as input	-			FALSE			
11	Input discharge coefficient	-	0	1	1			
12	Input Measured/Actual flowrate	kg/s	0		1.5			
13	Velocity	m/s			10	100	20	0
14	Diameter	m			0.025	0.05	0.1	0.025
15	Ratio of length to diameter	-	0	100	1			
	Atmospheric data							
16	Atmospheric pressure	Pa			101325			
17	Atmospheric temperature	K			293.15	273.15	283.15	
18	Atmospheric humidity	-			0.7	0.7	0.7	
19	Windspeed	m/s	0		0			
	Expansion method							
20	Expansion method (0 - min change, 1 - isentropic, 2 - cons moment, 3 - instantaneous, 4 - DNV GL recommended)	-	0	4	2			3
	PARAMETERS (values to be changed by expert users only)							
21	Multi-component flag (1 - MC, 0 - PC)	-	0	1	0			
22	Droplet correlation (0-original CCPS, 1- JIPII, 2-TNO, 3-Tilton, 4- Melhem, 5-JIPIII, 6-modified CCPS, 7-modified CCPS excl. 2PH pipe)	-	0	7	6			
23	Force mechanical or flashing breakup (0 - No, 1 - force mechanical, 2 - force flashing)	-	0	2	0			
24	Atmospheric molecular weight	kg/kmol			28.966			
25	Maximum velocity capping method (0 - user input, 1 - sonic velocity)	-	0	1	0			
25	Maximum velocity	m/s			1.00E+08			
26	Critical Weber number (for PHAST mechanical correlation)	-			12.5			
27	Minimum droplet size	m			1.00E-08			
28	Maximum droplet size	m			0.01			
Outputs								
Output Index	**Description**	**Units**						
	ERROR STATUS				OK	WARN	OK	OK
	Storage state							
1	Pressure	Pa			101325	1000000	101325	5000000
2	Temperature	K			260	170	300	387.6467
3	Liquid fraction (MASS basis)	kg/kg			1	0	1	1
	Exit state							
4	Pressure	Pa			101325	1000000	101325	5000000
5	Temperature	kg/kg			260	170	300	387.6467
6	Liquid fraction (MASS basis)	-			1	0	1	1
	Final (post-expansion) state							
7	Temperature	K			239.7476	111.666	300	239.1593
8	Liquid fraction (MASS basis)	kg/kg			0.932197	4.14E-02	1	0.572843
9	Velocity	m/s			1.00E+01	5.00E+02	20	2.76E+02
	Droplet data							
10	Droplet diameter	m			3.58E-03	5.15E-07	1.82E-03	3.69E-06
11	Flashing or mechanical (1 - mechanical, 2 - flash, 3 - transition)	-			1	1	1	1
12	JIP Rossin-Rammler 'b' coefficient	-			Undefined	Undefined	Undefined	Undefined
	Other data							
13	ATEX expansion method (1 - isentropic, 2 - cons moment, 3 - instantaneous, 4 - DNV GL recommended)	-			2	2	Undefined	3
14	Expanded diameter	m			1.79E-01	5.82E-02	1.00E-01	0.00E+00
15	Expansion energy	J/kg			Undefined	Undefined	0	37993.9
16	Partial expansion energy	J/kg			0	49626	0	37993.9
17	Superheat at exit	K			20.25243	58.33397	-73.16784	148.4874
18	Velocity at vena contracta	m/s			10	100	20	0
19	Corrected velocity at exit (i.e. dVenaVelocity * discharge Coefficient)	m/s			10	100	20	0
20	Actual/measured flowrate	kg/s			3.218397	2.507381	1.56E+02	0.00E+00

Table 0-1 ATEX model input and output

Input Data:

1. Material name. The user specifies the name for the material stored in the vessel.

2. Storage state.

The vessel stagnation data used to define the state of the stored material. The storage state can be specified in a number of ways, as described below.

2.1. Specification flag. A material at equilibrium can be specified using any 2 of pressure (P_{st}), temperature (T_{st}) , or liquid mass fraction (f_L) . A material not at equilibrium must have all 3 specified. This input flag tells the model how determine the state:
2.1.1. A value of 1 indicates P_{st} and T_{st} are specified; f_L is ignored.
2.1.2. A value of 6 indicates P_{st} and f_L are specified; T_{st} is ignored.
2.1.3. A value of 7 indicates T_{st} and f_L are specified; P_{st} is ignored.
2.1.4. A value of 0 indicates the material is not at equilibrium, and all 3 of P,T and f_L are used
2.2. Pressure (P_{st}). Storage pressure, including any liquid head for continuous releases. For instantaneous releases, the pressure should be that at half the liquid height in the vessel.
2.3. Temperature (T_{st}). Storage temperature.
2.4. Liquid fraction (f_L). Storage liquid mole fraction.

The above storage data are used only for the CCPS flashing droplet-size correlation in case of the old Weber/CCPS 6.54 droplet-size correlation (see Droplet Size Validation Document). Otherwise these data will not affect the results.[20]

3. Exit state (data at the orifice prior to atmospheric expansion). Exit state used for continuous releases only and not for instantaneous releases.

3.1. Input of orifice pressure, temperature and liquid fraction:

3.1.1. Specification flag. A material at equilibrium can be specified using any 2 of orifice pressure (P_o), orfice temperature (T_o) , or orifice liquid mass fraction (f_{Lo}) . A material not at equilibrium must have all 3 specified. This input flag tells the model how determine the state:
3.1.1.1. A value of 1 indicates P_o and T_o are specified; f_{Lo} is ignored.
3.1.1.2. A value of 6 indicates P_o and f_{Lo} are specified; T_o is ignored.
3.1.1.3. A value of 7 indicates T_o and f_{Lo} are specified; P_o is ignored.
3.1.1.4. A value of 0 indicates the material is not at equilibrium, and all 3 of P_o,T_o and f_{Lo} are used
3.1.2. Pressure (P_o). Orifice pressure
3.1.3. Temperature (T_o). Orifice temperature.
3.1.4. Liquid fraction (f_{Lo}). Orifice Storage liquid mole fraction.

3.2. Input of flow rate or velocity
3.2.1. Specification flag – flow rate supplied: TRUE (specify flow rate) or false (specify velocity)
3.2.2. If TRUE, specify flow rate Q. If flow rate is known, orifice velocity u_o can be calculated using material density at the exit:

$$u_o = \frac{Q}{0.25\pi\, d_o^{\,2} \rho_o(P_o, T_o, f_{Lo})}\ ;\ u_{vc} = \frac{Q}{0.25\pi\, d_{vc}^{\,2} \rho_o(P_o, T_o, f_{Lo})} \qquad \textbf{(43)}$$

3.2.3. If FALSE, specify the orifice velocity u_o. The vena contract velocity u_{vc} is derived from this as follows: $u_{vc} = u_o / C_d$; vena contracta diameter $d_{vc} = C_d^{0.5}\, d_o$. Note that u_{vc} is currently output by DISC and Phast and labelled in the Phast reports as 'orifice velocity'.

[20] JS: check usage of storage/exit data for instantaneous release.

3.3. Discharge coefficient[21] (should normally be obtained from DISC or GASPIPE/PIPEBREAK,)
- C_d = 0.6 for metastable liquid releases from leak
- C_d is calculated for other leak releases
- C_d = 1 for line rupture and long pipe releases

3.4. Exit diameter. Pipe or orifice diameter.
3.5. Ratio of L/D. The ratio of length to diameter of the orifice, pipe or nozzle. Only used for the JIP correlation. The Phase II JIP model enforces cut-offs of 2 and 50, while the Phase III JIP model enforces cut-offs of 0.1 and 50; see Droplet Size Model Validation document for details.

4. Atmospheric expansion data. Atmospheric pressure, temperature and humidity at the discharge height. Also the wind speed at the discharge height needs to be specified, but this is used by the Melhem correlation only.

Parameters (to be changed only by expert users):

1. Multi-component modelling flag. A value = 0 enables multi-component modelling for mixtures, rather than the pseudo-component approach (= 1) in PHAST 6.4 and earlier releases. Note that use of the JIP droplet correlation for mixtures is not currently recommended. Instead the Melhem correlation could be considered in addition to the old Weber/CCPS droplet size correlation.

2. Expansion method. For continuous releases, the default (= 2) is the recommended conservation of momentum / conservation of energy method[22]. The other continuous methods are isentropic (=1); the 'minimum thermodynamic change' method, (=0) where both methods are applied and the one that yields the highest final temperature is chosen; and DNV recommended (=4) which applies conservation of momentum when rainout is not expected. See Section 3.1. For instantaneous releases, there is only one method (see Section 3.2). Method 0 and 4 is recommended in combination with the old Weber/CCPS droplet size correlation (Method 2 should never be used in this case), while method 2 is recommended for the new JIP droplet correlations.

3. Droplet size calculation method. Sets which one of the droplet correlation methods is used for calculating droplet size in ATEX. See Droplet Size Validation Document for further details.

   3.1. Available droplet correlations:
      3.1.1.0 – the original CCPS (Phast 6.4) method – default in Phast 6.6 and earlier versions.
      3.1.2.1 – the JIP method uses the correlation proposed by the Flashing Liquid Jets Phase II project.
      3.1.3.2 – the TNO Yellow Book correlation
      3.1.4.3 – the droplet size correlation developed by Tilton and Farley
      3.1.5.4 – the Melhem correlation.
      3.1.6.5 – the correlation proposed in the JIP Phase III
      3.1.7.6 – the Modified CCPS correlation – new default in Phast 6.7
      3.1.8.7 – the Modified CCPS correlation but not for two-phase pipes
   3.2. Of these only the Original CCPS, Modified CCPS, Melhem and JIP phase III correlations are available in Phast, with the Modified CCPS correlation as the default.

4. Force mechanical or flashing break-up. If > 0, and where applicable, this forces the use of the flashing (= 2) or mechanical (= 1) break-up correlation used by a particular method (Weber/CCPS,; not applicable to or TNO as described above).

   4.1. Weber/CCPS. Can force either flashing or mechanical break-up.
   4.2. JIP-II, JIP-III. Can force mechanical break-up only
   4.3. TNO. Purely a mechanical break-up correlation, so this parameter has no effect.
   4.4. Melhem and Tilton and Farley. This parameter has no effect.

5. Atmospheric molecular weight. Should normally never be modified.

6. Specification of maximum velocity

[21] JS: move discharge coefficient to below specification of flow rate or velocity
[22] Not currently the default in PHAST

6.1. 'Maximum velocity capping method' (0 = user input, 1 = sonic velocity)
6.2. For user input =0: 'Maximum velocity'. This velocity should be at least equal to the sonic velocity at atmospheric pressure. The default option of 0 is in practice no capping of velocity as the default value is 1e8 m/s. Note that the sonic velocity is considered to be a lower limit for the final velocity in case of choked flow.

7. Critical Weber number. This is used only for the Weber/CCPS and Melhem mechanical droplet size correlation. The critical weber number is hardcoded as 15 for the TNO correlation.

8. Minimum and maximum droplet diameter.

Output Data:

1. Storage state. The storage state specified by the user, with all 3 of P_i , T_i and f_{Li}

2. Exit state. The material state at the orifice, prior to atmospheric expansion conditions. The model returns all 3 of P_o , T_o and f_{Lo}.

3. Final (post-expansion) state. The material state after the expansion to ambient conditions. The model returns T_f and f_{Lf} . The final pressure $P_f = P_a$. The model also returns final velocity u_f.

4. Droplet data.

   4.1. Droplet diameter.
   4.2. Flashing (=1) or mechanical (=2) droplet size correlations used. For the JIP correlation, a value of 3 is possible, indicating the droplets are in the transitional zone between flashing and mechanical break-up.
   4.3. Rossin-Rammler coefficients: a_{RR}[23] and b_{RR}. Used in determining the droplet size distribution.

5. Other data

   5.1. ATEX expansion method used. If the 'minimum thermodynamic change' method has been chosen, this output will indicate which of the two expansion methods was actually used.
   5.2. Expanded diameter.
   5.3. Expansion energy, E_{exp}.
   5.4. Partial expansion energy, E_p.
   5.5. Superheat at exit, ΔT_{sh}. Equals $T_o - T_{sat}(P_a)$
   5.6. Velocity at vena contracta, u_{vc}
   5.7. Corrected velocity at exit, $u_o = C_d\, u_{vc}$
   5.8. Flow rate

A.2 Model warnings and errors

Below are descriptions of the possible ATEX model error and warning messages.

```
2     "Unrecognised droplet calculation method"
3     "Unrecognised expansion method flag"
4     "Atmospheric pressure out of range"
5     "Maximum velocity out of range"
6     "Atmospheric temperature out of range"
7     "Atmospheric relative humidity out of range"
8     "Atmospheric molecular weight out of range"
9     "Critical Weber number out of range"
10    "Droplet minimum diameter out of range"
11    "Droplet maximum diameter out of range"
12    "Final (pseudo) velocity out of range"
```

[23] JS: ARR now doubles up as partial expansion energy - to change in future

```
13    "L/D ratio less than zero"
14    "Exit diameter out of range"
15    "Exit velocity out of range"
16    "Instantaneous model and JIP droplet correlation not allowed"
```

The JIP droplet correlation is derived from a continuous release from a vessel orifice. It cannot be applied to instantaneous releases.

```
17    "Specified exit flowrate is out of range"
18    "Specified wind speed is out of range"
19    "Specified discharge coefficient is out of range"
20    "Velocity capping method is out of range"
21    "Cannot calculate sonic velocity cap"
22    "Invalid value of droplet flag for chosen droplet correlation"
24    "Scenario flag invalid for the model"
```

The messages are:

```
2004 "Entropy or enthalpy not conserved during expansion to atmospheric pressure"
```

The isentropic/conservation of energy expansion calculations have not converged within the accepted tolerance. The closest solution discovered will be employed.

```
2005 "Isentropic expansion fails: simulated results are invalid (i.e. positive enthalpy difference). Using forced-phase expansion [see theory document for details]"
```

The instantaneous isentropic expansion calculations have encountered an unrealistic solution which will result in the simulation of a negative final velocity. A special logic based on forced-phase expansion is applied (see Appendix B for details). This may occur due to the incorrect/inconsistent set-up of a new pure component's material (especially vapour pressure) properties or the use of the pseudo-component modelling logic for wide-boiling mixtures.

```
2006 "Chosen droplet correlation invalid for instantaneous releases, using original CCPS correlation (Phast 6.54)"
```

Some droplet correlations depend on data that are not available or relevant for the instantaneous scenario, e.g. orfice data. If such a correlation is chosen for an instantaneous release, then the original CCPS correlation is automatically chosen instead.

APPENDIX B. SPECIAL LOGIC FOLLOWING FAILURE OF INSTANTANEOUS ISENTROPIC EXPANSION CALCULATIONS

There are special instances in which the instantaneous isentropic expansion model described in section 3.2 fails to simulate positive expansion energies. This is usually observed when the Pseudo-component thermodynamic assumption is applied to wide boiling mixtures. Where this occurs, the atmospheric expansion model (i.e. ATEX) carries out the following:

- For fluids existing as two-phase mixtures at stagnation condition, ATEX conducts an irreversible adiabatic expansion (i.e. isenthalpic expansion) from the stagnation state (P_{st} and S_{st} i.e. stagnation pressure and entropy) to ambient pressure (i.e. P_a, S_f).
- For fluids existing as single-phase mixtures at orifice conditions, ATEX conducts a forced phase (i.e. liquid-liquid or vapour-vapour) expansion from the fluid's stagnation state to its saturated state at ambient pressure (i.e. P_a, $S_f = S_{sat}$); see Figure 0-1

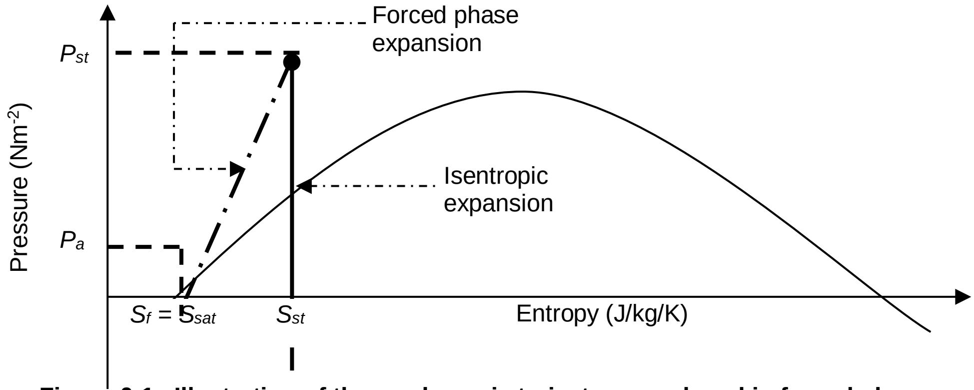

Figure 0-1 Illustration of thermodynamic trajectory employed in forced phase expansion calculations for anomalous instantaneous releases

The expansion energy for these special cases is defined as[24]:

$$E_{\exp} = T_{sat}\left(S_{st} - S_f\right) - \left(P_{st} - P_a\right)v_{st} \qquad \textbf{(44)}$$

The above expansion energy is subsequently substituted in equation **(16)** to obtain the final velocity (see section 3.2).

[24] JUSTIFY: The use of this approach could result in discontinuous behaviour in simulated final velocities. Furthermore, the equation adopted for the expansion energy has no theoretical basis. In all, this logic has only been retained as an artefact of the defunct atmospheric expansion models (i.e. EXPNZE/ADIAX/ADIAX0). It is envisaged that with the rigorous multi-component modelling, the need would no longer exist for the use of this special logic.

About DNV

We are the independent expert in risk management and quality assurance. Driven by our purpose, to safeguard life, property and the environment, we empower our customers and their stakeholders with facts and reliable insights so that critical decisions can be made with confidence. As a trusted voice for many of the world's most successful organizations, we use our knowledge to advance safety and performance, set industry benchmarks, and inspire and invent solutions to tackle global transformations.

Digital Solutions

DNV is a world-leading provider of digital solutions and software applications with focus on the energy, maritime and healthcare markets. Our solutions are used worldwide to manage risk and performance for wind turbines, electric grids, pipelines, processing plants, offshore structures, ships, and more. Supported by our domain knowledge and Veracity assurance platform, we enable companies to digitize and manage business critical activities in a sustainable, cost-efficient, safe and secure way.

DNV | digital@dnv.com | dnv.com/digital